Genetic analysis of F1 cluster phages that infect *Mycobacterium smegmatis* identifies two distinct holin-like proteins that regulate the host lysis event

Richard S. Pollenz[1*], Kira Ruiz-Houston[2], Wynter Dean[1], Loc Nguyen[1]

[1]Department of Molecular Biosciences, University of South Florida, Tampa, Florida, United States of America

[2]Department of Microbiology, University of Wisconsin, Madison, Wisconsin, United States of America

[*]Corresponding Author:

E-mail: pollenz@usf.edu (RSP)

ABSTRACT

Phages Girr and NormanBulbieJr (NBJ) infect Gram-positive *Mycobacterium smegmatis* mc^2 155. Both phages contain conserved lysis cassettes that harbor two endolysin genes (*lysin A* and *lysin B*) and two genes encoding transmembrane domain (TMD) holin-like proteins. The first holin-like protein, termed LysF1a is 88 amino acids, has two TMDs and a predicted N-in-C-in membrane topology. The second, termed LysF1b, has a single N-terminal TMD and a predicted N-out-C-in topology making it distinct from the type III holins or spanins in size and membrane topology. Deletion of *lysF1b* results in severe lysis defect phenotypes manifest by reduced plaque size and changes to lysis timing in liquid culture. Deletion of both *lysF1a* and *lysF1b* genes results in phages that show the same lysis phenotypes as the single *lysF1b* deletion. Phages with only *lysF1b* are lysis competent and trigger lysis prematurely when exposed to energy poisons while phages with *lysF1a* or *lysF1a/lysF1b* deletions do not trigger prematurely. Deletion of genes upstream of the lysis cassette did not impact lysis phenotypes. Lysis recovery mutants were isolated from phages lacking the *lysF1b* gene and these mutants generated wild type plaque size but triggered lysis prematurely and showed ~65% reductions in burst size. Genome sequencing identified different point mutations that mapped to TMD1 or the C-terminal region of the *lysF1a* gene. Infection of an *M. smegmatis* strain that does not produce lipomannan and lipoarabinomannan by either wild type phages or phages carrying the *lysF1b* deletion showed modest plaque size increases but did not fully complement the lysis defect of phages lacking the *lysF1b* gene. Collectively, the findings show that both LysF1a and LysF1b proteins are required for efficient bacterial lysis by these F1 cluster phages. LysF1a does not function as a pure antiholin but requires the expression of the LysF1b protein for efficient lysis functioning.

41 **INTRODUCTION**

42 With an estimated 10^{31} different bacteriophage particles in the world, the pathway
43 whereby dsDNA phages lyse their bacterial hosts after infection and replication is one of the
44 most common cell fates on earth [1]. Extensive biochemical and genetic work with dsDNA
45 phages that infect Gram-negative hosts has established a general three-step model for the
46 triggering of the lysis pathway that involves three distinct sets of proteins. The first are
47 endolysin/s that have defined catalytic activity to lyse the peptidoglycan (PG) layer [2]. The
48 second are holin or antiholin proteins that have between 1-4 transmembrane domain helices
49 (TMD). These proteins work together to, 1) control the timing of the lysis event following phage
50 infection [3, 4], 2) assist with the destabilization of the membrane proton motive force (PMF) [3,
51 4] and 3) in the canonical holin models, generate large 1μm "pores" in the inner membrane (IM)
52 to allow the exit of the endolysin enzymes to the periplasmic space where they can access and
53 cleave the PG layer [5, 6]. Finally, there are secreted membrane proteins and lipoproteins
54 termed spanins that are associated with the IM and outer membrane (OM). There proteins
55 interact after the PG layer is cleaved to generates the lesion across the IM and OM that allows
56 for the efficient release of the phage progeny [7-9].

57 dsDNA phages such as lambda, P2, and phage 21 all have genomes < 50,00bp and
58 have a clustered lysis cassette that contain all the genes necessary to mediate the bacterial
59 lysis event [10-12]. Phage lambda encodes the canonical type I holin protein that has 3TMDs
60 and forms large oligomers that create 1μm holes in the IM to allow exit of the endolysin from the
61 cytoplasm to the periplasmic space [12]. Phage 21 defines the type II pinholin lysis pathway and
62 utilizes a 2TMD holin protein that forms ~1,000 heptamers in the IM. The pinholins create only
63 nanometer size holes that are not big enough to allow exit of the endolysin, and they function to
64 disrupt the PMF and trigger lysis. Thus, phages that encode pinholins also encode endolysins
65 that carry secretion-arrest-release (SAR) signals and the SAR-endolysin is held in an inactive

66 state in the IM prior to triggering. The disruption of the PMF causes the release of the IM
67 tethered SAR-endolysin to the periplasmic space where it cleaves the PG [4, 13, 14]. In both
68 lambda and phage 21, a single open reading frame with two in-frame start codons (dual start
69 motif) encodes two holin proteins that only differ by the addition of 1-2 N-terminal amino acids
70 [10, 11, 14, 15]. The longer version of each holin functions as the inactive antiholin and in both
71 cases a percentage of the holin forms dimers with the antiholin that holds that holin in an
72 inactive state prior to triggering. Upon triggering, the antiholin assumes active holin function
73 greatly increasing the amount of active holin protein available for hole formation. In phages with
74 large genomes, such as P1 and T4, the holin, antiholin, endolysin, spanin and lysis inhibiter
75 (LIN) rI and rIII genes can be bioinformatically characterized throughout the genome and are not
76 in a defined cassette [10, 11, 16, 17]. The type III holin from phage T4 has a single N-terminal
77 TMD with an N-in-C-out topology with the bulk of the sequence oriented in the periplasmic
78 space [16, 17]. T4 phage encodes two different antiholins and LIN proteins that modulate the
79 holin lysis timing and participate in the lysis inhibition activity of phage T4 [16, 17]. Thus, a
80 common theme in the phage-mediated lysis pathway of lambda, P1, P2 and T4 is the utilization
81 of holins and antiholins to regulate the lysis event. Phage T7 on the other hand, has only 1
82 annotated holin and no identified antiholin and deletion of the holin is not lethal but results in
83 various lysis phenotypes suggesting that other unidentified proteins may also participate in the
84 lysis pathway [18]. Another variation of the lysis pathway has recently been shown for the
85 Enterococcal phage Mu [19]. Mu does not utilize canonical holins and antiholins in the bacterial
86 lysis pathway and instead uses a novel 1TMD protein termed a releasin protein to release the
87 SAR-endolysin from the IM so it can cleave the PG [19]. As with lambda and phage 21, Mu
88 contains canonical spanins to create the final lesion for progeny release once the PG has been
89 cleaved. It is speculated that Mu does not utilize the holin/antiholin regulated lysis mechanism
90 because it copies its genome via replicative transposition during the lytic cycle and has less
91 selective pressure due to transposition immunity [19]. This pathway adds yet another variation

92 in phage-mediated bacterial lysis and it is striking that all the *E. coli* phages that have been
93 rigorously studied utilize a similar set of tools to complete the lysis pathway through distinct
94 molecular mechanisms.

95 There are 1000s of annotated dsDNA phages that infect Gram-positive hosts, yet the
96 molecular mechanism that these pages use to lyse their hosts is not resolved to the level of the
97 *E. coli* phages. Although it is hypothesized that the lysis mechanism in these phages will utilize
98 a similar set of proteins as described for phages that infect Gram-negative bacteria, the bulk of
99 biochemical and genetic work has focused more on the enzymes that target the cell wall than on
100 the holins, possibly because these enzymes may be employed as antibiotic agents [20-22].
101 Gram-positive bacteria lack a formal OM and instead have a much more complex PG layer and
102 an extended structural cell wall components beyond the PG such as arabinogalactans and
103 mycolic acids [23-26]. Thus, addition of an endolysin to Gram-positive bacteria can result in cell
104 death. Bioinformatic, biochemical and genetic analysis has identified several types of phage-
105 encoded endolysins that target different regions of the cell wall. The first type of endolysin is
106 termed lysin A and targets distinct domains of the peptidoglycan [21, 27]. These enzymes are
107 highly modular, do not contain canonical SAR domains, and deletion studies show that the lysin
108 A is essential to phage propagation [28, 29]. It is unknown if the lysin A is released to the
109 peptidoglycan layer through holins since some studies show that exogenous expression of
110 selected lysin A enzymes can be cytotoxic to *M. smegmatis* [21, 30-33]. Many phages that infect
111 Gram-positive hosts also contain a second endolysin termed lysin B that targets the linkages in
112 the mycolic acid layer of the cell wall [28, 31, 34, 35]. It has been hypothesized that lysin B
113 provides a fitness advantage for optimal bacterial lysis and phage release since deletion of lysin
114 B results in viable phages with reduced plaque and burst size [28].

115 In phages that infect Gram-positive hosts the presence of genes that encode holin-like
116 proteins has primarily been characterized by bioinformatic analysis and many of the phages
117 contain more than one gene encoding a TMD protein that could serve as a holin or antiholin.

118 Currently there are reports on host lysis by phages that infect *Staphylococcus aureus* [36-38],
119 *Bacillus sp*. [39,40], *Lactococcal sp*. [41], *Oenococcus oeni* [42, 43], *Streptococcus sp* [44],
120 *Gordonia rubripertincta* [45-47] and *Mycobacterium sp*. [48-55]. The holin function for the
121 encoded TMD proteins in most of these reports is based primarily on the proximity of the TMD
122 gene/s near an endolysin. Where biochemical work is reported, the majority has been carried
123 out using exogenous expression of the TMD genes in *E. coli*. However, there are several
124 reports on phages that infect *Mycobacterium smegmatis* where gene deletion has been utilized
125 to evaluate lysis function of the predicted holin proteins.

126 The first study evaluated two genes encoding TMD proteins that are found directly
127 downstream of the *lysin A* and *lysin B* in the F1 cluster phage Ms6 [50-52]. Ms6 gene *26*
128 encodes an 88 amino acid protein with 2TMDs while gene *27* encodes a 124 amino acid protein
129 with 1TMD. Deletion of gene *26* resulted in reduced lysis timing, reduced plaque size but wild
130 type burst size, while deletion of gene *27* resulted in delayed lysis timing, increased plaque size
131 and increased burst size. However, there are limitations to these findings because holin function
132 was not verified using energy poisons and the mutant phages were not tested in liquid lysis
133 assays in the *M. smegmatis* host versus *E. coli*. In addition, the experiments to assess function
134 and interaction of the two proteins were carried out using recombinant *E. coli* expression
135 systems that are not physiologic. Thus, while it appears that both proteins are needed for the
136 lysis event, it is unclear how each is contributing to the lysis of the *M. smegmatis* host.

137 The second set of studies evaluated phage D29, a cluster A2 phage that also infects *M.*
138 *smegmatis* [53-56]. D29 has a lysis cassette with a *lysin A* (gene *10*), 2TMD holin (gene *11*) and
139 a *lysin B* (gene *12*). It is important to note that the 2TMD holin of D29 is not an ortholog to the
140 2TMD protein in Ms6 and differs significantly in amino acid sequence and size. The lysis
141 cassette that is also distinct from most other actinobacteriophages in that it has no other genes
142 encoding holin-like TMD proteins within or near the putative lysis cassette. Deletion of gene *11*
143 results in a viable phage with a different phenotype that the 2TMD deletion in Ms6 [53].

144 D29_Δ*11* phage shows a modest 30% reduced plaque size, slightly delayed lysis timing and
145 reduced burst size [53]. The lack of a more severe lysis phenotype is surprising given that gp11
146 is the only defined holin, especially since the D29 lysin A does not have a defined signal peptide
147 or SAR-like domain for export [32, 33]. However, it has been reported that the D29 lysin A may
148 be exported prior to lysis in a yet to be defined pathway that appears to be independent of the
149 holin [32, 33]. Alternatively, the modest lysis phenotype could also indicate that D29 has
150 additional holin-like genes that are not located within the defined "lysis cassette" region. Such a
151 scenario has recently been described in a bioinformatic study of the lysis cassettes of 77
152 phages that infect the Gram-positive *Gordonia rubripertincta* strain [46]. This study showed that
153 there was a high level of diversity of the lysis cassette gene organization and that putative holin-
154 like genes could be identified in genomic regions distal to the endolysin containing lysis
155 cassettes [46]. This study also showed that most of the phages evaluated had at least two holin-
156 like genes.

157 In summary, there is limited biochemical and genetic analysis of host lysis pathways by
158 phages that infect Gram-positive hosts, especially within the host bacteria. One of the most
159 intriguing findings from the annotation of phages that infect Gram-positive hosts is the presence
160 of multiple genes that encode predicted holin-like TMD proteins in the defined lysis cassettes.
161 Since antiholins have not been experimentally identified in phages that infect Gram-positive
162 hosts, one interpretation of these data are that holins and antiholins are expressed from distinct
163 genes as shown for *E. coli* phages P2 and T4 [16, 17, 57, 58]. It is also possible that some of
164 the TMD genes encode proteins with spanin-like functions that interact with the complex cell
165 wall of the Gram-positive bacteria. This hypothesis is supported by a report that identified a 177
166 amino acid protein termed LysZ, that is encoded by phages that infect *Corynebacterium*
167 *glutamicum* and may function to disrupt the integrity of the bacterial cell wall [59]. The current
168 study aims to evaluate how two predicted holin-like TMD proteins encoded by phages Girr and

169 NormanBulbieJr (NBJ) function in the lysis pathway of *Mycobacterium smegmatis* mc^2 155 by
170 utilizing recombineered phages and multiple lysis assays under physiological growth conditions.

171 **MATERIALS AND METHODS**

172 **Bioinformatic analysis of transmembrane domains and AlphaFold3 analysis**

173 The identification of transmembrane domains (TMD) and protein topologies was carried
174 out essentially as described by Pollenz et al., 2024 [46] utilizing Deep TMHMM (v1.0.24) [60,
175 TOPCONS (v2.0) [61], SignalP-5.0 and SignalP-6.0 [62], LipoP 1.0 [61] and HHpred
176 (databases: PDB_mmCIF70_30_Mar; Pfam-A_v37) [64]. All membrane proteins described in
177 this report had 100% consensus predictions of TMD domain location, number and protein
178 topology in all programs. Structural predictions of proteins and protein-protein interactions were
179 determined using AlphFold3 [65]. For single proteins, pTM scores >50% indicate high
180 confidence in the model predictions. For protein-protein interactions, ipTM scores <90% are
181 considered low confidence and should be used with caution [63]. All amino acid alignments
182 were performed using Clustal Omega [66].

183 **Bacterial strains, growth and plaque assay**

184 The list of bacterial strains, phage and plasmids utilized in this study is presented in
185 Table 1. *Mycobacterium smegmatis* mc^{2}155 [67] was used as wild type host for all phage
186 related experiments. *M. smegmatis* ∆mtpA and *M. smegmatis* ∆mtpA-comp are described in
187 [68]. *M. smegmatis* strains were propagated on Middlebrook 7H10 agar supplemented with 10%
188 Albumen Dextrose Complex (ADC; 5% albumen, 2% dextrose, 154mM NaCl) at 37ºC. To
189 generate saturated stock cultures, a single colony of *M. smegmatis* was propagated in 25ml of
190 Middlebrook 7H9 media supplemented with 10% ADC, 1mM $CaCl_2$, 0.5% glycerol and 0.05%

191 Table 1. Bacterial Strains, Phages and Plasmids

Bacterial Strains	Genotype/Features	Reference/Source
M. smegmatis	*Mycobacterium smegmatis* mc^2 155	67
M. smegmatis ∆mptA	*Mycobacterium smegmatis* mc^2 155	68

	lacking the mptA enzyme	
M. smegmatis ΔmptA-comp	*ΔmptA* strain carrying complementing mtpA expression plasmid	68
E. coli	*Escherichia coli* NEB5α F'I^Q	New England Biolabs
Bacteriophage	**Genotype/Features**	**Source**
Phage Girr_WT	Mycobacteriophage Girr	70. PhagesDB: https://phagesdb.org/phages/Girr
Phage Girr_*Δ26*	Girr_WT with deletion of gene *26*	This study
Phage Girr_*Δ29*-20	Girr_WT with deletion of gene *29* clone 20	This study
Phage Girr_*Δ29*-25	Girr_WT with deletion of gene *29* clone 25	This study
Phage Girr_*Δ27-30*	Girr_WT with deletion of genes 27-30	This study
Phage Girr_*ΔlysF1a*	Girr_WT with deletion of gene *34*	This study
Phage Girr_Δ*lysF1b*	Girr_WT with deletion of gene *35*	This study
Phage Girr_Δ*lysF1a*/_Δ*lysF1b*	Girr_WT with deletion of gene *34* and gene *35*	This study
Phage NBJ_WT	Mycobacteriophage NormanBulbieJr	71. PhagesDB: https://phagesdb.org/phages/NormanBulbieJr
Phage NBJ_*Δ29*	NBJ_WT with deletion of gene *29*	This study
Phage NBJ_*ΔlysF1a*	NBJ_WT with deletion of gene *33*	71
Phage NBJ_*ΔlysF1b*	NBJ_WT with deletion of gene *34*	This study
Phage NBJ_Δ*lysF1a*/_Δ*lysF1b*	NBJ_WT with deletion of gene 32 and gene *33*	This study
Phage D29_	Mycobacteriophage D29	56
Plasmids	**Features**	**Source**
pExTra-Girr_*29*	pExTra01::(Ptet-Girr_*34*-mcherry); Kan^R	70
pExTra-Girr_*34*	pExTra01::(Ptet-Girr_*34*-mcherry); Kan^R	70
pExTra-Girr_*35*	pExTra01::(Ptet-Girr_*35*-mcherry); Kan^R	70
pExTra-NBJ_*29*	pExTra01::(Ptet-NBJ_*29*-mcherry); Kan^R	71
pExTra-NBJ_*32*	pExTra01::(Ptet-NBJ_*32*-mcherry); Kan^R	71
pExTra-NBJ_*33*	pExTra01::(Ptet-NBJ_*33*-mcherry); Kan^R	71
pExTra-Waterfoul_*32*	pExTra01::(Ptet-Waterfoul_*32*-mcherry); Kan^R	69

pExTra-Waterfoul_*32*ΔN	pExTra01::(Ptet-Waterfoul_*32(truncation of N-terminal TMD)*-mcherry); Kan^R	This study
pExTra-Waterfoul_*32*ΔC-40	pExTra0 ::(Ptet-Waterfoul_*32(truncation of C-terminal 40aa)*-mcherry); Kan^R	This study
pJV53	Acetamide inducible plasmid with Ched9c gene *60-61*. Kan^R	73

192

193 Tween-80 with shaking (225rpm) at 37°C. For all liquid lysis and one-step experiments, 100ul of
194 saturated stock was added to 250ml baffled flasks containing 55ml of supplemented 7H9
195 without Tween. Cultures were shaken (225rpm) overnight at 37°C and utilized in experiments
196 the next day while in log phase growth (OD_{600} <0.8). Titering experiments showed that an *M.*
197 *smegmatis* culture at an OD_{600} of 1.0 was equal to ~6.5 x 10^7 CFU/ml. This value was utilized
198 when phages were infected at different MOIs. Plaque assays were completed by mixing the
199 appropriate amount of phage with 250ul of saturated *M. smegmatis* in Middlebrook 7H9 media
200 supplemented with 10% ADC, 1mM $CaCl_2$ and 0.5% glycerol. The mixture was vortexed and
201 incubated at 22°C for 10 minutes. Following the infection, the sample was mixed with 4-5ml of
202 top agar (Middlebrook 7H9, 1mM $CaCl_2$, 0.5% agar) and plated immediately onto 7H10 agar
203 plates. Plates were allowed to harden and placed in a 37°C bacterial incubator for 16-48 hrs.
204 Competent *M. smegmatis* cells for recombineering or for plasmid transfection and
205 complementation studies were prepared as described previously [29, 69-71]. *Escherichia coli*
206 NEB5α $F'I^Q$ (New England Biolabs) was used for plasmid amplification and purification and
207 grown in LB broth or on LB agar supplemented with 50ug/ml kanamycin sulfate and.

208 **Plasmid constructs, *M. smegmatis* transformation and complementation analysis**

209 All PCR primers utilized in this study are shown in S1 Table 1. To generate the inducible
210 expression plasmids pExTra_Waterfoul_*32ΔN*, pExTra_Waterfoul_*32ΔC40*,
211 pExTra_Waterfoul_32 was PCR amplified with Q5 DNA polymerase (New England Biolabs)

212 using Waterfoul specific primers containing with pExTra homology regions (Table S1). Purified
213 PCR products (were ligated into linearized pExTra01 using isothermal assembly (NEB HiFi 2x
214 Master Mix) as described [67-69]. Recombinant plasmids were recovered by transformation of
215 *E. coli* NEB5α F′I^Q and colonies selected on LB agar supplemented with 50μg/μl kanamycin
216 sulfate. Plasmid DNA was purified using the GeneJet kit (Fisher) and all plasmids were
217 sequence-verified by Sanger sequencing using the pExTra Seq primer (Azenta). For generating
218 complementing strains, competent *M. smegmatis* cells were prepared as described [67-69] and
219 40μl mixed with 100ng plasmid DNA in a 1mm electroporation cuvette. The sample was
220 electroporated with 1800V and the time constant set to 5.0 msec. Following electroporation, the
221 sample was mixed with 950μl of supplemented 7H9 media without Tween and shaken (225rpm)
222 at 37ºC for 120 minutes. Following the recovery period, 10μl-100μl aliquots were spread on
223 7H10 agar plates supplemented with 10μg/μl kanamycin sulfate and incubated at 37ºC for 3-5
224 days. To generate cultures for plaque assay, single colonies of *M. smegmatis* carrying the
225 appropriate plasmid were harvested into 25ml of supplemented 7H9 media containing 10μg/μl
226 kanamycin sulfate. Cultures were shaken (225rpm) at 37ºC for 24-48 hours. Saturated cultures
227 at OD_{600} > 1.5 were centrifuged at 6200rpm for 10 minutes and the pellets resuspended in
228 supplemented 7H9 media (without Tween) to a final OD_{600} of 2.0. These cells were utilized for
229 phage infection and then mixed with 4.5ml top agar supplemented with 10ng/μl kanamycin
230 sulfate with or without 100ng/μl anhydrotetracycline (aTc). The mixture was added to 7H10 agar
231 containing 10μg/μl kanamycin sulfate supplemented with or without 100ng/μl aTc and incubated
232 at 37ºC for the times indicated in the results section.

233 **Bacteriophage recombineering and genome sequencing**

234 All gblocks and PCR primers utilized in this study are shown in Table S1. The deletion of
235 genes in phage Girr and NBJ were carried out using the Bacteriophage Recombineering of
236 Electroporated DNA (BRED) procedure as described [29, 72], with the following modifications.

237 Phage genomic DNA was purified using the Wizard DNA Clean up kit (Promega). dsDNA
238 recombineering substrates were synthesized as gblocks (Integrated DNA Technologies). To
239 generate µg quantities of dsDNA substrates, gblocks were solubilized in water to 10ng/µl and
240 PCR amplified with gblock specific primers using 2X Q5 master mix (New England Biolabs).
241 PCR products were purified using Zymoclean DNA recovery (Zymoresearch). To generate
242 recombinant phage, 200-400ng dsDNA substrate was mixed with 100ng phage genomic DNA
243 and incubated on ice for 10min. The DNA mixture was added to 100µl of recombineering *M.*
244 *smegmatis* in a 2mm electroporation cuvette and electroporated at 2500V with the time constant
245 set to 20.0 msec. Following electroporation, 900µl of supplemented 7H9 media was added to
246 the cells and they were shaken (225rpm) at 37°C for 90 minutes. Following the recovery period,
247 the sample was mixed with 250µl of saturated *M. smegmatis* and plated with 5ml 7H9 top agar
248 onto 7H10 agar plates. Plates were incubated at 37°C for 18-24 hours to recover primary
249 plaques. Primary plaques were picked into 120µl of phage buffer (10 mM Tris-HCl, pH 7.5; 10
250 mM $MgSO_4$, 68.5 mM NaCl; 1mM $CaCl_2$), vortexed, and incubated at 22°C for 2-8 hrs. The
251 presence of mutant phage genomes was determined by Deletion Amplification Detection Assay
252 (DADA) PCR [29] using a 20µl reaction with: 1µl of plaque sample, 2µl of 0.2 µM DADA primer
253 mix (1:1 mix of For and Rev primers), 5µl glycerol (40%), 2µl water and 10µl OneTaq 2x Master
254 Mix (New England Biolabs). PCR conditions were: 94°C for 1 minute followed by 35 cycles of
255 94°C-1min/66°C 1min and a final 66°C step for 5 minutes. Positive primary plaque samples
256 were serially diluted and plated on wild type or complementing *M. smegmatis* as indicated.
257 Secondary plaques were picked as above and screened by standard PCR using gene specific
258 flanking primers. Pure populations of mutant phage were evaluated by full genome sequencing
259 as described [73, 74]. Briefly, Genomic DNA was used to create sequencing libraries with the
260 NEB XLEP-P1 kit. Sequencing was performed by the Pittsburgh Bacteriophage Institute and the
261 library run on an Illumina NextSeq 1000 instrument. Raw reads were trimmed with cutadapt 4.7
262 (using the option: –nextseq-trim 30) and filtered with skewer 0.2.2 (using the options: -q 20 -Q

263 30 -n -l 50) prior to assembly. The resulting sequences were assembled using Consed (v29.0)
264 with Unicycler (v5.0) and contigs checked for completeness, accuracy, and genome termini.
265 Final phage contigs were aligned to wild type phage to identify deletions and point mutations.

266 **Plaque size analysis**

267 Plaques were generated using the plaque assay procedure described above. For
268 experiments where plaque size would be evaluated between several different phages, identical
269 bacterial samples, incubation times, phage concentrations and top agar amounts were utilized.
270 Plaque size was evaluated using ImageJ software [75] and by manual measurement using
271 photos embedded in PowerPoint and custom rulers. In most experiments, results are presented
272 for an average of 50 plaques and the statistical significance of measurements determined by
273 unpaired t-test (https://www.graphpad.com/quickcalcs/ttest1/). Plaque volume was calculated by
274 the formula $\pi r^2 h$ where r is the radius of the plaque and h was set to 1mm for the top agar
275 thickness.

276 **Liquid lysis assay and cell viability assay from liquid cultures**

277 Liquid lysis assays were carried out essentially as described by Payne et al., 2009 [28]
278 with the following modifications. Briefly, overnight cultures of *M. smegmatis* in log phase growth
279 were diluted to an OD_{600} of 0.25-0.30 in supplemented 7H9 without Tween and 40ml of culture
280 was added to 250ml baffled flasks. High titer phage lysate was added to the cultures to create
281 an MOI of 10 and the mixture set at 37°C for 30 minutes without shaking. T_0 for all experiments
282 was the time of phage addition. After 30 minutes (T_{30}), the cultures were constantly shaken a
283 225rpm and aliquots of cells removed with a syringe and sterile needle from the shaking culture
284 without stopping the incubator. The OD_{600} of the sample was immediately recorded for each
285 aliquot using a GENESYS spectrophotometer (Fisher Scientific). In some experiments, KCN
286 (1M in water), or $CHCl_3$ (100%) was added directly to the shaking culture to produce a final
287 concentration of 10mM or 1%, respectively. All liquid lysis experiments were repeated at least
288 five separate times and representative experiments are presented.

289 To assess if there were viable cells surviving in the phage infected cultures, bacteria was
290 aliquoted from a single stock sample at an OD_{600} of 0.25-0.27 and infected at an MOI of 10 as
291 described above. An aliquot of culture was removed from uninfected and infected cultures at the
292 times specified in the experiment, evaluated at OD_{600} and serial diluted in 7H9 neat. 250µl
293 aliquots of the dilutions were spread on 7H10 agar plates and incubated at 37°C until colonies
294 could be counted (4-5 days). To assure that surviving colonies all arose from infected cells and
295 were not the result of phage resistant *M. smegmatis* or contamination, lytic phage D29 [56] was
296 used as a positive control with an expected outcome of zero viable cells.

297 **ATP assay**

298 The presence of ATP in culture supernatants was determined utilizing the ENLIGHTEN
299 kit (Promega). Briefly, liquid lysis assays were carried out as described above. A 500ul aliquot of
300 culture was removed at indicated time points and immediately passed through a 0.2µ syringe
301 filter to remove bacteria. The sample was frozen at -20°C prior to analysis. The presence of ATP
302 in culture supernatants was determined by mixing 5µl with 50µl ENLIGHTEN reagent
303 (Promega), mixing for 5 seconds and then reading the integrated luminescence over 10
304 seconds using a GloMax luminometer (Promega). To assure that the readings were within the
305 linear range of the instrument an ATP standard curve was utilized.

306 **One-step growth curves and burst size determination**

307 Several experimental procedures have been utilized for one-step growth curves with
308 Gram-positive bacteria [33, 49, 51, 53]. In our hands, none of these procedures generated
309 consistent results or provided the ability to directly measure burst size. Thus, we developed a
310 one-step protocol that is illustrated in S2 Figure 1 and described below. To prepare the cells, the
311 OD_{600} of fresh overnight cultures of *M. smegmatis* in log growth were determined and 10ml
312 centrifuged at 3,000rpm for 10 minutes. The cells were resuspended in supplemented 7H9 to a
313 final concentration equal to an OD_{600} of 3.2/ml. 250µl of cells (~5 x 10^7 cfu) were added to
314 microfuge tubes and ~5 x 10^7 phage added to the cells to create an MOI of 1. The same amount

315 of phage was also added to 250µl of supplemented 7H9 media without cells to verify the titer
316 and determine the level of phage adsorption. The mixture was vortexed and set at 37ºC for 30
317 minutes without shaking. T_0 for all experiments was the time of phage addition to the cells. After
318 30 minutes, 750µl of supplemented 7H9 was added to all samples. Samples were vortexed and
319 centrifuged at 6,200rpm for 4 minutes to separate unabsorbed phage. The supernatant was
320 saved for analysis of titer and adsorption, and the cell pellet immediately resuspended in 1ml
321 supplemented 7H9, vortexed and diluted 1:10,000 into 70ml of supplemented 7H9 in baffled
322 250ml flasks. An aliquot was removed and 5µl, 12.5µl and 25µl used for plaque assay to
323 determine the number of infectious centers to determine the precise number of infected cells. A
324 second aliquot was removed and filtered through a 0.2µ syringe filter and 150µl utilized for
325 plaque assay to test for unabsorbed (free) phage at T_{45} minutes (the first one-step data point).
326 The flask was placed in a 37ºC incubator and constantly shaken at 225rpm for the duration of
327 the experiment. At specified time points, 500µl aliquots were removed from the shaking flasks
328 and each sample immediately passed through a 0.2µ syringe filter to remove cells and collect
329 free phage. The amount of phage in each sample was determined by performing plaque assays
330 using 150µl of serially diluted samples (usually 10^0 to 10^{-4} dilutions were sufficient). The phage
331 titer in the flask, expressed as PFU/ml was determined at each time point by counting the
332 plaques on each plate, dividing by the volume of phage used in the infection (150µl), multiplying
333 by the dilution factor and then multiplying by 10^3. The number of infectious centers in the
334 infected 70ml culture was determined by counting the plaques, dividing by the volume used for
335 the plaque assay and multiplying by 70,000. The original phage titer and the percentage of
336 adsorbed phage was determined by spot titers and plaque assay of the serially diluted
337 supernatants collected from the samples of phage with and without the added cells. Since the
338 number of cells and phage used in these experiments was held constant, this procedure
339 consistently produced ~3.5-5.5 x 10^7 infectious centers. This procedure also resulted in
340 essentially zero unabsorbed phage in the culture at the start of the one-step assay. Burst size at

341 all time points could be directly determined by dividing the total phage in the 70ml culture by the
342 number of infectious centers. All phages were evaluated through a minimum of three separate
343 assays. A representative data set showing the raw data for adsorption, infections centers and a
344 one-step assay is provided in S3 Figure 2 and S4 Figure 3.

345 **RESULTS AND DISCUSSION**

346 **Topologies of Holin-like TMD Proteins Within the Lysis Cassettes of F1 Cluster Phages**
347 **Girr and NormanBulbieJr.**

348 To investigate the contribution of predicted holin-like proteins in the lysis of *M.*
349 *smegmatis*, it was desirable to begin work in phages that had a defined lysis cassette and prior
350 wet-lab data. F1 cluster phages Girr and NormanBulbieJr (NBJ) were selected since both
351 phages have a define lysis cassette and a full genome cytotoxicity screen has been reported for
352 both phages [70, 71]. Girr and NBJ have an average nucleotide identity of 89.86% but only
353 share 69 of 102 genes. Both phages have a defined lysis cassette organization located
354 downstream of the *tape measure* and *minor tail* genes and encode a Lysin A enzyme predicted
355 to target the peptidoglycan layer and a Lysin B that targets the linkage of the arabinogalactins to
356 the mycolic acids (Figure 1A). The *lysin B* gene is directly followed by two genes encoding
357 proteins that have predicted TMDs (Girr *34* and *35* and NBJ *32* and *33*).

358 It was first important to bioinformatically evaluate the predicted topologies of these TMD
359 proteins and determine how they compared to previously characterized holins or other phage
360 proteins involved in bacterial lysis. Girr *34* and NBJ *32* encode small 80aa and 77aa proteins,
361 respectively, that have two predicted TMD regions and an N-in-C-in topology by all TMD
362 prediction programs (Figure 1B). The proteins are 97% identical and have cytoplasmic N and C-
363 terminal domains that each contain four charged amino acids. The presence of two TMDs and
364 the N-in-C-in topology is like the phage 21 S^{21} type II pinholin (Figure 1BC). However, the
365 presence of a pinholin is typically associated with a SAR-endolysin that is secreted to the
366 periplasmic space prior to lysis triggering [10, 11, 13]. Analysis of the Girr or NBJ Lysin A

367 proteins by the various TMD prediction programs and AlpahFold3 (S5 Figure 4), show no
368 evidence of SAR domains or signal sequences and this is consistent with previous analysis of
369 Lysin A proteins from phages that infect *M. smegmatis* [21]. Thus, it is critical to contrast several
370 structural differences of gp32 and gp34 to the canonical $S^{21}68$ pinholin and $S^{21}71$ antiholin.
371 First, the $S^{21}68$ holin protein has only 3 N-terminal amino acids prior to the TMD1 and
372 this feature is a critical to its function as a holin and allows the TMD1 to become cytoplasmic
373 (Figure 1BC) [11-15]. Second, the S^{21} gene has a dual start motif that produces both the $S^{21}68$
374 holin protein and the $S^{21}71$ antiholin after phage infection [11-15]. The difference in the two
375 proteins is the addition of the extra basic K residue to the N-terminal cytoplasmic domain of
376 $S^{21}71$ that limits the TMD1 from exiting the membrane to the same degree as the $S^{21}68$ holin
377 (Figure 1BC; [11-15]). Thus, the expression of $S^{21}71$ keeps a percentage of the $S^{21}68$ in an
378 inactive dimer until triggering at which time the $S^{21}71$ converts to an active holin [13-15, 76, 77].
379 Third, the $S^{21}68_{IRS}$ protein is an engineered version of $S^{21}68$ that adds the MRYIRS motif and 4
380 charged residues in the N-terminal cytoplasmic domain that creates a dominant negative
381 version of the antiholin that is poorly triggered to an active holin [76]. Neither Girr gene *34* nor
382 NBJ gene *32* have a dual start motif that generates multiple products of the same open reading
383 frame. Genes *34* and *32* encode a single protein product that has a predicted N-terminal
384 cytoplasmic domain of 13-16 amino acids of which four are charged and two others are polar.
385 Therefore, the N-terminal topology and the number of charged amino acids in Girr gp34 and
386 NBJ gp32 are more similar with the $S^{21}71$ antiholin and $S^{21}68_{IRS}$ and would predict that TMD1 of
387 these proteins remains embedded in the membrane. In addition, the TMDs of S^{21} both contain
388 GxxxG motifs that are predicted to contribute to homotypic and/or heterotypic helix interactions
389 of the monomers that facilitate the formation of the pinholes [76, 77]. While TMD1 and TMD2 of
390 Girr and NBJ have a high percentage of GA residues (Figure 1B), they lack defined GxxxG
391 domains found in S^{21}. Finally, although AlphaFold3 does not model membrane proteins as well
392 as soluble proteins, Girr gp34 was not modeled with high confidence into either a monomer or a

393 heptamer compared to $S^{21}68$ (S6 Figure 5). Taken together, this data suggests that Girr gp34 or
394 NBJ gp32 are unlikely to function as a type II holin. Based on the literature we will designate
395 these proteins as LysF1a due to a predicted function in lysis (lys) and being first identified in F1
396 cluster phages.

397 Since there is a second gene encoding a protein with a single TMD directly downstream
398 of the *lysF1a* gene, we hypothesized that this protein may also be involved in the lysis pathway.
399 Girr *35* and NBJ *33* both have -4bp ATGA overlaps to the upstream *lysF1a* gene and encode
400 98% identical 124aa proteins with a single N-terminal TMD and a predicted N-out-C-in topology
401 by all TMD prediction programs (Figure 2A). Both proteins have a 22 amino acid extracellular
402 domain followed by the single TMD. There are four basic residues following the TMD and
403 AlphaFold3 predicts an extended helical cytoplasmic C-terminal domain that contains ~50%
404 KRDE charged residues typical of holins [10, 11]. Figure 3B shows the AlphaFold3 models and
405 predicted topologies of representative proteins with a single TMD that are implicated in phage-
406 mediated bacterial lysis compared gp33 and gp35. Most pertinent is the type IIIa holin typified
407 by the T protein of phage T4 that forms large 1um holes like canonical type I holins [16, 17] and
408 the recently identified type IIIb holin identified in jumbophage PhiKZ [78]. Neither type III holin
409 has >20% amino acid identity to gp33 and gp35, and both are much larger with the T having the
410 opposite membrane topology with a globular extracellular domain critical to its holin function
411 (Figure 2B). Although the PhiKZ holin has an extended cytoplasmic domain, the protein has a
412 C-out-N-in topology and also has a globular cytoplasmic domain. Nether have the highly
413 charged cytoplasmic regions found in the proteins, It noteworthy that spanins also have a single
414 TMD and model with an extended helical prediction, but like the T holin, these proteins are also
415 oriented in a N-in-C-out topology that has been shown experimentally and is also predicted by
416 the TMD prediction programs (Figure 2B; [10, 11]). Interestingly, there is a recent report
417 regarding phages that infect the Gram-positive *Corynebacterium glutamicum* strain. The authors
418 have characterized a protein with 1 TMD that is termed LysZ and is proposed to interact with

419 lipid-anchored glycans on the extracellular side of the IM to promote efficient lysis [59].
420 However, like the type IIIa holin, LysZ is much larger than the Girr and NBJ proteins and it is
421 proposed to have a N-in-C-out topology that allows it to interact with the lipid-anchored glycans
422 [59]. Thus, Girr gp35 and NBJ gp33 are most similar in structure and membrane topology to the
423 recently identified phage Mu releasin protein (Figure 2B) [19]. Releasin however, is named due
424 to its function to release the Mu SAR-endolysin from the membrane in a holin independent
425 manner [19]. Mu also has <20% amino acid identity to gp33 and gp35 and does not possess the
426 highly charged cytoplasmic domain. Thus, of all the characterized proteins involved in lysis that
427 have 1 TMD, gp35 and gp33 appear to represent a novel class of proteins and will be termed
428 LysF1b since the gene is downstream of the *lysF1a*.

429 **Deletion of Individual *lysF1a* and *lysF1b* Genes in F1 Phage are Viable and Results in**
430 **Reduced Plaque size**

431 To evaluate the function of the *lysF1a* and *lysF1b* genes, the BRED recombineering
432 method was utilized to delete them in both Girr and NBJ as described in Methods. Several
433 primary plaques were positive for each deletion and pure populations of Girr_*ΔlysF1a*,
434 Girr_*ΔlysF1b*, NBJ_*ΔlysF1a*, and NBJ_*ΔlysF1b* were recovered from secondary plaques. Figure
435 3 shows the lysis cassette organizations of the Girr mutants and the PCR verification of the
436 gene deletions from clonal high titer lysates. The data for NBJ is shown in S7 Figure 6 and
437 deletion of gene *33* is also presented in Wise et al. [71]. The genome structure of all deletions
438 was confirmed by sequencing the immediate region of the deletion and by whole genome
439 sequencing to validate that there were no point mutations outside of the targeted gene deletion
440 region.

441 To assess the phenotypes of the mutant phage, equal concentrations of Girr_WT,
442 Girr_*ΔlysF1a* and Girr_*ΔlysF1b* were used to infect *M. smegmatis* and the total number of
443 recovered plaques and plaque sizes evaluated. All phages formed plaques with equivalent

444 efficiencies under the standard assay conditions described in Methods suggesting no defects in
445 adsorption (S8 Figure 7). However, both Girr_Δ*lysF1a* and Girr_Δ*lysF1b* presented with
446 significantly smaller plaques than Girr_WT (Figure 4) as did NBJ_Δ*lysF1a* and NBJr_Δ*lysF1a*
447 (S9 Figure 8). A summary of the plaque size data for both Girr and NBJ is presented in Table 2.
448 Deletion of the *lysF1a* gene from Girr or NBJ results in ~40% reduction in plaque diameter and

449 **Table 2 Plaque sizes in WT Girr and *lysF1a* and *lysF1b* deletion mutants.**

PHAGE	Plaque size (mm)	% of WT (diam.)	Plaque (vol, mm^3)	% of WT (plaque vol)
NBJ_WT	3.49 +/- 0.533	100	11.479	100
NBJ_Δ*lysF1b*	1.23 +/- 0.225*	35.24*	1.425*	12.42*
NBJ_Δ*lysF1a*	2.05 +/- 0.660*	58.73*	3.96*	34.50*
Girr_WT	3.88 +/- 0.731	100	14.188	100
Girr_Δ*lysF1b*	1.28 +/- 0.376*	32.98*	1.544*	10.88*
Girr_Δ*lysF1a*	2.31 +/- 0.719*	59.53*	5.029*	35.44*

450

451 *M. smegmatis* was infected with identical numbers of phage and plaque size determined after
452 36 hrs. of growth at 37°C. Plaque diameter was measured using ImageJ. Data is presented as
453 average +/- standard deviation for a minimum of 50 individual plaques. * = statistically significant
454 from Girr or NBJ WT phage *p<0.0001.*
455

456 a 65% reduction in plaque volume, while deletion of the *lysF1b* is more severe showing a ~65%
457 reduction in plaque diameter and near 90% reduction in plaque volume. To validate that these
458 plaque size reductions were directly related to the loss of *lysF1a* or *lysF1b* genes, *M. smegmatis*
459 containing complementing expression plasmids were infected with the mutant phages and
460 plaque size evaluated as described in Methods. Since both Girr LysF1b and NBJ LysF1b are
461 highly toxic when exogenously expressed in *M. smegmatis* [70, 71], complementation of the
462 *lysF1b* deletions first utilized Waterfoul gp32. Waterfoul is a K5 cluster phage with a canonical
463 lysis cassette and gene *32* encodes a 1TMD with the same general size and membrane
464 topology as Girr LysF1b (Figure 2D) and is not toxic when induced by aTc in *M. smegmatis* [67].
465 When M. *smegmatis* transfected with Waterfoul gp32 is infected with Girr_Δ*lysF1b* in the

466 presence of aTc, there is a significant increase in plaque size compared to untreated cells
467 (Figure 5A). Importantly, the increase in plaque size was not observed when the N-terminal
468 TMD domain or the highly charged C-terminal 40 amino acids of Waterfoul gp32 were truncated
469 (Figure 5A). Thus, the complementation by Waterfoul gp32 requires the full-length protein.
470 Recently it has been reported that the pTet promoter in pExTra is leaky and that it is possible to
471 complete complementation analysis in the absence of aTc [71]. Thus, *M. smegmatis* was
472 transfected with pExTra-Girr*35* and pExTra-NBJ*33* and the resulting cells infected with
473 Girr_Δ*lys1b* as described in Methods. Figure 5B shows that there is a significant increase in
474 plaque size when Girr_Δ*lys1b* is plated on the complementing strains expressing the LysF1b
475 proteins compared to cells with the base pExTra01 vector. These results support that the
476 reduced plaque size of Girr_*ΔlysF1b* is directly attributable to the loss of *lysF1b.* Similarly, the
477 wild type plaque size is restored when *M. smegmatis* harboring the pExTra-Girr_*34* plasmid is
478 infected with Girr_*ΔlysF1a* (Figure 6). Thus, the loss of either *lysF1* gene appears to create a
479 lysis defect phenotype that is like the phenotype when the *lysin B* is deleted in phage Giles and
480 the cell wall components remain a barrier to efficient phage release [28].

481 **Deletion of Individual *lysF1* Genes Result in Distinct *M. smegmatis* Liquid Lysis**
482 **Phenotypes and ATP Release.**

483 A main function of holins is the control of the lysis timing by the destruction of the proton
484 motive force (PMF) [10, 11]. To assess lysis timing of Girr, NBJ and the *lysF1* mutants, liquid
485 lysis assays were performed where the optical density (OD_{600}) of infected log growth *M.*
486 *smegmatis* cultures is measured over time. Importantly, in all studies, once phage had been
487 allowed to absorb for 30 minutes, cultures were continually shaken even while samples were
488 withdrawn so that lysis would not be prematurely triggered by changing the culture conditions
489 [11, 79]. The data show that cultures infected with Girr_WT grow steadily until ~110 minutes
490 post infection. Beginning at 110 minutes, there is a significant drop in the OD_{600} of the culture

491 (triggering event) until it reaches a baseline of OD_{600} 0.10 at about 200 minutes (Figure 7A). In
492 contrast, Girr_*ΔlysF1a* grows until ~130 minutes and then shows a reduction in OD_{600} until 300
493 minutes that does not reach the same OD_{600} baseline as Girr_WT even after 480 minutes of
494 incubation (Figure 7A). Strikingly, cultures infected with Girr_*ΔlysF1b* do not show a drop in
495 OD_{600} but appear to cease growing after ~200 minutes with only a slight decrease in OD_{600} over
496 the remaining growth period out to 480 minutes (Figure 7A). For NBJ_WT, OD_{600} begins to drop
497 after 130 minutes and like Girr_WT reaches a baseline of around OD_{600} 0.10 (Figure 7B).
498 NBJ_*ΔlysF1a* shows a delay in lysis timing like Girr_*ΔlysF1a*, but the delay is more pronounced
499 as the OD_{600} does not begin to drop until ~180 minutes post infection (Figure 9B). Just like
500 Girr_*ΔlysF1b*, NBJ_*ΔlysF1b* ceases to grow after ~200 minutes and does not show a significant
501 reduction in OD_{600} even after 480 minutes of growth (Figure 7B). Thus, in both phages, deletion
502 of *lysF1a* results in a triggering delay while deletion of *lysF1b* results in no defined triggering
503 event in this assay. It is interesting that Girr_WT and NBJ_WT show a ~20-minute difference in
504 triggering time and that a difference is also observed between Girr_*ΔlysF1a* and NBJ_*ΔlysF1a.*
505 These results may be due to differences in how the lysis cassette genes are expressed since
506 Girr has an HNH endonuclease gene between the *lysin A* and *lysin B* (Figure 1A) and the
507 intergenic region between the *lysin B* gene and the *lysF1a* is 8bp in NBJ but 38bp in Girr (S10
508 Figure 9).
509 ATP release has been used as a measure of cell viability and membrane integrity
510 following phage infection [27, 53]. Figure 7C shows the ATP release from the same experiment
511 that is presented in Figure 7AB. As expected, ATP release for Girr_WT, NBJ_WT, Girr_*ΔlysF1a*
512 and NBJ_*ΔlysF1a* generally mirrors the time at which lysis is triggered and the culture OD_{600}
513 begin to decline. ATP levels in the media also peak when the OD_{600} baseline is reached at about
514 300 minutes (Figure 7C). In contrast, there is delayed but gradual increase in the amount of
515 ATP released from the cultures infected with Girr_*ΔlysF1b* and NBJ_*ΔlysF1b* out to 300

516 minutes. Although the ATP level does not reach that of Girr_WT or NBJ_WT, the release of ATP
517 confirms that cell integrity has been comprised after infection with the *lysF1b* mutants. To
518 directly assess this contention, aliquots of the cultures were removed at 100- and 260-minutes
519 post infection, serial diluted and plated on 7H10 agar to assess colony growth as detailed in
520 Methods. Both Girr and NBJ are temperate phages, thus, it was expected that the infected
521 cultures would show a small percentage of surviving lysogens as reported in Wise et. al. 2025.
522 A representative data set with NBJ is shown in S11 Figure 10. Girr showed similar results. Cells
523 infected with NBJ_WT or NBJ_Δ*lysF1b* show >90% reduced colonies 100-minutes post
524 infection when compared to the uninfected culture that was essentially at the same OD_{600}. When
525 the cultures were reevaluated at 260-minutes post infection, the colony counts for both NBJ_WT
526 and NBJ_Δ*lysF1b* show a slight 1.4-fold rise due to lysogeny growth, but are still 90% reduced
527 in viable cells compared to the number at the start of the experiment. The lytic phage D29 kills
528 all cells in the culture, validating that the surviving cells are not the result of infection resistant
529 cells or contamination. Thus, this data clearly supports the hypothesis that the lack of a defined
530 OD_{600} decline in the Δ*lysF1b* infected cells is due to inefficient lysis and not due to having more
531 viable cells than those infected with Girr_WT.
532 Collectively, the important finding from this data set is that an F1 phage with only the
533 1TMD LysF1b protein can trigger the lysis event in the absence of the 2TMD lysF1a protein, but
534 that the lysF1a protein does not support significant bacterial lysis as measured by a drop in
535 OD_{600}. The lack of OD_{600} decline is not due to there being a high population of viable cells,
536 although there is a small percentage (<10% of the starting cell population) of surviving lysogens.
537 In fact, the liquid lysis results for Girr_Δ*lysF1b* and NBJ_Δ*lysF1b* is like the lethal *lysin A*
538 deletion in phage Giles where the cultures stopped growing after infection and the OD_{600} gently
539 rose and then plateaued but did not show a sharp triggering decline up through 360-minutes
540 post infection [28]. The similarity in these results suggest that the lysis defects in the Δ*lysF1b*

541 phage may be related to the inability of the endolysins to efficiently cleave the cell wall
542 components because they are either not efficiently released from the infected cell or are
543 exported but cannot be released from the membrane or activated in some manner.

544 **Energy Poisons Cause Early Triggering of F 1Cluster Phages with Deletion of the *lysF1a***
545 **Gene but not the *lysF1b* Gene in Liquid Lysis Assays**

546 The results presented so far indicate that the expression of both TMD proteins are
547 required for phage viability, but phages that express only the LysF1b protein can support
548 bacterial lysis while phages that express only LysF1a are viable but severely lysis
549 compromised. The diagnostic assay for holin function is the ability to cause early triggering of an
550 infected culture by the addition of energy poisons (e.g., cyanide or the protonophore
551 dinitrophenol) due to the disruption of the proton motive force (PMF) [11, 79]. This type of assay
552 has been utilized in nearly all the pioneering work on holin function of phages that infect *E. coli.*
553 [10, 11, 19] and both Girr_WT and NBJ_WT can be triggered early if infected cells are treated
554 with CN (S12 Figure 11). To assess the effect of CN on the various mutants, *M. smegmatis* was
555 infected with Girr_WT or Girr_*ΔlysF1a* and the OD_{600} of the culture measured as described in
556 Methods. At 110 minutes after infection, KCN (final concentration of 10mM) was added directly
557 to one culture of Girr_*ΔlysF1a* and to a culture of uninfected cells. Figure 8A shows that
558 Girr_WT triggers at ~110 minutes while Girr_*ΔlysF1a* triggers at 130 minutes just as in Figure
559 9A. However, when KCN is added to a culture infected with Girr_*ΔlysF1a*, there is a drop in
560 OD_{600} beginning at ~120 minutes that clearly precedes the drop in the untreated Girr_*ΔlysF1a*
561 culture. KCN addition to uninfected cells results in immediate cessation of growth, but not a
562 significant drop in OD_{600}.To validate these results, studies were repeated with the NBJ mutants.
563 NBJ_WT triggers later than Girr_WT at ~130 minutes and declines to OD_{600} 0.10 by 300
564 minutes as expected (Figure 10B). NBJ_*ΔlysF1a* shows delayed triggering just as in Figure 8B
565 and addition of KCN to a culture infected with NBJ_*ΔlysF1a* at 120 minutes results in lysis

566 triggering by 130 minutes with a gradual reduction in OD_{600} that mirrors the NBJ_WT. The ability
567 of Girr_*ΔlysF1a* and NBJ_*ΔlysF1a* to trigger lysis, identifies the 1TMD LysF1b protein as a
568 putative holin and not a releasin, since energy poisons do not trigger lysis prematurely in phage
569 Mu [19].

570 The next set of studies focused on the phages with deletion of the 1TMD *lysF1b* genes
571 to determine if they could also be triggered by the addition of KCN. Figure 8C shows the results
572 for Girr_*ΔlysF1b*. As previously shown in Figure 8A, *M. smegmatis* infected with Girr_*ΔlysF1b*
573 does not exhibit a defined triggering event as the cells simply cease growing with a slight
574 reduction in OD_{600} out to 480 minutes. Addition of KCN to the Girr_*ΔlysF1b* culture at 180
575 minutes results in a modest 30% reduction of OD_{600} between 180-240 minutes compared to the
576 Girr_*ΔlysF1b* untreated culture. However, following this initial decline, the level of change in
577 OD_{600} generally mirrors that of the untreated Girr_*ΔlysF1b* culture and the KCN treated *M.*
578 *smegmatis* control. In contrast, addition of 1% $CHCl_3$ to the Girr_*ΔlysF1b* culture at 180 minutes,
579 results in an immediate precipitous drop in OD_{600} to the level of Girr_WT indicating that the
580 endolysin enzymes are present and active in the cells. The results for NBL_*ΔlysF1b* are shown
581 in Figure 8D and exhibit near identical results to Girr_*ΔlysF1b* in that addition of KCN cause a
582 modest drop during the first hour after addition, and then an OD_{600} decline that mirrors the
583 untreated NBJ_Δ*lysF1b* culture and the KCN treated *M smegmatis*. Addition of $CHCl_3$ results in
584 the same type of sharp decline in OD_{600} to the level of the NBJ_WT baseline. Collectively, these
585 results show that phages expressing only the 2TMD LysF1a protein are not efficiently triggered
586 following disruption of the PMF but that the cells have the requisite enzymes for lysis since lysis
587 occurs immediately after addition of 1% $CHCl_3$. The inability of the LysF1a proteins to be
588 triggered by KCN is like the $S^{21}71$ or $S^{21}68_{IRS}$ antiholins [13, 76, 77].

589 **F1 Cluster Phage Deleted for *lysF1a* have Delayed Burst Timing While Phage Deleted for**
590 ***lysF1b* Deletion have Reduced Timing and Greatly Reduced Burst Size**

591 The previous results show that infection of *M. smegmatis* with either Girr_*ΔlysF1a* or
592 NBJ_*ΔlysF1a* results in a defined triggering (lysis) event that can be prematurely initiated by
593 addition of KCN. However, the results do not establish if phage have been efficiently released
594 from the lysed cells, the timing of the burst event and the burst size. Since it is not possible to
595 utilize lysogens to study phage release in *M. smegmatis*, one-step grow curves were utilized to
596 evaluate the various *lysF1a* and *lysF1b* mutant phages. The experimental set up for these
597 studies is fully described in the methods and representative raw data sets are also shown in S3
598 Figure 2 and S4 Figure 3. The one-step results from three different experiments utilizing Girr
599 phages are presented in Figure 9. Phage release from Girr_WT shows a lag time of ~180
600 minutes from the time of infection and then a gradual phage release for 90 minutes before
601 reaching a plateau at ~300 minutes (Figure 9A). The slow release of phage over a 90-minute
602 period is consistent with the liquid lysis assays that showed an ~60-minute timeline of OD_{600}
603 decline after triggering. This is an important observation because there should not be a sharp,
604 immediate lysis of all cells and accompanying phage release since the phage infections are not
605 synchronized but carried out over a 30-minute period and the efficient release of phage from
606 Gram-positive bacteria may also be hampered by the extensive cell wall. Girr_*ΔlysF1a* shows a
607 delayed lag time by ~20 minutes compared to Girr_WT and a more prolonged period of phage
608 release over 150 minutes before reaching a plateau. The overall burst size for Girr_WT over
609 three experiments was 277 +/- 81 PFU/cell. Girr_*ΔlysF1a* showed a lower burst of 255 +/- 75
610 PFU/cell but this was not statistically different from the for Girr_WT. In contrast, Girr_*ΔlysF1b*
611 shows a very small but defined burst at ~ 210 minutes that is best illustrated when the data is
612 plotted independent of the other phages (Figure 9B). The overall burst size for Girr_*ΔlysF1b* is
613 only ~29.2 +/- 36 PFU/cell suggesting very poor efficiency of phage release from the infected
614 cells. Overall, this data is consistent with the plaque size and liquid lysis results and supports
615 the hypothesis that *M. smegmatis* integrity is compromised when infected with Girr_*ΔlysF1b* but

616 the release of phage progeny is severely impacted. In addition, the near wild type burst size
617 observed in cells infected with Girr_*ΔlysF1a*, further support the holin function of the LysF1b
618 protein.

619 **Deletion of both *lysF1a* and *lysF1b* is not Lethal to Phage Viability and Shows Similar**
620 **Phenotypes to the Δ*lysF1b* Mutants**

621 Since deletion of either of the individual TMD genes resulted in viable phage, it was of
622 interest to test whether a double deletion of both TMD genes was viable. Both Girr and NBJ
623 were used for these studies and the NBJ data set is shown in Figure 10. BRED was utilized was
624 utilized to delete *lysF1b* from NBJ_*ΔlysF1a* DNA. Figure 11A/B shows the genomic context of
625 the double deletion and the PCR confirmation that both *lysF1a* and *lysF1b* is deleted. The
626 deletion was confirmed by Sanger sequencing of the deleted region and full genome
627 sequencing confirmed that there we no additional nucleotide changes to the genome. A viable
628 double deletion of *lysF1a* and *lysF1b* was also produced in phage Girr that showed identical
629 results to NBJ. Interestingly, while NBJ_*ΔlysF1a/ΔlysF1b* had dramatically reduced plaque size
630 compared to the NBJ_WT phage, the plaques were essentially the same size as the single
631 mutation NBJ_*ΔlysF1b* phage (Figure 10C). Liquid lysis data in Figure 10D show that NBJ_WT
632 triggers lysis as expected at ~130-140-minutes while NBJ_*ΔlysF1b* and the
633 NBJ_*ΔlysF1a/ΔlysF1b* phage causes reduced culture growth but no defined triggering.
634 Importantly, the addition of KCN was able to prematurely trigger the NBJ_WT but did not trigger
635 the NBJ_*ΔlysF1b* or trigger NBJ_*ΔlysF1a/ΔlysF1b.* The finding that the double deletion of
636 *lysF1a* and *lysF1b* is viable and has essentially the same phenotypes as the NBJ_*ΔlysF1b*,
637 support the hypothesis that the LysF1a protein does not contribute to lysis in the absence of
638 LysF1b. These findings also suggest that the F1 phage encoded lysins can be released from
639 the cell independent of LysF1a and LysF1b proteins as suggested for Mycobacteriophage D29
640 and others [21, 30-32],

641 **Lysis Recovery Mutants Isolated from Girr_*ΔlysF1b* or NBJ_*ΔlysF1b* Show Wild Type**

642 **Plaque Size and have Point Mutations in the *lysF1a* Gene**

643 Since both Girr_*ΔlysF1b* and NBJ_*ΔlysF1b* show significant plaque size defects it was

644 possible to screen for lysis recovery mutants (LRM) by assessing changes to the small plaque

645 size following multiple rounds of infection and replication. Figure 11A shows the presence of a

646 large plaque in a Girr_*ΔlysF1b* plaque assay after the second round of harvest and infection.

647 **Table 3. Lysis Recovery Mutants (LRM) from Δ*lysF1b* Phages.**

Phage	Type of mutation	Genetic location	Mutation Result
Girr_Δ*lysF1b*-LRM1	point mutation-nucleotide substitution	gene *35 (lysF1a)*	G66D
Girr_Δ*lysF1b*-LRM2	point mutation-nucleotide substitution	gene *35 (lysF1a)*	R19H
Girr_Δ*lysF1b*-LRM6	point mutation-nucleotide deletion	gene *35 (lysF1a)*	missense coding after A63 and premature stop at aa74: A63APRQPRNGFGD.STOP
Girr_Δ*lysF1b*-LRM7	point mutation-nucleotide substitution	gene *35 (lysF1a)*	G66D
Girr_Δ*lysF1b*-LRM8	point mutation-nucleotide insertion	gene *35 (lysF1a)*	stop after G66
Girr_Δ*lysF1b*-LRM11	point mutation-nucleotide insertion	gene *35 (lysF1a)*	stop after G66
Girr_Δ*lysF1b*-LRM12	point mutation-nucleotide insertion	gene *35 (lysF1a)*	stop after G66
Girr_Δ*lysF1b*-LRM14	point mutation-nucleotide substitution	gene *35 (lysF1a)*	G66D
Girr_Δ*lysF1b*-LRM15	point mutation-nucleotide insertion	gene *35 (lysF1a)*	stop after G66
Girr_Δ*lysF1b*-LRM16	point mutation-nucleotide substitution	gene *35 (lysF1a)*	A31T
NBJ_Δ*lysF1b*-LRM1	point mutation-nucleotide substitution	gene *33* (*lysF1a*)	A68E
NBJ_Δ*lysF1b*-LRM2	point mutation-nucleotide substitution	gene *33* (*lysF1a*)	A68E
NBJ_Δ*lysF1b*-LRM3	point mutation-nucleotide substitution	gene *33* (*lysF1a*)	A68E

NBJ_Δ*lysF1b*-LRM7	point mutation-nucleotide substitution	gene *33* (*lysF1a*)	D9A

648

649 When phages were recovered from the large plaque, serial diluted and replated, the wild type
650 plaque size was recovered across the full phage population (Figure 11B). This type of
651 experiment was repeated multiple times with Girr_Δ*lysF1b* and NBJ_Δ*lysF1b* and ten
652 independent Girr_Δ*lysF1b*-LRMs and four independent NBJ_Δ*lysF1b*-LRMs were recovered. All
653 Girr LRM mutants showed a large plaque phenotype compared to the parent Girr_Δ*lysF1b* (S13
654 Figure 12) and PCR analysis of the *lysF1a*-*lysF1b* genomic region confirmed that all the LRM
655 mutants contained the expected Δ*lysF1b* deletion (S13 Figure 12). To determine the location of
656 any nucleotide mutations within the genome of the LRM mutants, DNA was extracted and the
657 genomes were sequenced as detailed in Methods. In all cases, the Girr_Δ*lysF1b*-LRMs and
658 NBJ_Δ*lysF1b*-LRMs contained the expected *lysF1b* deletion but all phage also contained either
659 nucleotide insertions, deletions or substitutions within the *lysF1a* open reading frame that
660 altered the amino acid sequence of the LysF1a protein. A summary of all LRM mutants is
661 provided in Table 3 and a schematic showing the amino acid changes to the different
662 Girr_lysF1a-LRMs is presented in S14 Figure 13.

663 Six different mutations were identified in the ten Girr_Δ*lysF1b*-LRMs and two in the four
664 NBJ_Δ*lysF1b*-LRMs.The mutations mapped to three different domains of the LysF1a protein:
665 the N-terminal cytoplasmic domain, the first TMD or the beginning of the cytoplasmic C-terminal
666 domain. No mutants were recovered that impacted the second TMD or distal regions of the
667 cytoplasmic C-terminal domain. In the Girr LRM mutants, two different missense mutations were
668 found in TMD1 of LysF1a that result in R19H and A31T while one of the NBL LRM mutants
669 changed the charged cytoplasmic D9 to A. In addition, three G66D mutants were recovered in
670 the Girr LRMs, and three A68E mutants were recovered in the NBJ LRMs. All of these change a
671 small hydrophobic amino acid to a negatively charged amino acid just after the end of the TMD2

672 at the beginning of the cytoplasmic C-terminal domain. Finally, four mutants generate a
673 nonsense mutation that either truncates the Girr LysF1a protein after G66 or create a frame shift
674 after A63 that results in missense coding and a premature stop after amino acid 73. All LRM
675 mutations result in changes to the LyF1a protein that likely alter its conformation, thus, the
676 findings support that the LysF1a protein can in fact efficiently function in the lysis pathway and
677 that the protein does not exclusively function as an antiholin to the LysF1b as suggest earlier.
678 Importantly, plaques were also evaluated for LRM mutants after multiple rounds of plating of the
679 *ΔlysF1a/ΔlysF1b* double mutants, but even after six rounds of infection and plating, we failed to
680 identify any changes to plaque sizes, and this suggests that there are no other negative
681 regulators (putative antiholins) of the lysis pathway in these phages.

682 **Lysis Recovery Mutants Exhibit Early Lysis and Reduced Burst Size**

683 Since the LRMs generate a wild type plaque size (Figure 11A; S13 Figure 12), it was
684 pertinent to evaluate the lysis timing in liquid culture and determine lag time and burst size. *M.*
685 *smegmatis* was infected with Girr_WT, Girr_*ΔlysF1b* and three different Girr_*ΔlysF1b*-LRMs and
686 the OD_{600} of the culture measured as described in Methods. Figure 12A shows that Girr_WT
687 triggers lysis as expected at ~110-minutes while Girr_*ΔlysF1b* causes reduced culture growth
688 but no defined triggering as also shown in Figures 8 and 9. In stark contrast, Girr_*ΔlysF1b*-
689 LRM1, Girr_*ΔlysF1b*-LRM2 and Girr_*ΔlysF1b*-LRM16, all trigger lysis prematurely at ~90
690 minutes and ultimately reduce the OD_{600} to the same baseline as Girr_WT. When NBJ_WT,
691 NBJ_*ΔlysF1b*, NBJ_*ΔlysF1b*-LRM1 and NBJ_*ΔlysF1b*-LRM7 were tested in the liquid lysis
692 assay, the NBJ-LRMs also trigger lysis prematurely and reduce the OD_{600} to the same level as
693 NBJ_WT (Figure 11B). To validate the early triggering time and assess its impact on burst size,
694 one-step growth curves were completed as described in Methods. Figure 12C shows a
695 representative one-step experiment with Girr_WT and two LRM mutants. Phage release from
696 Girr_*ΔlysF1b*-LRM1 and Girr_Girr_*ΔlysF1b*-LRM2 is detected by 150 minutes and plateaus by

697 200-minutes, a time point at which Girr_WT has achieved <10% burst size. The two Girr LMRs
698 average burst size is also only 95.5 +/- 12.5 PFU/cell compared to 289.6 +/- 65 PFU/cell for the
699 Girr_WT. The reduced burst size is likely the result of lysis triggering well before all phage
700 progeny have been full assembled and is consistent with reports that have evaluated early
701 triggering in *E. coli* phages [11, 12, 76]. The current results also indicate that plaque size in our
702 experimental system is not a function of burst size since a >65% reduction in burst size is still
703 able to generate wild type-sized plaques (Figure 12A; S13 Figure 12). These findings add
704 further support to the hypothesis that the small plaque phenotypes of the various LysF1 mutants
705 is the result of inefficient cell wall lysis that hampers phage release.

706 **Analysis of *lysF1b* Phage Plaque Sizes in *M. smegmatis* Lacking the Lipoarabinomannan**
707 **Layer of the Cell Wall**

708 A recent study proposes a 1TMD protein termed LysZ may function as a spanin-like
709 protein to disrupt the integrity of the Gram-positive *Corynebacterium glutamicum* cell wall by
710 interacting with the lipoarabinomannan (LAM) layer [59]. In these studies, deletion of *lysZ* from
711 phages CL31 or Cog results in a small plaque phenotype that is rescued if phage were plated
712 on a *Corynebacterium glutamicum* strain that is defective in the synthesis the LAM. Since both
713 LysZ and LysF1b have a single TMD and deletion of the genes results in small plaques, it was
714 pertinent to determine whether an *M. smegmatis* strain lacking the mtpA enzyme required to
715 synthesize LAM (*M. smegmatis* ∆mtpA) [68], would complement the small plaque phenotype of
716 Girr_∆*lysF1b*. Wild type *M. smegmatis*, *M. smegmatis* ∆mtpA, and *M. smegmatis* ∆mtpA-comp
717 (∆mtpA carrying complementing mtpA expression plasmid), were grown to saturation and set to
718 OD_{600} of 2.0 prior to infection. Equal amounts of phage were used to infect and cells and
719 plaques evaluated after incubation for 48 hrs. at 37°C. Figure 13A shows that both wild type Girr
720 and Girr_∆*lysF1b* exhibit a modest but significant increase in plaque size when infected into the
721 *M. smegmatis* ∆mtpA strain compared to the wild type *M. smegmatis* or the *M. smegmatis*

722 ΔmtpA-comp strain. Girr_WT plaques increased by 1.4-fold from 2.8mm to 3.9mm while
723 Girr_Δ*lysF1b* increased by 1.8-fold from 0.93mm to 1.7mm (Figure 13B). To account for the
724 possibility that the change is plaque size were caused by reduced cell growth and less *M.*
725 *smegmatis* ΔmtpA bacteria growing over the courses of the experiment, studies were repeated
726 using high density cultures at 2 x 10^8 CFU/infection. This level of bacteria will exacerbate small
727 plaque phenotypes since the increased cells enhance absorption and reduce phage diffusion
728 [28; 84-86]. In these studies, both Girr_WT and Girr_Δ*lysF1b* showed similar plaques size
729 increases as the low-density experiments verifying that *M. smegmatis* lacking a formal LAM
730 layer is generally less restrictive to lysis and phage release. Since both Girr_WT and
731 Girr_Δ*lysF1b* show increased plaque size and the plaques of Girr_Δ*lysF1b* do not reach
732 Girr_WT size, the results indicate that the lack of the LAM layer does not effectively complement
733 the deletion of *lyF1b*. This is consistent with the proposed holin function of the LysF1b and
734 supports the hypothesis that the LysF1b and LysZ proteins have distinct functions in the lysis
735 pathway in their respective bacterial hosts although holin function for LysZ has not been
736 formally evaluated.

737 **Analysis of Additional Genes Proposed to be Involved in the Lysis Pathway of F1 Cluster**
738 **Phages**

739 It is currently unknown how the various endolysins encoded by actinobacteriophages
740 gain access to the peptidoglycan layer following phage infection. Although exogenous
741 expression of the lysin A from some phages is cytotoxic to *M. smegmatis*, there is no evidence
742 of signal sequences or SAR domains in these proteins [21, 30--34]. However, *Mycobacterium*
743 *sp.* appear to have several different secretion systems that do not require a signal sequence
744 [80-83]. Additionally, it has been proposed that phage Ms6 encodes a small chaperone protein
745 (gp23) required for the export of Lysin A because the deletion of the gene results in a small
746 plaque phenotype [50, 52]. Since both phage Girr and NBJ encode a homolog to gp23 in the

747 same general genomic area upstream of the Lysin A (gene *29*; Figure 14A), it was of interest to
748 determine if deletion caused a lysis defect in Girr and NBJ. Figure 14D shows that Girr gp29 is
749 73 amino acids and shares 76.2% identity to Ms6 gp23 while NBJ gp29 shares 76 of 77 amino
750 acids with gp23. BRED was utilized to delete gene *29* from Girr and two independent Girr_Δ*29*
751 phage mutants were isolated (Figure 14B). Girr_Δ*29-20* and Girr__Δ*29-25* showed no lysis
752 defect when compared to Girr_WT in the liquid lysis assay (Figure 15C) and showed identical
753 plaque size to Girr_WT (Figure 14E). BRED deletion of NBJ *29* (NBJ_Δ*29*) also showed wild
754 type plaque size (Figure 14E) and no difference in liquid lysis when compared to NBJ_WT.
755 To explore the possible interaction of the Lysin A and gp29 further, the proteins were
756 modeled using AlphaFold3. The results presented in S15 Figure 14 to S17 Figure 16 show that
757 all models produced data with ipTM values <0.4 indicating a very low confidence in the
758 interactions of the soluble Lysin A and gp29 proteins. Thus, these results suggest that gp29
759 from phage Girr or NBJ is not involved in the lysis pathway. A plausible explanation for the lysis
760 defects observed in the Ms6 studies is that the method of deletion of gene *23* somehow
761 impacted the expression of Lysin A (gene *24*) to generate a lysis phenotype. Full genome
762 sequencing data of the Ms6 mutants was not presented or discussed [50, 52] and the
763 requirement of a phage encoded chaperone has not been identified in any other phage.

764 **IMPLICATIONS AND FUTURE DIRECTIONS**

765 The results presented in this report identify the novel LysF1a and LysF1b proteins as
766 holin-like components required for efficient lysis of *M. smegmatis* by F1 cluster phages. The
767 data support that LysF1a and LysF1b function together to time the lysis event and disrupt the
768 PMF, however, it appears that LysF1a requires the presence of the LysF1b protein to be active
769 as a putative holin. Holin function is based on several key findings. First, holin function for the
770 LysF1b protein is directly demonstrated by the ability of energy poisons to trigger premature
771 lysis in phages that do not express LysF1a (Figure 10). While it could be argued that the energy

772 poison might trigger lysis by releasing a lysin that was previously exported and tethered to the
773 outer membrane, this hypothesis is not supported by the fact that CN treatment does not trigger
774 lysis in the Δ*lysF1*a/Δ*lysF1b* double mutant. Second, holin function is supported for LysF1b
775 instead of releasin function because there is no defined SAR-endolysins in F1 cluster phages
776 and the energy poisons do not trigger early lysis by releasin in phage Mu [18]. Finally, holin
777 function is supported for LysF1a by the ability to recover LRM mutants in the Δ*lysF1b*
778 background of both Girr and NBJ that map to the LysF1a protein and create phage that trigger
779 lysis early but otherwise are fully lysis competent (Figure 12).
780 The 1TMD LysF1b proteins represent a new class of holins and appear to be found
781 predominantly in phages that infect Gram positive hosts. HHpred analysis shows that the
782 LysF1b proteins have a high probability hit to Pfam PF10874 (DUF2746) that contains 906
783 proteins. Within this Pfam are hits to phages that infect *Mycobacterium sp, Gordonia sp,* and
784 *Streptomyces sp* and hits to *Micromonospora sp, Rothia sp, Saccharothrix sp, Nocardia*
785 *terpenica, Propionicmonas paludicola, Microbacterium talmoniae, Xylanimonas oleitrophica and*
786 *Actinacidiphilia glaucinigra* where the later hits are likely to proteins that are encoded by
787 prophages within the host bacteria. To assess whether additional phages in the
788 Actinobacteriophage Database at PhagesDB.org express a LysF1b-like homolog [87], phages
789 infecting *M. smegmatis* were bioinformatically evaluated as described in Methods to identify the
790 lysis cassette and associated genes that encode proteins with 1TMD and 2TMD in the same
791 cassette. Of the ~2,600 phages in the database that infect *M. smegmatis*, ~50% (from 22 of the
792 32 clusters) encode a LysF1b-like protein with a predicted N-out-C-in membrane topology and
793 also have an associated gene encoding a protein with N-in-C-in 2TMD in a defined lysis
794 cassette (S18 Figure 17, S19 Figure 18). Of the remaining 50% of annotated *M. smegmatis*
795 phages, 30% encode a LysF1b-like homolog but do not have an associated gene that encodes
796 a 2TMD protein, but instead have a gene encoding a protein with 4TMD. Thus, ~80% of the

797 phages that infect *M. smegmatis* have a LysF1b homolog with the predicted N-out-C-in
798 topology. These lysF1a-like proteins are grouped to 20 different phams based on their amino
799 acid identity [88, 89]. Representative LysF1a-like proteins from each pham are presented in S20
800 Figure 19. The proteins differ in size from 92-150 amino acids, have several basic amino acids
801 after the TMD as highlighted in Figure 2 and have between 30%-50% DEKRH charged amino
802 acids in the C-terminal cytoplasmic domain (S20 Figure 19). Multiple sequence alignment
803 indicates minimal amino acid identity between the proteins (S21 Figure 20) and the alignment
804 also failed to identify any domains of high identity. Thus, while ~80% of the phages that infect
805 *M. smegmatis* in the PhagesDB.org database express a LysF1b-like protein, it is unclear
806 whether they all function like the LysF1b proteins from Girr and NBJ.
807 Since the F1 phages evaluated in this study can clearly perform lysis independent of the
808 LysF1a, and the double deletion of both *lysF1a* and *lysF1b* has the same phenotype as the
809 Δ*lysF1b*, what then is the function of the 2TMD LysF1a proteins in the lysis pathway? As
810 discussed throughout this report, a role of LysF1a as a type II pinholin is not supported by the
811 sequence data (Figure 1BC). In fact, the amino acid sequence data and lack of lysis function in
812 the absence of LysF1b, better supports LysF1a as an pure antiholin like P2 phage LysA [55,56].
813 However, deletion of the *lysF1a* gene results in a lysis triggering *delay* in both Girr_Δ*lysF1b* and
814 NBJ_ Δ*lysF1b* with the later delayed over 60 minutes compared to NBJ_WT (Figure 8). A lysis
815 delay is not consistent with the function of LysF1a as a pure antiholin to the LysF1b, since it
816 would be expected that deletion of the antiholin would result in *early* host lysis by Girr_Δ*lysF1a*
817 or Girr_Δ*lysF1a* since the LysF1b would not be inhibited from forming active multimers as
818 shown for lambda S_{105} and phage 21 $S^{21}68$ [10-12]. In this context, the key findings are 1) that
819 destabilization of the PMF alone is not sufficient to “activate” LysF1a into a lesion that supports
820 wild type lysis or phage release (Figure 8), and 2) that LRMs can be recovered in the Δ*lysF1b*
821 background that have point mutations LysF1a that result in a fully lysis competent LysF1a

822 protein that happens to trigger premature (i.e. unregulated) lysis (Figure 12). These findings
823 suggest that amino acid changes to the protein may induce conformational changes to the
824 LysF1a that allow it to fully support bacterial lysis and phage release in the absence of the
825 LysF1b. Thus, an attractive working model is that LysF1a is not an antiholin to LysF1b but
826 simply is not lysis active without LysF1b. Therefore, as expression of both proteins increases
827 following infection, they reach a concentration at which they can formally interact, and this
828 interaction facilitates conformational changes in the LysF1a that allow it to become active in
829 lysis. The two proteins then function together to facilitate the release of endolysins and/or phage
830 particles. Such a model would be like the holin/antiholin system in phage lambda and phage 21
831 where the phages express both active holins and inactive antiholins and triggering results in an
832 instantaneous conversion of all proteins to active holins [10-12].
833 Currently, it is unclear how the LysF1a and LysF1b proteins interact and whether both
834 proteins together actively participate in the creation a heteromeric lesion in the inner membrane.
835 Clearly, LysF1b alone can trigger lysis and initiate the process of phage release, but as stated
836 above, lysis timing and the efficiency of phage release are still not optimal. Phage SSP1
837 appears to have two distinct holins that support lysis when expressed exogenously, but it has
838 not been formally demonstrated that they both form a heteromeric lesion [40]. In addition, the
839 lysis pathway of phage P2 utilizes two distinct proteins, holin Y and antiholin LysA, but LysA
840 protein appears to be fully regulatory to holin Y and is not converted into an active holin like the
841 antiholins S_{107} or $S^{21}71$ [11, 57, 58]. Thus, the interaction of two distinct holin monomers that
842 have different membrane topologies will require direct study of LysF1a and LysF1b proteins
843 within membranes to resolve the structure. Such work could also directly address whether the
844 LysF1b also has interactions with cell wall components to facilitate phage release as suggested
845 for the LysZ proteins of *Corynebacterium* phages [59]. Whether the other Mycobacteriophages
846 that express different variants of the LysF1a and LysF1b proteins also utilize them in the same
847 way as Girr and NBJ will require additional deletion and complementation studies. The current

848 study therefore provides a framework to evaluate lysis under physiological conditions in Gram-
849 positive hosts. It is exciting to speculate that due to the presence of *lysF1*-like and *lysZ*-like
850 genes in so many phages, it may be that the phages that infect Gram-positive hosts use a
851 similar set of tools to complete the lysis pathway through distinct molecular mechanisms just as
852 observed for phages that infect *E. coli.*

853 **LIMITATIONS**

854 The focus of the current report was to genetically evaluate the function of LysF1a and
855 LysF1b proteins in the physiological context of phage infection in *M. smegmatis*. There are
856 several limitations to the current data set. First, Girr and NBJ are temperate phages and do not
857 kill the entire liquid cultures even at an MOI of 10:1. This is one reason that the culture OD_{600} in
858 our experiments does not drop below 0.10. Although we have shown that the residual surviving
859 bacteria is <10% of the starting culture and does not impact the ability to assess lysis timing, we
860 have a limited window of analysis of ~6-8 hrs. after infection before the lysogens increase the
861 OD_{600} and begin to interfere with the analysis. Thus, we don't have time points past 480 minutes
862 and it's possible that the various *lysF1b* mutants ultimately lyse the infected cells if allowed to
863 grow for 24 hrs. Second, due to the lysogens present in the experiments, the ability to evaluate
864 the infected bacteria via microscopy (especially electron microscopy) is challenging. Microscopy
865 data is therefore not presented since infected cells and lysogens can't be distinguished prior to
866 lysis and even after lysis the images have lysogens that interfere with the analysis. Third, the
867 LysF1 proteins are integral membrane proteins and AlphaFold3 modeling has reduced
868 confidence for membrane proteins and usually shows low confidence pTM scores of <0.5.
869 Additionally, using AlphaFold3 to assess protein-protein interactions for membrane proteins is
870 also poor with ipTM scores generally <0.5 (low confidence). Finally, the ability to exogenously
871 express LysF1a and LysF1b proteins from plasmids to assess possible interactions and
872 phenotypes in the *M. smegmatis* host is not possible due to the strong cytotoxicity of the LysF1b
873 [70, 71].

874 **DATA AVAILABILITY STATEMENT**

875 The authors affirm that all data necessary for confirming the conclusions of this article are
876 represented fully within the article and its tables and figures. Full genome sequences of Girr and
877 NBJ are available in GenBank through accession numbers MH669003 and MH399784,
878 respectively. Extended data, including all original gel figures are posted to FileShare
879 https://doi.org/10.6084/m9.figshare.31562248

880 **ACKNOWLEDGMENTS**

881 We are grateful to the members of the Science Education Alliance for their invaluable research
882 support and for supplying phage and plasmid reagents, particularly Dainelle Heller, Viknesh
883 Sivanathan, Graham Hatfull, Deborah Jacobs-Sera, Becky Garlena and Dan Russell. We also
884 thank the Pittsburgh Bacteriophage Institute for genome sequencing of the phages described in
885 this study. We want to thank A. McKitterick for helpful discussions regarding LysZ. We want to
886 thank Y. Morita for generously sending the ΔmtpA *M. smegmatis* strains. We thank Welkin Pope
887 for helpful discussions regarding infectious centers.

888 **REFERENCS**

889 1. Mushegian AR. Are There 10(31) Virus Particles on Earth, or More, or Fewer? J Bacteriol.
890 2020;202(9).
891 2. Oliveira H, Melo LD, Santos SB, Nobrega FL, Ferreira EC, Cerca N, et al. Molecular aspects
892 and comparative genomics of bacteriophage endolysins. J Virol. 2013;87(8):4558-70.
893 3. Ryan GL, Rutenberg AD. Clocking out: modeling phage-induced lysis of Escherichia coli. J
894 Bacteriol. 2007;189(13):4749-55.
895 4. Pang T, Fleming TC, Pogliano K, Young R. Visualization of pinholin lesions in vivo. Proc Natl
896 Acad Sci U S A. 2013;110(22):E2054-63.
897 5. Savva CG, Dewey JS, Deaton J, White RL, Struck DK, Holzenburg A, et al. The holin of
898 bacteriophage lambda forms rings with large diameter. Mol Microbiol. 2008;69(4):784-
899 93.

900 6. Savva CG, Dewey JS, Moussa SH, To KH, Holzenburg A, Young R. Stable micron-scale
901 holes are a general feature of canonical holins. Mol Microbiol. 2014;91(1):57-65.
902 7. Summer EJ, Berry J, Tran TA, Niu L, Struck DK, Young R. Rz/Rz1 lysis gene equivalents in
903 phages of Gram-negative hosts. J Mol Biol. 2007;373(5):1098-112.
904 8. Rajaure M, Berry J, Kongari R, Cahill J, Young R. Membrane fusion during phage lysis. Proc
905 Natl Acad Sci U S A. 2015;112(17):5497-502.
906 9. Berry J, Rajaure M, Pang T, Young R. The spanin complex is essential for lambda lysis. J
907 Bacteriol. 2012;194(20):5667-74.
908 10. Young R. Phage lysis: three steps, three choices, one outcome. J Microbiol.
909 2014;52(3):243-58.
910 11. Cahill J, Young R. Phage Lysis: Multiple Genes for Multiple Barriers. Adv Virus Res.
911 2019;103:33-70.
912 12. Cahill J, Holt A, Theodore M, Moreland R, O'Leary C, Martin C, et al. Spatial and temporal
913 control of lysis by the lambda holin. mBio. 2024;15(2):e0129023.
914 13. Park T, Struck DK, Dankenbring CA, Young R. The pinholin of lambdoid phage 21: control
915 of lysis by membrane depolarization. J Bacteriol. 2007;189(24):9135-9.
916 14. Barenboim M, Chang CY, dib Hajj F, Young R. Characterization of the dual start motif of a
917 class II holin gene. Mol Microbiol. 1999;32(4):715-27.
918 15. Blasi U, Young R. Two beginnings for a single purpose: the dual-start holins in the
919 regulation of phage lysis. Mol Microbiol. 1996;21(4):675-82.
920 16. Ramanculov E, Young R. An ancient player unmasked: T4 rI encodes a t-specific antiholin.
921 Mol Microbiol. 2001;41(3):575-83.
922 17. Ramanculov E, Young R. Genetic analysis of the T4 holin: timing and topology. Gene.
923 2001;265(1-2):25-36.
924 18. Chamblee JS, Ramsey J, Chen Y, Maddox LT, Ross C, To KH, et al. Endolysin Regulation
925 in Phage Mu Lysis. mBio. 2022;13(3):e0081322.

926 19. Xu H, Bao X, Hong W, Wang A, Wang K, Dong H, Hou J, Govinden R, Deng B, Chenia HY.
927 Biological Characterization and Evolution of Bacteriophage T7-△holin During the Serial
928 Passage Process. Font. Microbiology. 2021;12.
929 20. Raman SK, Siva Reddy DV, Jain V, Bajpai U, Misra A, Singh AK. Mycobacteriophages:
930 therapeutic approach for mycobacterial infections. Drug Discov Today.
931 2024;29(7):104049.
932 21. Payne KM, Hatfull GF. Mycobacteriophage endolysins: diverse and modular enzymes with
933 multiple catalytic activities. PLoS One. 2012;7(3):e34052.
934 22. Schmelcher M, Donovan DM, Loessner MJ. Bacteriophage endolysins as novel
935 antimicrobials. Future Microbiol. 2012;7(10):1147-71.
936 23. Arenskotter M, Broker D, Steinbach A. Biology of the metabolically diverse genus Gordonia.
937 Appl Environ Microbiol. 2004;70(6):3195-204.
938 24. Goodfellow M, Jones AL. Corynebacteriales ord. nov. Bergey's Manual of Systematics of
939 Archaea and Bacteria. 2015. p. 1-14.
940 25. Brennan PJ. Structure, function, and biogenesis of the cell wall of Mycobacterium
941 tuberculosis. Tuberculosis (Edinb). 2003;83(1-3):91-7.
942 26. Hart EM, Bernhardt TG. The mycomembrane. Curr Biol. 2025;35(3):R85-R6.
943 27. Catalao MJ, Pimentel M. Mycobacteriophage Lysis Enzymes: Targeting the Mycobacterial
944 Cell Envelope. Viruses. 2018;10(8).
945 28. Payne K, Sun Q, Sacchettini J, Hatfull GF. Mycobacteriophage Lysin B is a novel
946 mycolylarabinogalactan esterase. Mol Microbiol. 2009;73(3):367-81.
947 29. Marinelli LJ, Piuri M, Swigonova Z, Balachandran A, Oldfield LM, van Kessel JC, et al.
948 BRED: a simple and powerful tool for constructing mutant and recombinant
949 bacteriophage genomes. PLoS One. 2008;3(12):e3957.

950 30. Joshi H, Seniya SP, Suryanarayanan V, Patidar ND, Singh SK, Jain V. Dissecting the
951 structure-function relationship in lysozyme domain of mycobacteriophage D29-encoded
952 peptidoglycan hydrolase. FEBS Lett. 2017;591(20):3276-87.
953 31. Singh AK, Gangakhedkar R, Thakur HS, Raman SK, Patil SA, Jain V. Mycobacteriophage
954 D29 Lysin B exhibits promising anti-mycobacterial activity against drug-resistant
955 Mycobacterium tuberculosis. Microbiol Spectr. 2023;11(6):e0459722.
956 32. Pohane AA, Joshi H, Jain V. Molecular dissection of phage endolysin: an interdomain
957 interaction confers host specificity in Lysin A of Mycobacterium phage D29. J Biol Chem.
958 2014;289(17):12085-95.
959 33. Nair G, Jain V. An intramolecular cross-talk in D29 mycobacteriophage endolysin governs the
960 lytic cycle and phage-host population dynamics. Sci. Adv.2024;10(6):
961 34. Gil F, Catalao MJ, Moniz-Pereira J, Leandro P, McNeil M, Pimentel M. The lytic cassette of
962 mycobacteriophage Ms6 encodes an enzyme with lipolytic activity. Microbiology
963 (Reading). 2008;154(Pt 5):1364-71.
964 35. Gil F, Grzegorzewicz AE, Catalao MJ, Vital J, McNeil MR, Pimentel M. Mycobacteriophage
965 Ms6 LysB specifically targets the outer membrane of Mycobacterium smegmatis.
966 Microbiology (Reading). 2010;156(Pt 5):1497-504.
967 36. Loessner MJ, Gaeng S, Wendlinger G, Maier SK, Scherer S. The two-component lysis
968 system of Staphylococcus aureus bacteriophage Twort: a large TTG-start holin and an
969 associated amidase endolysin. FEMS Microbiol Lett. 1998;162(2):265-74.
970 36. Kwan T, Liu J, DuBow M, Gros P, Pelletier J. The complete genomes and proteomes of 27
971 Staphylococcus aureus bacteriophages. Proc Natl Acad Sci U S A. 2005;102(14):5174-
972 9.
973 38. Vybiral D, Takac M, Loessner M, Witte A, von Ahsen U, Blasi U. Complete nucleotide
974 sequence and molecular characterization of two lytic Staphylococcus aureus phages:
975 44AHJD and P68. FEMS Microbiol Lett. 2003;219(2):275-83.

976 39. Godinho LM, El Sadek Fadel M, Monniot C, Jakutyte L, Auzat I, Labarde A, et al. The
977 Revisited Genome of Bacillus subtilis Bacteriophage SPP1. Viruses. 2018;10(12).
978 40. Fernandes S, São-José C. Probing the function of the two holin-like proteins of
979 bacteriophage SPP1. Virology. 2017;500:184-189.
980 41. Escobedo S, Campelo AB, Wegmann U, Garcia P, Rodriguez A, Martinez B. Insight into the
981 Lytic Functions of the Lactococcal Prophage TP712. Viruses. 2019;11(10).
982 42. Sao-Jose C, Parreira R, Vieira G, Santos MA. The N-terminal region of the Oenococcus
983 oeni bacteriophage fOg44 lysin behaves as a bona fide signal peptide in Escherichia coli
984 and as a cis-inhibitory element, preventing lytic activity on oenococcal cells. J Bacteriol.
985 2000;182(20):5823-31.
986 43. Gindreau E, Lonvaud-Funel A. Molecular analysis of the region encoding the lytic system
987 from Oenococcus oeni temperate bacteriophage phi 10MC. FEMS Microbiol Lett.
988 1999;171(2):231-8.
989 44. Nelson D, Schuch R, Zhu S, Tscherne DM, Fischetti VA. Genomic sequence of C1, the first
990 streptococcal phage. J Bacteriol. 2003;185(11):3325-32.
991 45. Pope WH, Mavrich TN, Garlena RA, Guerrero-Bustamante CA, Jacobs-Sera D,
992 Montgomery MT, et al. Bacteriophages of Gordonia spp. Display a Spectrum of Diversity
993 and Genetic Relationships. mBio. 2017;8(4).
994 46. Pollenz RS, Bland J, Pope WH. Bioinformatic characterization of endolysins and holin-like
995 membrane proteins in the lysis cassette of phages that infect Gordonia rubripertincta.
996 PLoS One. 2022;17(11):e0276603.
997 47. McGarrah CEE, Algarin-Martinez ED, Cavasini MED, Correa V, Danielson DF, Dean WR, et
998 al. Isolation and Annotation of Azira, a CT Cluster Phage That Infects Gordonia
999 rubripertincta. Microbiol Resour Announc. 2023;12(7):e0034723.

1000 48. Dedrick RM, Marinelli LJ, Newton GL, Pogliano K, Pogliano J, Hatfull GF. Functional
1001 requirements for bacteriophage growth: gene essentiality and expression in
1002 mycobacteriophage Giles. Mol Microbiol. 2013;88(3):577-89.
1003 49. Sandoval AM, Abram AM, Alhabib ZM, Antonyan AS, Brikho SM, Buhay SI, et al. Complete
1004 Genome Sequences of Cluster G Mycobacteriophage Darionha, Cluster A
1005 Mycobacteriophage Salz, and Cluster J Mycobacteriophage ThreeRngTarjay. Microbiol
1006 Resour Announc. 2020;9(20).
1007 50. Catalao MJ, Gil F, Moniz-Pereira J, Pimentel M. Functional analysis of the holin-like proteins
1008 of mycobacteriophage Ms6. J Bacteriol. 2011;193(11):2793-803.
1009 51. Garcia M, Pimentel M, Moniz-Pereira J. Expression of Mycobacteriophage Ms6 lysis genes
1010 is driven by two sigma(70)-like promoters and is dependent on a transcription
1011 termination signal present in the leader RNA. J Bacteriol. 2002;184(11):3034-43.
1012 52. Catalao MJ, Gil F, Moniz-Pereira J, Pimentel M. The mycobacteriophage Ms6 encodes a
1013 chaperone-like protein involved in the endolysin delivery to the peptidoglycan. Mol
1014 Microbiol. 2010;77(3):672-86.
1015 53. Bavda VR, Jain V. Deciphering the Role of Holin in Mycobacteriophage D29 Physiology.
1016 Front Microbiol. 2020;11:883.
1017 54. Bavda VR, Yadav A, Jain V. Decoding the molecular properties of mycobacteriophage D29
1018 Holin provides insights into Holin engineering. J Virol. 2021;95(10).
1019 55. Kamilla S, Jain V. Mycobacteriophage D29 holin C-terminal region functionally assists in
1020 holin aggregation and bacterial cell death. FEBS J. 2016;283(1):173-90.
1021 56. Ford ME, Sarkis GJ, Belanger AE, Hendrix RW, Hatfull GF. Genome structure of
1022 mycobacteriophage D29: implications for phage evolution. J Mol Biol. 1998;279(1):143-
1023 64.
1024 57. To KH, Dewey J, Weaver J, Park T, Young R. Functional analysis of a class I holin, P2 Y. J
1025 Bacteriol. 2013;195(6):1346-55.

1026 58. Christie GE, Calendar R. Bacteriophage P2. Bacteriophage. 2016;6(1):e1145782.
1027 59. McKitterick AC, Lyerly EW, Bernhardt TG. Bacteriophages target membrane-anchored
1028 glycopolymers to promote host cell lysis and progeny release. bioRxiv.
1029 2025:2025.06.24.661397.
1030 60. Hallgren J, Tsirigos KD, Pedersen MD, Almagro Armenteros JJ, Marcatili P, Nielsen H, et al.
1031 DeepTMHMM predicts alpha and beta transmembrane proteins using deep neural
1032 networks. bioRxiv. 2022:2022.04.08.487609.
1033 61. Tsirigos KD, Peters C, Shu N, Kall L, Elofsson A. The TOPCONS web server for consensus
1034 prediction of membrane protein topology and signal peptides. Nucleic Acids Res.
1035 2015;43(W1):W401-7.
1036 62. Almagro Armenteros JJ, Tsirigos KD, Sonderby CK, Petersen TN, Winther O, Brunak S, et
1037 al. SignalP 5.0 improves signal peptide predictions using deep neural networks. Nat
1038 Biotechnol. 2019;37(4):420-3.
1039 63. Juncker AS, Willenbrock H, Von Heijne G, Brunak S, Nielsen H, Krogh A. Prediction of
1040 lipoprotein signal peptides in Gram-negative bacteria. Protein Sci. 2003;12(8):1652-62.
1041 64. Soding J, Biegert A, Lupas AN. The HHpred interactive server for protein homology
1042 detection and structure prediction. Nucleic Acids Res. 2005;33(Web Server
1043 issue):W244-8.
1044 65. Abramson J, Adler J, Dunger J, Evans R, Green T, Pritzel A, et al. Accurate structure
1045 prediction of biomolecular interactions with AlphaFold 3. Nature. 2024;630(8016):493-
1046 500.
1047 66. Madeira F, Madhusoodanan N, Lee J, Eusebi A, Niewielska A, Tivey ARN, Lopez, R,
1048 Butcher S. The EMBL-EBI Job Dispatcher sequence analysis tools framework in 2024.
1049 Nucleic acids research. 2024;52(W1):W521–W525.

1050 67. Snapper SB, Melton RE, Mustafa S, Kieser T, Jacobs WR, Jr. Isolation and characterization
1051 of efficient plasmid transformation mutants of Mycobacterium smegmatis. Mol Microbiol.
1052 1990;4(11):1911-9.
1053 68. Sparks IL, Kado T, Prithviraj M, Nijjer J, Yan J, Morita YS. Lipoarabinomannan mediates
1054 localized cell wall integrity during division in mycobacteria. Nat Commun.
1055 2024;15(1):2191.
1056 69. Heller D, Amaya I, Mohamed A, Ali I, Mavrodi D, Deighan P, et al. Systematic
1057 overexpression of genes encoded by mycobacteriophage Waterfoul reveals novel
1058 inhibitors of mycobacterial growth. G3 (Bethesda). 2022;12(8).
1059 70. Pollenz RS, Barnhill K, Biggs A, Bland J, Carter V, Chase M, et al. A genome-wide
1060 cytotoxicity screen of cluster F1 mycobacteriophage Girr reveals novel inhibitors of
1061 Mycobacterium smegmatis growth. G3 (Bethesda). 2024;14(5).
1062 71. Wise B, Edwards K, Jirsa C, [student authors], Kanther M, Payne K, Pollenz RS, Heller DM.
1063 Identification and characterization of host-modulating effectors encoded by the Cluster F1
1064 mycobacteriophage NormanBulbieJr. bioRxiv 2025.
1065 72. van Kessel JC, Hatfull GF. Mycobacterial recombineering. Methods Mol Biol. 2008;435:203-
1066 15.
1067 73. Gordon D, Abajian C, Green P. Consed: a graphical tool for sequence finishing. Genome
1068 Res. 1998;8(3):195-202.
1069 74. Russell DA. Sequencing, Assembling, and Finishing Complete Bacteriophage Genomes.
1070 Methods Mol Biol. 2018;1681:109-25.
1071 75. Schneider CA, Rasband WS, Eliceiri KW. NIH Image to ImageJ: 25 years of image analysis.
1072 Nat Methods. 2012;9(7):671-5.
1073 76. Pang T, Park T, Young R. Mutational analysis of the S21 pinholin. Mol Microbiol.
1074 2010;76(1):68-77.

1075 77. Park T, Struck DK, Deaton JF, Young R. Topological dynamics of holins in programmed
1076 bacterial lysis. Proc Natl Acad Sci U S A. 2006;103(52):19713-8.
1077 78. Manohar P, Wan J, Ganser G, Sharp K, Young R. The Lysis cassette of jumbophage PhiKZ.
1078 Sci Rep. 2026;16(1):5840.
1079 79. Doermann AH. The intracellular growth of bacteriophages. I. Liberation of intracellular
1080 bacteriophage T4 by premature lysis with another phage or with cyanide. J Gen Physiol.
1081 1952;35(4):645-56.
1082 80. Rigel NW, Gibbons HS, McCann JR, McDonough JA, Kurtz S, Braunstein M. The Accessory
1083 SecA2 System of Mycobacteria Requires ATP Binding and the Canonical SecA1. J Biol
1084 Chem. 2009;284(15):9927-9936.
1085 81. Abdallah A, Gey van Pittius N, DiGiuseppe Champion P, Cox J, Luirink J, et. al. Type VII
1086 secretion — mycobacteria show the way. Nat Rev Microbiol. 2007;5:883–891.
1087 82. Bendtsen JD, Kiemer L, Fausbøll A, Brunak S. Non-classical protein secretion in bacteria.
1088 BMC Microbiol. 2005;5:58.
1089 83. Zhang Z, Dong L, Li X, Deng T, Wang Q. The PE/PPE family proteins of Mycobacterium
1090 tuberculosis: evolution, function, and prospects for tuberculosis control. Front. Immunol.
1091 2025;16:1606311.
1092 84. Ameh EM, Tyrrel S, Harris JA, Pawlett M, Orlova EV, Ignatiou A, et al. Lysis Performance of
1093 Bacteriophages with Different Plaque Sizes and Comparison of Lysis Kinetics After
1094 Simultaneous and Sequential Phage Addition. Phage (New Rochelle). 2020;1(3):149-57.
1095 85. Abedon ST, Yin J. Bacteriophage plaques: theory and analysis. Methods Mol Biol.
1096 2009;501:161-74.
1097 86. Dennehy JJ, Abedon ST, Turner PE. Host density impacts relative fitness of bacteriophage
1098 Phi6 genotypes in structured habitats. Evolution. 2007;61(11):2516-27.
1099 87. Russell DA, Hatfull GF. PhagesDB: the actinobacteriophage database. Bioinformatics.
1100 2017;33(5):784-6.

1101 88. Gauthier CH, Cresawn SG, Hatfull GF. 2022. PhaMMseqs: a new pipeline for constructing
1102 phage gene phamilies using MMseqs2. G3 Genes Genomes Genetics.
1103 2022;12(11):jkac233.

1104 89. Gauthier CH, Hatfull GF. PhamClust: a phage genome clustering tool using proteomic
1105 equivalence. mSystems. 2023;8(5):e00443-23.

1106

1107 **FIGURE LEGANDS**

1108

1109 **Figure 1. Lysis cassette organization of Girr and NormanBulbieJr (NBJ)** and **amino acid**
1110 **sequence and topology of Girr and NBJ LysF1a proteins and comparison to phage 21 S^{21}**
1111 **pinholin**. **A.** Predicted protein coding genes are shown as colored boxes. The genomic location
1112 is represented by the ruler, and the numbers represent the kilobase from nucleotide 1. Both
1113 lysis cassette regions are located upstream of the *tape measure* and *minor tail* genes. Genes
1114 above the genome are transcribed in the forward direct and genes below in the reverse
1115 direction. Genes with the same color encode proteins that are grouped to the same pham. Pink
1116 shading indicated nucleotide identity >90% in the shaded region. The *lysin A, lysin B,* 2TMD
1117 *lysF1a and* 1TMD *lysF1b* genes are identified. NKF = genes with no know function; *HNH* = HNH
1118 endonuclease. B. The amino acid sequences of Girr and NBJ LysF1a showing the location of
1119 the predicted TMDs and charged amino acids. **C.** The amino acid sequence of phage 21 $S^{21}68$
1120 holin, $S^{21}71$ antiholin and $S^{21}68_{IRS}$ showing the location of the predicted TMDs and charged
1121 amino acids. **D.** Predicted membrane topology of Girr LysF1a, $S^{21}68_{IRS}$ and the proposed
1122 topology of the $S^{21}68$ holin homodimer with cytoplasmic TMD1.

1123

1124 **Figure 2. Amino acid sequence and topology of lysis proteins with 1TMD**. **A.** The amino
1125 acid sequences of Girr LysF1b, NBJ LysF1b, Waterfoul gp32 and Mu releasin showing the
1126 location of the predicted TMD and the charged amino acids. **B.** AlphaFold3 structural
1127 predictions and membrane topologies of 1TMD proteins involved in lysis. pTM values: Mu, 0.51;
1128 NBJ LysF1b, 0.40; Girr LysF1b, 0.41; Rz, 0.57; T, 0.74; phiKZ, 0.58. **C.** Predicted topologies of
1129 Girr LysF1b and Waterfoul gp32.

1130

1131 **Figure 3. Deletion of Girr *lysF1a* and *lysF1b*. A.** Genomic structure and PCR primer set
1132 locations in Girr gene deletion mutants. Primer set 1 (P1) uses primers Girr-FL_*lysF1a* (F and

1133 R) and generates a 755bp fragment in Girr_WT and 487bp with *lysF1a* deletion. Primer set 2
1134 (P2) uses primers Girr-FL_*lysF1b* (F and R) and generates a 933bp fragment in Girr_WT and
1135 594bp with *lysF1b* deletion. Primer set 3 (P3) uses the forward Girr-FL_*lysF1a* and reverse Girr-
1136 FL_*lysF1b* and generates a 1189bp fragment in Girr_WT and either 921bp with *lysF1a* deletion
1137 or 818b with *lysF1b* deletion. **B.** PCR verification of high titer lysates of Girr_WT, Girr_Δ*lysF1a*
1138 and Girr_Δ*lysF1b* using the indicated primer sets. PCR band sizes are identified and show
1139 correct deletions of the indicated genes.
1140
1141 **Figure 4 Plaque sizes in Girr_WT, Girr_Δ*lysF1a* and Girr_Δ*lysF1b*.** *M. smegmatis* was
1142 infected with identical numbers of the indicated phage as detailed in Methods and plaque size
1143 determined after 36 hrs. of growth at 37°C. Scale = 1cm. Plaque volume schematics are
1144 presented to illustrate the plaque size differences.
1145
1146 **Figure 5. Complementation of plaque phenotype in Girr_Δ*lysF1b*. A.** Plaque assays were
1147 completed with *M. smegmatis* using Girr_WT or Girr_Δ*lysF1b* as described in Methods. Plaque
1148 assays were completed with *M. smegmatis* complementing strains carrying the indicated
1149 pExTra-Waterfoul expression plasmids using Girr_Δ*lysF1b* as described in Methods. Plaques
1150 were evaluated following incubation at 37°C for 36 hrs. Plaques sizes were quantified using
1151 ImageJ and the average diameter +/- standard deviation for > 50 plaques is shown. * =
1152 statistically different from Girr_WT, p <*0.0001*. ** = statistically different from Girr_Δ*lysF1b*
1153 infected on *M. smegmatis* with pExTra Waterfoul_*32* with no aTc, p <*0.0001*. Scale = 1cm. B.
1154 Plaque assays were completed with *M. smegmatis* using Girr_WT or Girr_Δ*lysF1b* as described
1155 in Methods. Plaque assays were completed with *M. smegmatis* complementing strains carrying
1156 the indicated pExTra-Waterfoul expression plasmids using Girr_Δ*lysF1b* as described in
1157 Methods. Plaques were evaluated following incubation at 37°C for 48 hrs. Plaques sizes were

1158 quantified using ImageJ and the average diameter +/- standard deviation for > 50 plaques is
1159 shown * = statistically different from Girr_WT, *p <0.0001*. ** = statistically different from
1160 Girr_Δ*lysF1b* infected on *M. smegmatis* with pExTra01, *p <0.0001*. Scale = 1cm.
1161
1162 **Figure 6. Complementation of plaque phenotype in Girr_Δ*lysF1a*.** Plaque assays were
1163 completed with *M. smegmatis* using Girr_WT or Girr_Δ*lysF1a* as described in Methods. Plaque
1164 assays were completed with *M. smegmatis* complementing strains carrying pExTra-Girr_*34*
1165 expression plasmid using Girr_Δ*lysF1a*as described in Methods. Plaques were evaluated
1166 following incubation at 37°C for 48 hrs. Plaques sizes were quantified using ImageJ and the
1167 average diameter +/- standard deviation for > 50 plaques is shown. * = statistically different from
1168 Girr_WT, *p <0.0001*. ** = statistically different from Girr_Δ*lysF1a* infected on *M. smegmatis* with
1169 pExTra-Girr_*34* with no aTc, *p <0.0001*. Scale = 1cm.
1170
1171 **Figure 7. Liquid lysis assay and ATP release from *M. smegmatis* after infection.** At T_0 a log
1172 growth culture of *M. smegmatis* at an OD_{600} of ~0.25 was infected with the indicated phage at
1173 an MOI of 10:1 and incubated at 37°C for 30 minutes without shaking. Control cultures (no
1174 phage) did not receive phage. At T_{30} minutes the culture was constantly shaken a 225rpm,
1175 aliquots removed at the indicated times and bacterial growth evaluated at OD_{600}. Open white
1176 arrow shows the 30-minute infection time. **A.** Representative results following infection with
1177 Girr_WT, Girr_Δ*lysF1a* and Girr_Δ*lysF1b*. **B**. Representative results following infection with
1178 NBJ_WT, NBJ_Δ*lysF1a* and NBJ_Δ*lysF1b.* **C.** Samples of culture were removed from the
1179 cultures represented in A and B at the times indicated by the solid black triangle on the x axis.
1180 The presence of ATP was evaluated as described in Methods.
1181

1182 **Figure 8. Energy poisons trigger early lysis by phage expressing LysF1b but not LysF1a.**
1183 At T_0 a log growth culture of *M. smegmatis* at an OD_{600} of ~0.25 was infected with the indicated
1184 phage at an MOI of 10:1 and incubated at 37°C for 30 minutes without shaking. Control cultures
1185 (no phage) did not receive phage. At T_{30} minutes the culture was constantly shaken a 225rpm,
1186 aliquots removed at the indicated times and bacterial growth evaluated at OD_{600}. **A**.
1187 Representative results following infection with Girr_WT, and Girr_Δ*lysF1a*. KCN (final
1188 concentration of 10mM) was added to a culture infected with Girr_Δ*lysF1a* and an uninfected
1189 culture at 110 minutes (open arrow). **B**. Representative results following infection with NBJ_WT,
1190 and NBJ_Δ*lysF1a.* KCN (final concentration of 10mM) was added to a culture infected with
1191 NBJ_Δ*lysF1a* and uninfected culture at 120 minutes (open arrow). **C.** Representative results
1192 following infection with Girr_WT, and Girr_Δ*lysF1b*. KCN (final concentration of 10mM) or $CHCl_3$
1193 (final concentration 1%) was added to cultures infected with Girr_Δ*lysF1b* and uninfected
1194 cultures at 180 minutes (open arrow). **D**. Representative results following infection with
1195 NBJ_WT, and NBJ_Δ*lysF1b.* KCN (final concentration of 10mM) or $CHCl_3$ (final concentration
1196 1%) was added to cultures infected with NBJ_Δ*lysF1b* and uninfected cultures at 180 minutes
1197 (open arrow).
1198
1199 **Figure 9. One-step growth curves of *M. smegmatis* infected with Girr_Δ*lysF1a* and**
1200 **Girr_Δ*lysF1b*. A**. One-step growth curves using Girr_WT, Girr_Δ*lysF1a* and Girr_Δ*lysF1b* were
1201 completed as described in Methods. Each time point represents the average and standard
1202 deviation from 3 different experiments. **B**. The data for Girr_Δ*lysF1b* from panel A replotted with
1203 a different Y axis than used in A. **C**. Burst size was determined as described in Methods. The
1204 average bust size +/- standard deviation is from three different experiments and represents the
1205 average of all points once the curve reached a plateau.
1206

1207 **Figure 10. Deletion of both lysF1a and lysF1b in NBJ. A.** Genomic structure and PCR primer
1208 set locations in NBJ_WT and NBJ_Δ*lysF1a*/Δ*lysF1b* mutant. **B**. PCR verification of
1209 *lysF1a/lysF1b* double deletion. Primer set 7 (P7) uses the forward NBJ-FL_*lysF1a* and reverse
1210 NBJ-FL_*lysF1b* and generates a 1179bp fragment in NBJ_WT, a 985bp fragment in
1211 NBJ_Δ*lysF1a*, 808bp fragment in NBJ_Δ*lysF1b* and a 580bp fragment in NBJ_Δ*lysF1a*/Δ*lysF1b*.
1212 **C.** *M. smegmatis* was infected with identical numbers of the indicated phage as detailed in
1213 Methods and plaque size determined after 36 hrs. of growth at 37ºC. Scale = 1cm. **D**. Liquid
1214 lysis assay. At T_0 a log growth culture of *M. smegmatis* at an OD_{600} of ~0.25 was infected with
1215 the indicated phage at an MOI of 10:1 and incubated at 37ºC for 30 minutes without shaking
1216 (indicated by white arrow). Control cultures (no phage) did not receive phage. At T_{30} minutes the
1217 culture was constantly shaken a 225rpm, aliquots removed at the indicated times and bacterial
1218 growth evaluated at OD_{600}. A separate culture of non-infected cells and NBJ_WT was treated
1219 with KCN (final concentration 10mm) at 100 minutes (black arrow). A separate culture of non-
1220 infected cells, NBJ_Δ*lysF1b* and NBJ_Δ*lysF1a*/Δ*lysF1b* was treated with KCN (final
1221 concentration 10mm) at 150 minutes (black arrow).
1222
1223 **Figure 11. Isolation of Girr_Δ*lysF1b*-LRM mutants**. **A**. *M. smegmatis* was infected with
1224 GirrΔ*lysF1b,* plate lysates recovered from the plaque assay and *M. smegmatis* infected with the
1225 recovered phage. Panel A shows a representative plaque assay following the second round of
1226 infection. A large plaque is circled. **B**. Phage were isolated from the large plaque in A, serial
1227 diluted and used for plaque assay. Plates were incubated at 37ºC for 36 hrs. **C**. Plaque assay
1228 from Girr_WT phage. Plates were incubated at 37ºC for 36 hrs. Scale bar = 1cm in all images.
1229
1230 **Figure 12. Liquid lysis and one-step assay of Girr and NBJ LRM mutants.** At T_0 a log
1231 growth culture of *M. smegmatis* at an OD_{600} of ~0.25 was infected with the indicated phage at

1232 MOI 10:1 for 30 minutes at 37°C without shaking. Control cultures (no phage) did not receive
1233 phage. At T_{30} minutes the culture was constantly shaken a 225rpm and aliquots removed over
1234 time. *M. smegmatis* growth was evaluated at OD_{600}. **A**. Representative results following infection
1235 with Girr_WT and indicated LRM mutants. **B**. Representative results following infection with
1236 NBJ_WT and indicated LRM mutants **C.** One-step growth curves using Girr_WT and
1237 Girr_Δ*lysF1b*-LRM1 and Girr_Δ*lysF1b*-LRM2 were completed as described in Methods. Each
1238 time point represents the average and standard deviation from 3 different experiments.
1239

1240 **Figure 13. Analysis of *lysF1b* phage plaque sizes in *M. smegmatis* lacking the**
1241 **lipoarabinomannan layer. A**. Representative plaque assays using Wild type *M. smegmatis, M.*
1242 *smegmatis* ΔmtpA-comp or *M. smegmatis* ΔmtpA cultures infected with the same amount of
1243 Girr_WT or Girr_Δ*lysF1b* and incubated for 48 hrs. at 37°C. Ruler = 1cm. **B**. Plaque sizes were
1244 determined as described in Methods. The average plaque diameter +/- standard deviation for 25
1245 plaques is shown.
1246

1247 **Figure 14. Analysis of NKF gene *29* in Girr and NBJ. A**. Gene organization of Girr, NBJ and
1248 Ms6 lysis cassette region. Predicted protein coding genes are shown as colored boxes. The
1249 genomic location is represented by the ruler, and the numbers represent the kilobase from
1250 nucleotide 1. Genes above the genome are transcribed in the forward direct and genes below in
1251 the reverse direction. Genes with the same color encode proteins that are grouped to the same
1252 pham. Pink shading indicated nucleotide identity >90% in the shaded region. *NKF* = Girr_*29*,
1253 NBJ_*29* and Ms6_*23*. **B**. PCR analysis of Girr_Δ*29*-20 and Girr_Δ*29*-25. **C**. Liquid lysis assay of
1254 the indicated phages was carried out as described in Methods. **D**. Amino acid alignment of Girr
1255 gp29, NBJ gp29 and Ms6 gp23 by Clustal Omega. **E**. Plaque assay of Girr_WT, Girr_Δ*29-20*,

1256 Girr Δ*29-25*, NBJ_WT, and NBJ_Δ*29.* Ruler = 1cm. Plaque sizes were determined as described

1257 in Methods. The average plaque diameter +/- standard deviation for 25 plaques is shown.

1258

1259

1260 SUPPLEMENTAL INFORMATION

1261 S1 Table 1. DNA gBLOCKS and Primers.

1262 S2 Figure 1. One-step growth curves schematic protocol.

1263 S3 Figure 2. One-step example data set: titers, adsorption and infectious centers.

1264 S4 Figure 3. One-step example data set: Girr_WT.

1265 S5 Figure 4. AlphaFold3 predictions of Girr and NBJ Lysin A.

1266 S6 Figure 5. AlphaFold3 predictions of Girr LysF1a and phage 21 S^{21}68.

1267 S7 Figure 6. Deletion of NBJ *lysF1a* and *lysF1b.*

1268 S8 Figure 7. Infection and adsorption of Girr_WT and TMD mutants.

1269 S9 Figure 8. Plaque sizes in NBJ_WT and *lysF1a* and *lysF1b* deletion mutants.

1270 S10 Figure 9. Genomic context of lysis cassette genes in Girr and NBJ.

1271 S11 Figure 10. Energy poisons and $CHCl_3$ treatment trigger early lysis by Girr_WT and

1272 NBJ_WT.

1273 S12 Figure 11. Cell viability of *M. smegmatis* infected with NBJ phages.

1274 S13 Figure 12. PCR analysis of Girr LRM variants and plaques.

1275 S14 Figure 13. Schematic of Girr_lysF1a-LRM amino acid sequences and membrane topology.

1276 S15 Figure 14. AlphaFold3 analysis of Ms6 chaperone and Lysin A interactions.

1277 S16 Figure 15. AlphaFold3 analysis of Girr gp29 and lysin A interactions.

1278 S17 Figure 16. AlphaFold3 analysis of NBJ gp29 and Lysin A interactions.

1279 S18 Figure 17. Part I: Identification of genes that encode *lysF1a* and *LysF1b* homologs in

1280 phages that infect *M. smegmatis.*

1281 S19 Figure 18. Part II: Identification of genes that encode *lysF1a* and *LysF1b* homologs in

1282 phages that infect *M. smegmatis.*

1283 S20 Figure 19. Identification of LysF1b homologs in phages that infect *M. smegmatis.*

1284 S21 Figure 20. . Percent identity of LysF1b homologs

A.

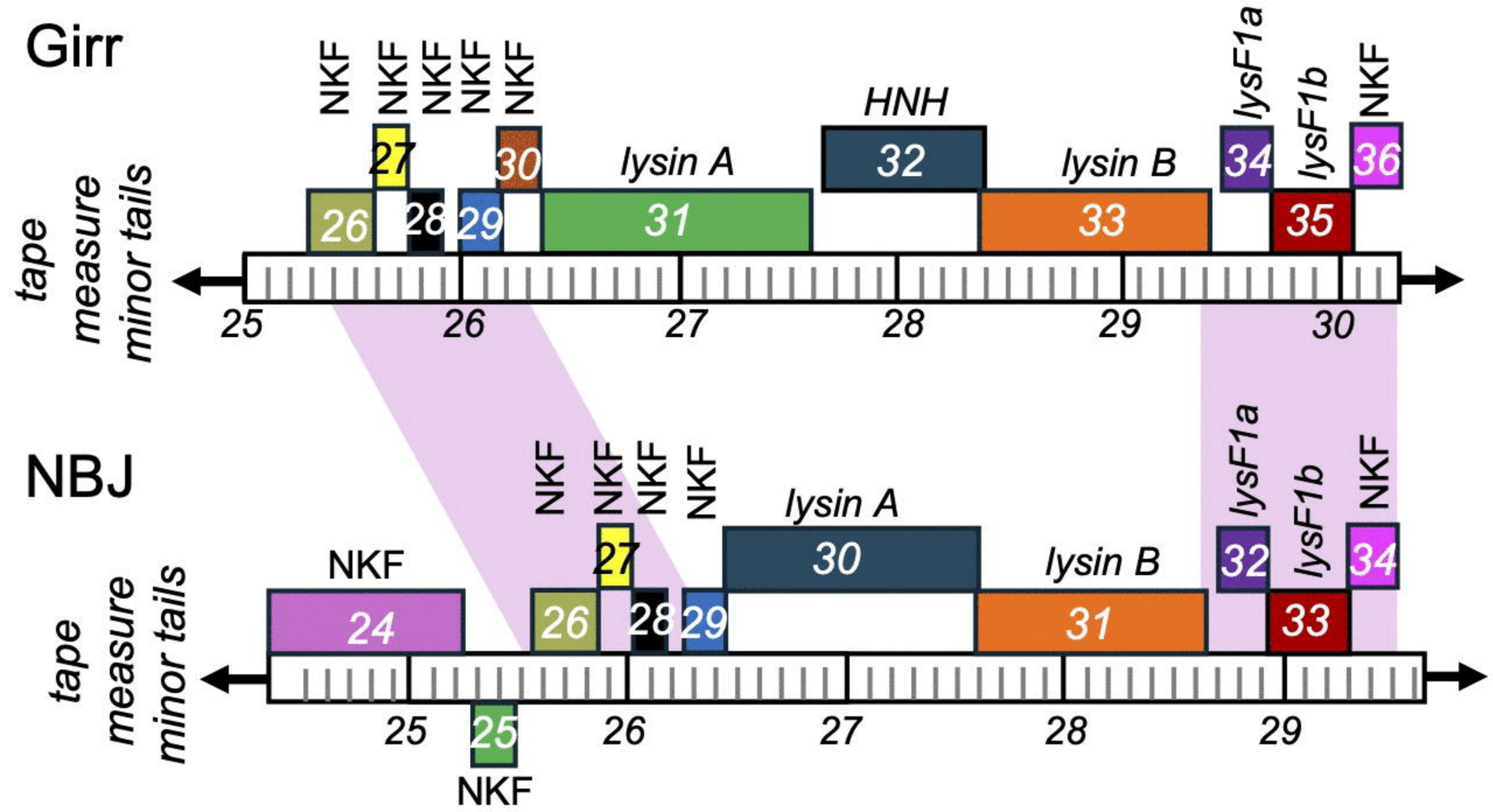
Girr
NKF
NKF
NKF
NKF
NKF
HNH
lysF1a
lysF1b
NKF
27
30
lysin A
32
lysin B
34
36
26
28
29
31
33
35
tape measure minor tails
25
26
27
28
29
30
NBJ
NKF
NKF
NKF
NKF
lysin A
lysF1a
lysF1b
NKF
NKF
27
30
lysin B
32
34
24
26
28
29
31
33
tape measure minor tails
25
25
26
27
28
29
NKF

B.

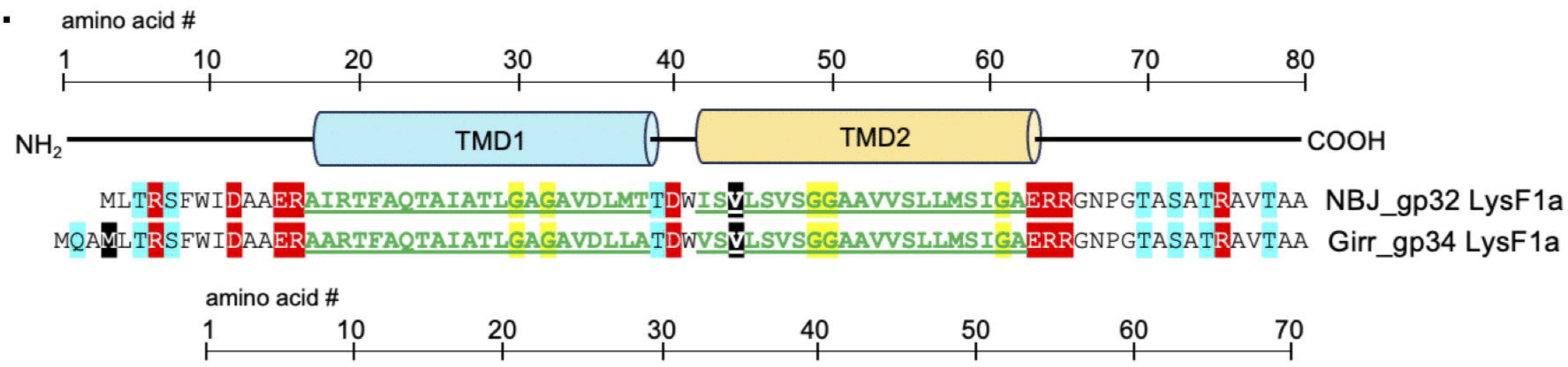
amino acid #
1
10
20
30
40
50
60
70
80
NH2
TMD1
TMD2
COOH
MLTRSFWIDAAERAIRTFAQTAIATLGAGAVDLMTTDWISVLSVSGGAAVVSLLMSIGAERRGNPGTASATRAVTAA NBJ_gp32 LysF1a
MQAMLTRSFWIDAAERAARTFAQTAIATLGAGAVDLLATDWVSVLSVSGGAAVVSLLMSIGAERRGNPGTASATRAVTAA Girr_gp34 LysF1a
amino acid #
1
10
20
30
40
50
60
70

C.

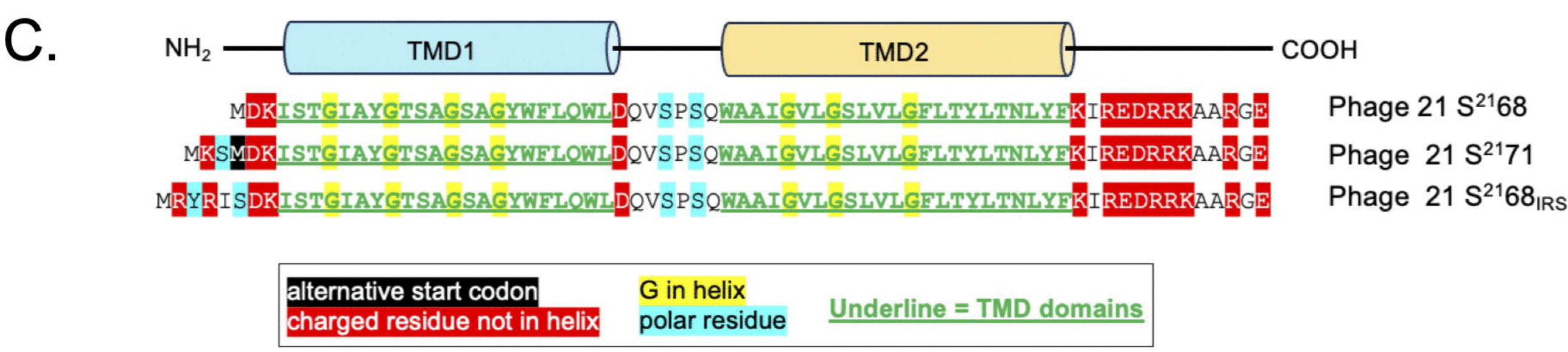
NH2
TMD1
TMD2
COOH
MDKISTGIAYGTSAGSAGYWFLQWLDQVSPSQWAAIGVLGSLVLGFLTYLTNLYFKIREDRRKAARGE Phage 21 S2168
MKSMDKISTGIAYGTSAGSAGYWFLQWLDQVSPSQWAAIGVLGSLVLGFLTYLTNLYFKIREDRRKAARGE Phage 21 S2171
MRYRISDKISTGIAYGTSAGSAGYWFLQWLDQVSPSQWAAIGVLGSLVLGFLTYLTNLYFKIREDRRKAARGE Phage 21 S2168IRS
alternative start codon
charged residue not in helix
G in helix
polar residue
Underline = TMD domains

D.

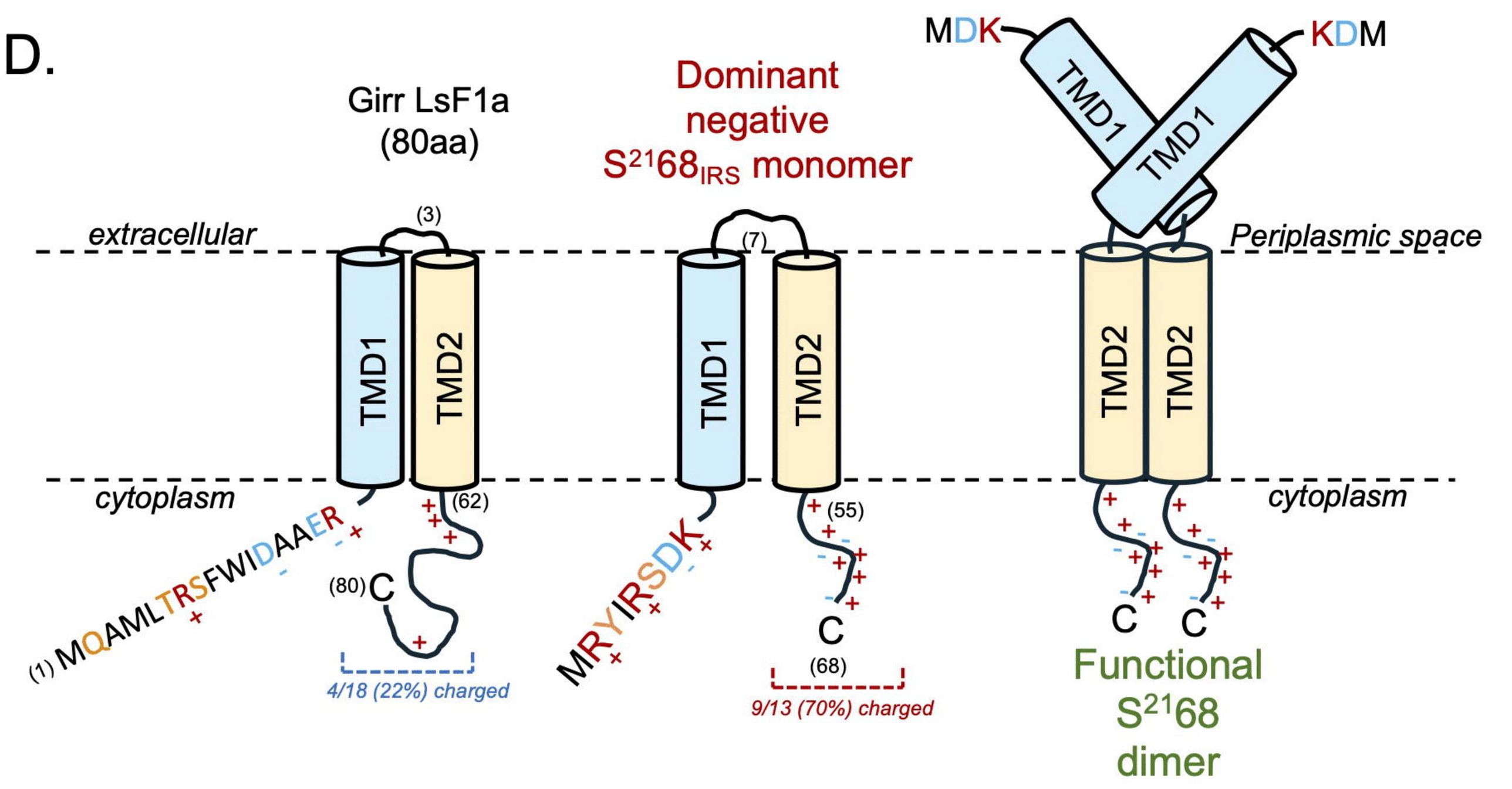
Girr LsF1a
(80aa)
Dominant
negative
S2168IRS monomer
MDK
KDM
TMD1
TMD1
extracellular
Periplasmic space
(3)
(7)
TMD1
TMD2
TMD1
TMD2
TMD2
TMD2
cytoplasm
cytoplasm
(62)
(55)
(1) MQAMLTRSFWIDAAER
(80) C
4/18 (22%) charged
MRYIRSDK
C
(68)
9/13 (70%) charged
C
C
Functional
S2168
dimer

A.

1 10 20 30 40 50 60 70 80 90 100 110 120 # amino acids

MIWESVREAVDAAYQPDDGIDLIGLLIIGLPSTIAAIGTGIVGVLTVRGQRKGRERARQIDAKTDEIHEQTVNTHDTNMRDDLDEIRDLVRDGFKQIQRDIGGLREELRTERLERIEGDKRRD Girr gp35 LysF1b

MIWESVREAVDAAYQPDDGIDLIGLLIIGLPSTIAAIGTGIVGVLTVRGQRKGRERARRIDAKTYEIHEQTVNTHDTNMRDDLDEIRDLVRDGFKQIQRDIGGLREELRTERLERIEGDKRRD NBJ gp33 LysF1b

MTGSAVSALPSDWYGLAGLAVVNAAGLLALFMKARGTHKQVANSHSTNLRDDIDGLRDHIVELGRDIGGMRTDVGQLRGEVRDDRTHTHHRFRRIEDKLDELAGRGARESG Waterfoul gp32

MDLISVLALWPYLLPVVAGGAVWAMRRSFASTERVERLENRMTEMETRYASIPGTEDVHEMRLQIAELSGDIRVLSQRVQSFSHQLELLLENAVNRSNS Mu releasin

Green = TMD domain | Basic region after TMD | + Charged | - Charged

B.

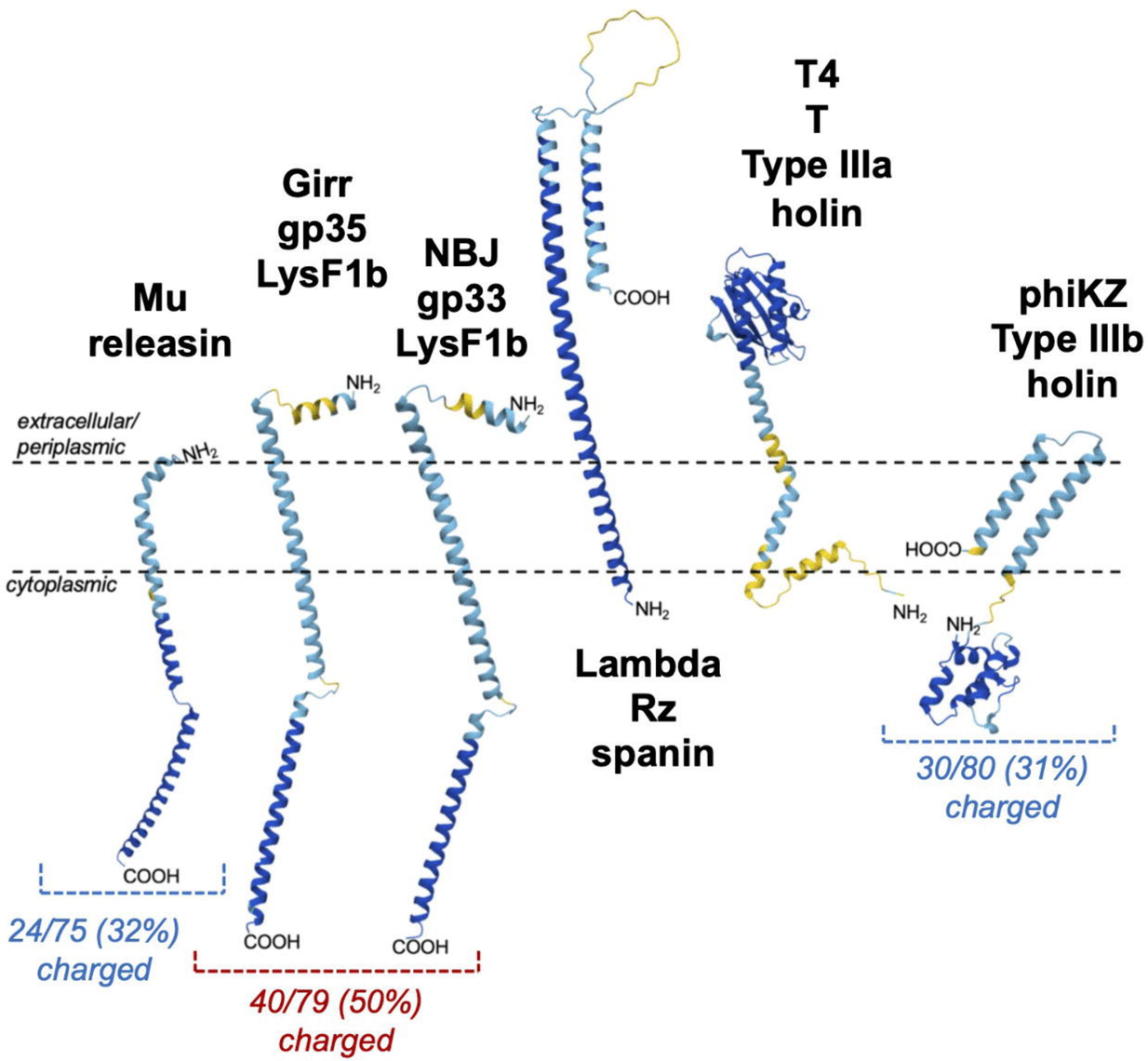

C.

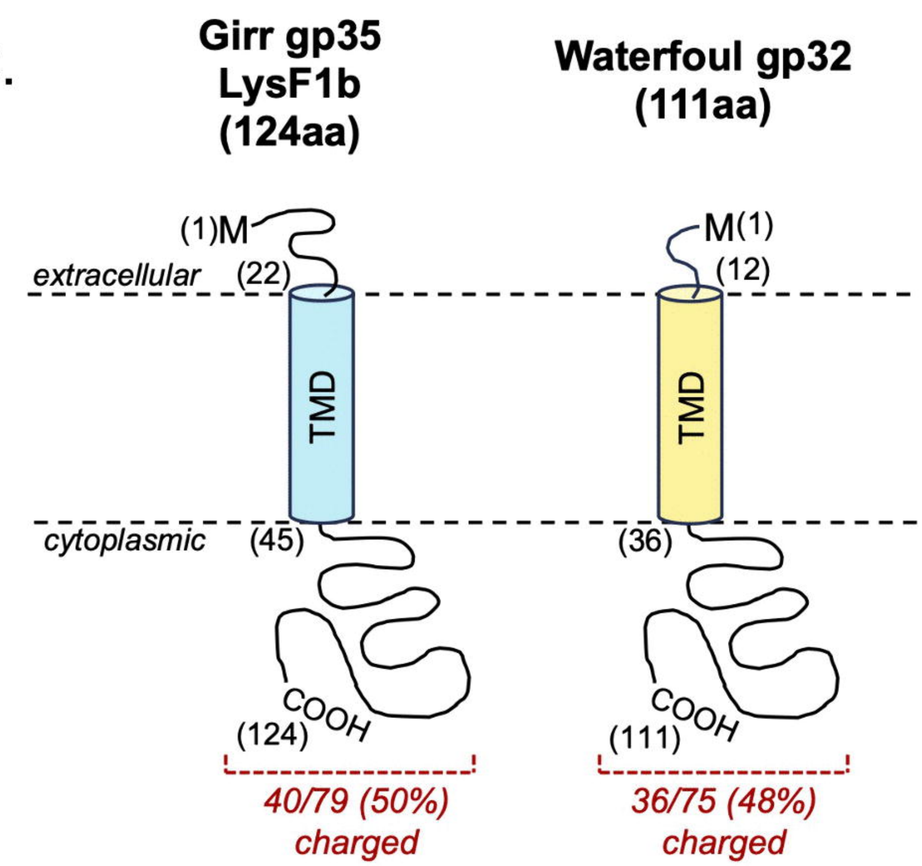

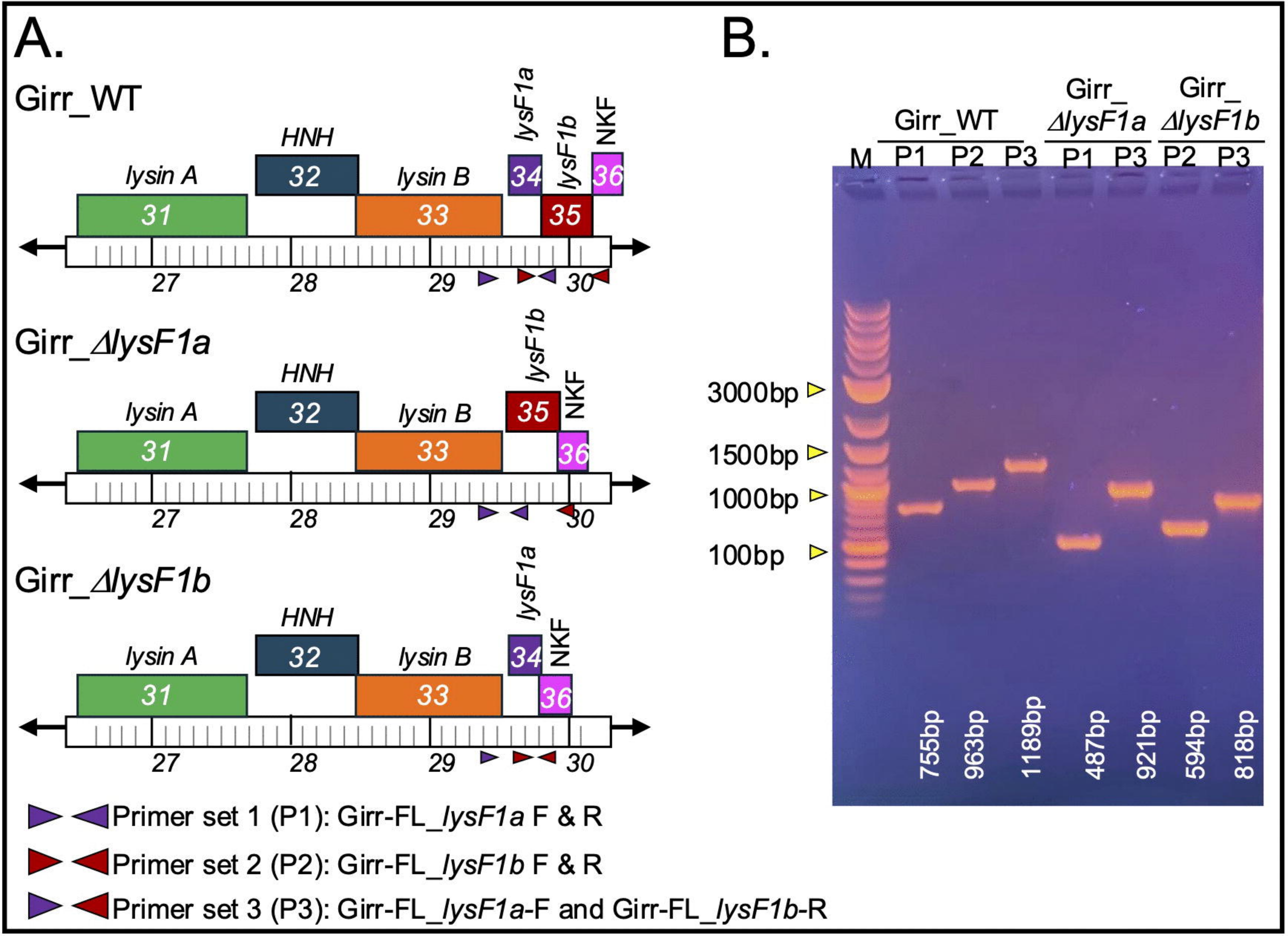
A.
Girr_WT
HNH
lysin A
lysin B
lysF1a
lysF1b
NKF
31
32
33
34
35
36
27
28
29
30
Girr_ΔlysF1a
HNH
lysin A
lysin B
lysF1b
NKF
31
32
33
35
36
27
28
29
30
Girr_ΔlysF1b
HNH
lysin A
lysin B
lysF1a
NKF
31
32
33
34
36
27
28
29
30
Primer set 1 (P1): Girr-FL_lysF1a F & R
Primer set 2 (P2): Girr-FL_lysF1b F & R
Primer set 3 (P3): Girr-FL_lysF1a-F and Girr-FL_lysF1b-R
B.
Girr_WT
Girr_ ΔlysF1a
Girr_ ΔlysF1b
M
P1
P2
P3
P1
P3
P2
P3
3000bp
1500bp
1000bp
100bp
755bp
963bp
1189bp
487bp
921bp
594bp
818bp

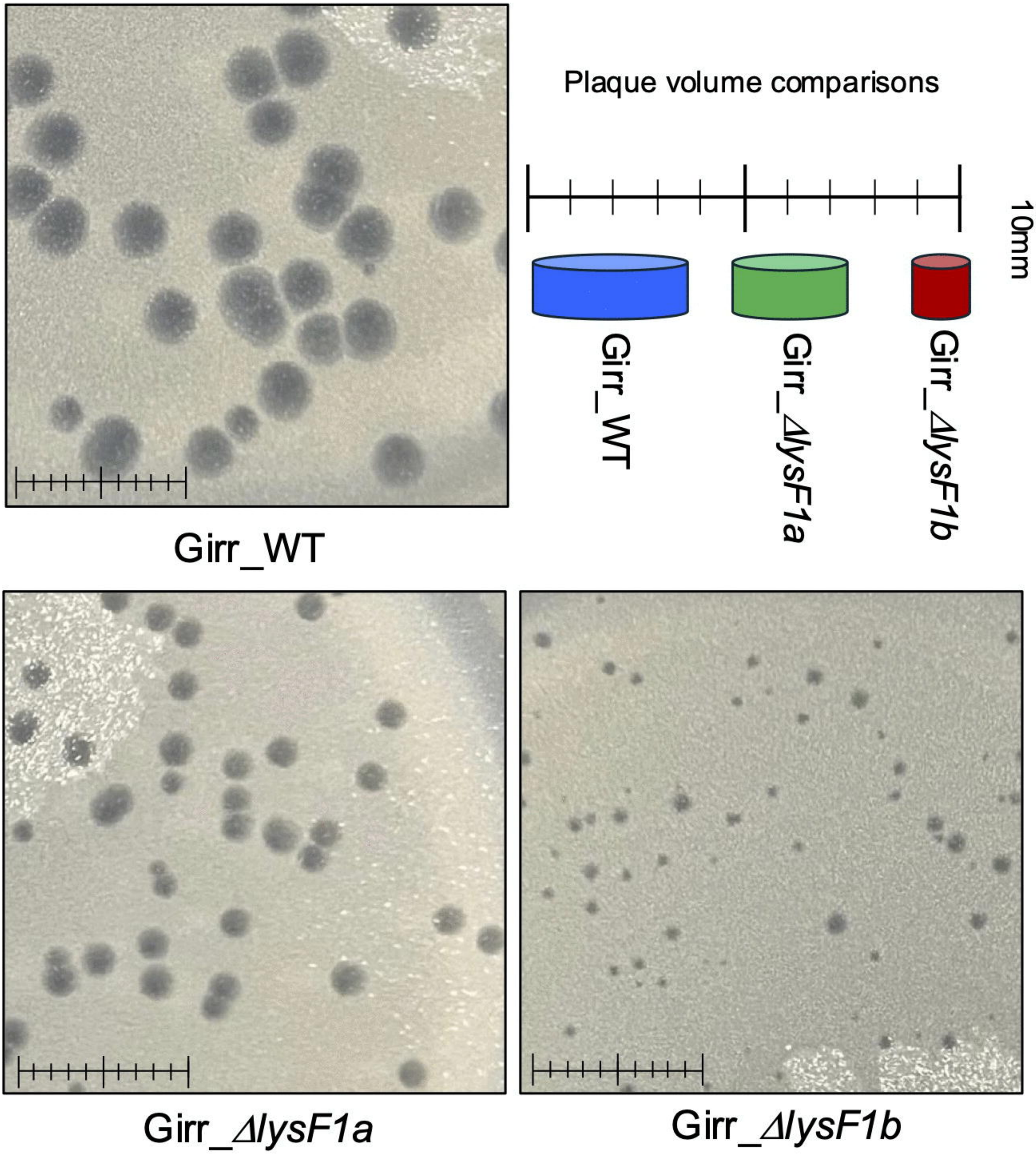
Plaque volume comparisons
10mm
Girr_WT
Girr_ΔlysF1a
Girr_ΔlysF1b
Girr_WT
Girr_ΔlysF1a
Girr_ΔlysF1b

A.

Girr_WT
M. Smegmatis
3.15 +/- 0.46 mm

Girr_*ΔlysF1b*
M. smegmatis
pExTra-Waterfoul_*32*
no aTc
0.85 +/- 0.25 mm

Girr_*ΔlysF1b*
M. smegmatis
pExTra-Waterfoul_*32Δ40C*
no aTc
0.89 +/- 0.30 mm

Girr_*ΔlysF1b*
M. smegmatis
pExTra-Waterfoul_*32ΔN*
no aTc
0.82 +/- 0.25 mm

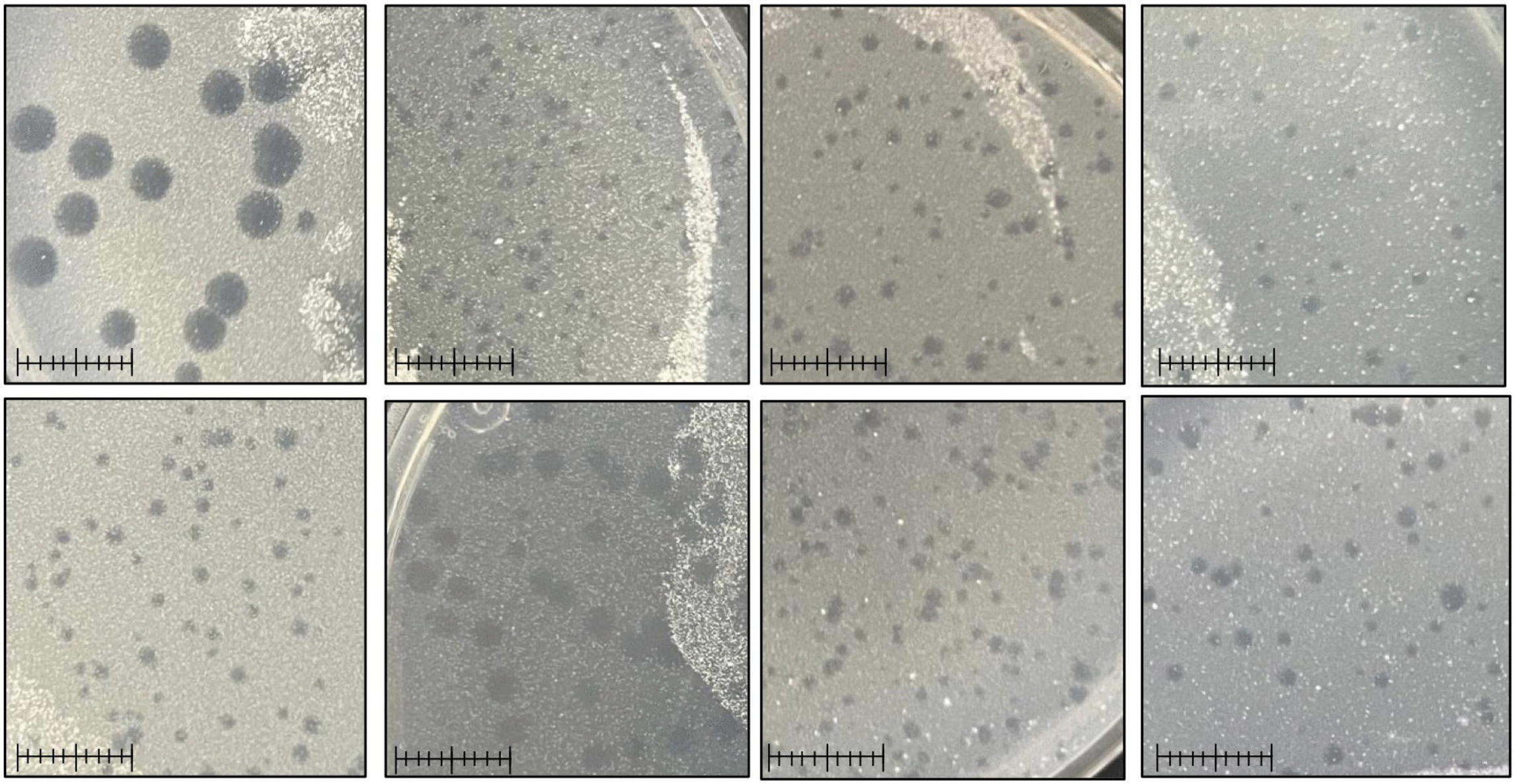

Girr_*ΔlysF1b*
M. Smegmatis
*0.79 +/- 0.20 mm

Girr_*ΔlysF1b*
M. smegmatis
pExTra-Waterfoul_*32*
+ aTc
**2.23 +/- 0.45 mm

Girr_*ΔlysF1b*
M. smegmatis
pExTra-Waterfoul_*32Δ40C*
+ aTc
0.88 +/- 0.29 mm

Girr_*ΔlysF1b*
M. smegmatis
pExTra-Waterfoul_*32ΔN*
+ aTc
0.84 +/- 0.31 mm

B.

Girr_WT
M. Smegmatis
4.15 +/- 0.65 mm

Girr_*ΔlysF1b*
M. Smegmatis
*0.95 +/- 0.36 mm

Girr_*ΔlysF1b*
M. Smegmatis
pExTra01
1.18 +/- 0.35 mm

Girr_*ΔlysF1b*
M. smegmatis/
pExTra-Girr_*35*
**2.33 +/- 0.367 mm

Girr_*ΔlysF1b*
M. Smegmatis
pExTra-NBJ_*33*
**2.19 +/- 0.298 mm

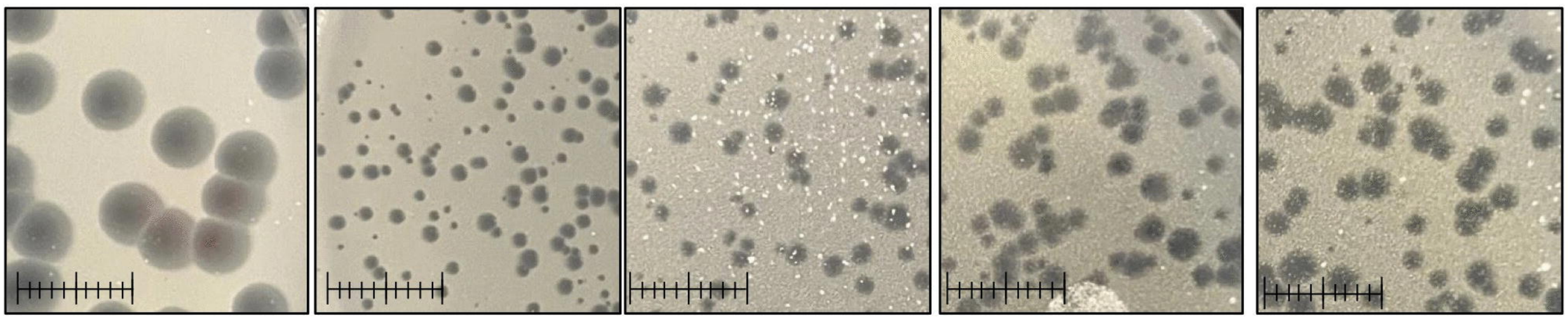

Girr_WT
M. Smegmatis
4.56 +/- 0.65 mm

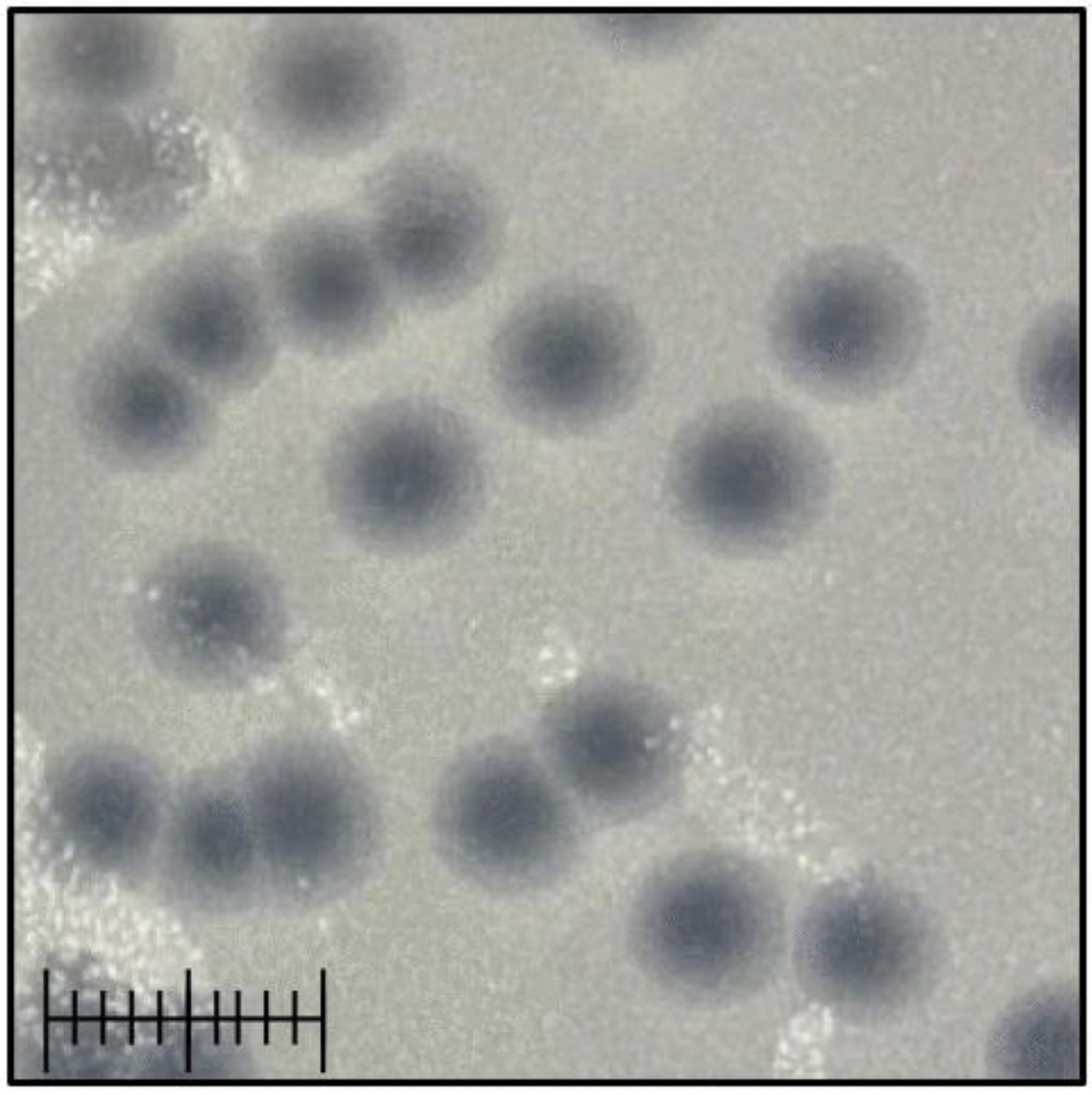

Girr_*ΔlysF1a*
M. Smegmatis
pExTra-Girr*34* + *aTc*
**4.15 +/- 0.55 mm

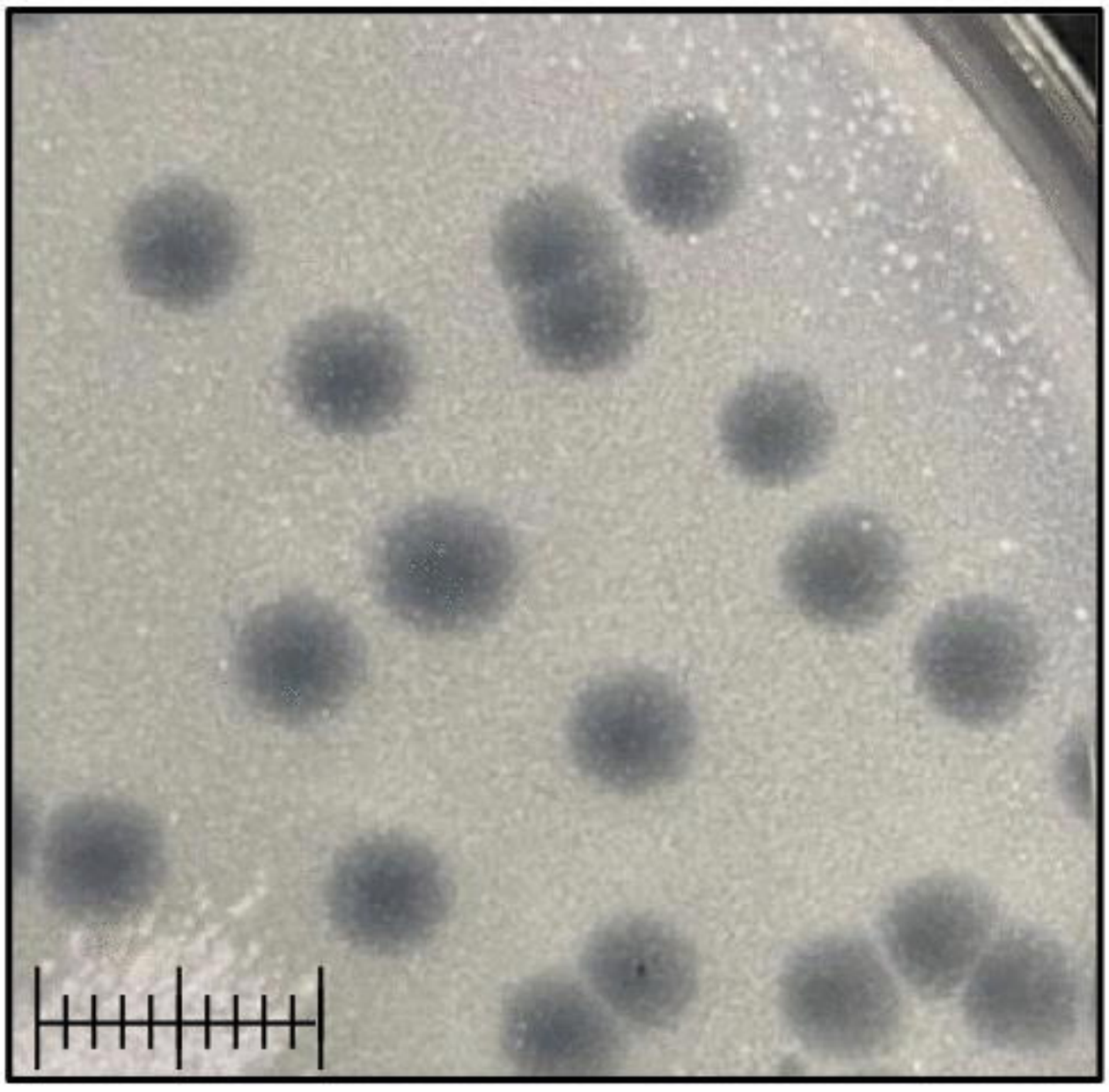

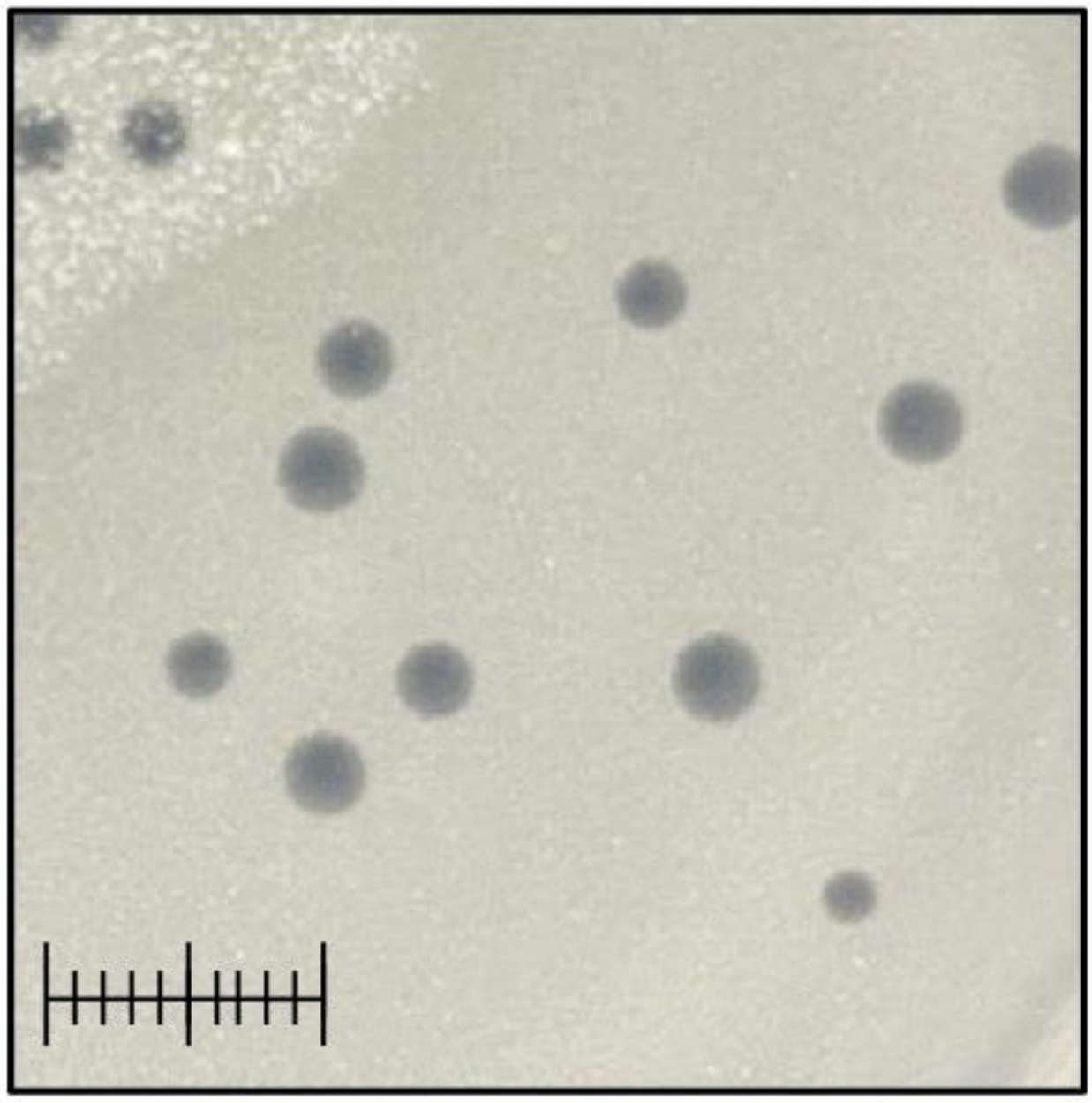

Girr_*ΔlysF1a*
M. Smegmatis
*2.79 +/- 0.55mm

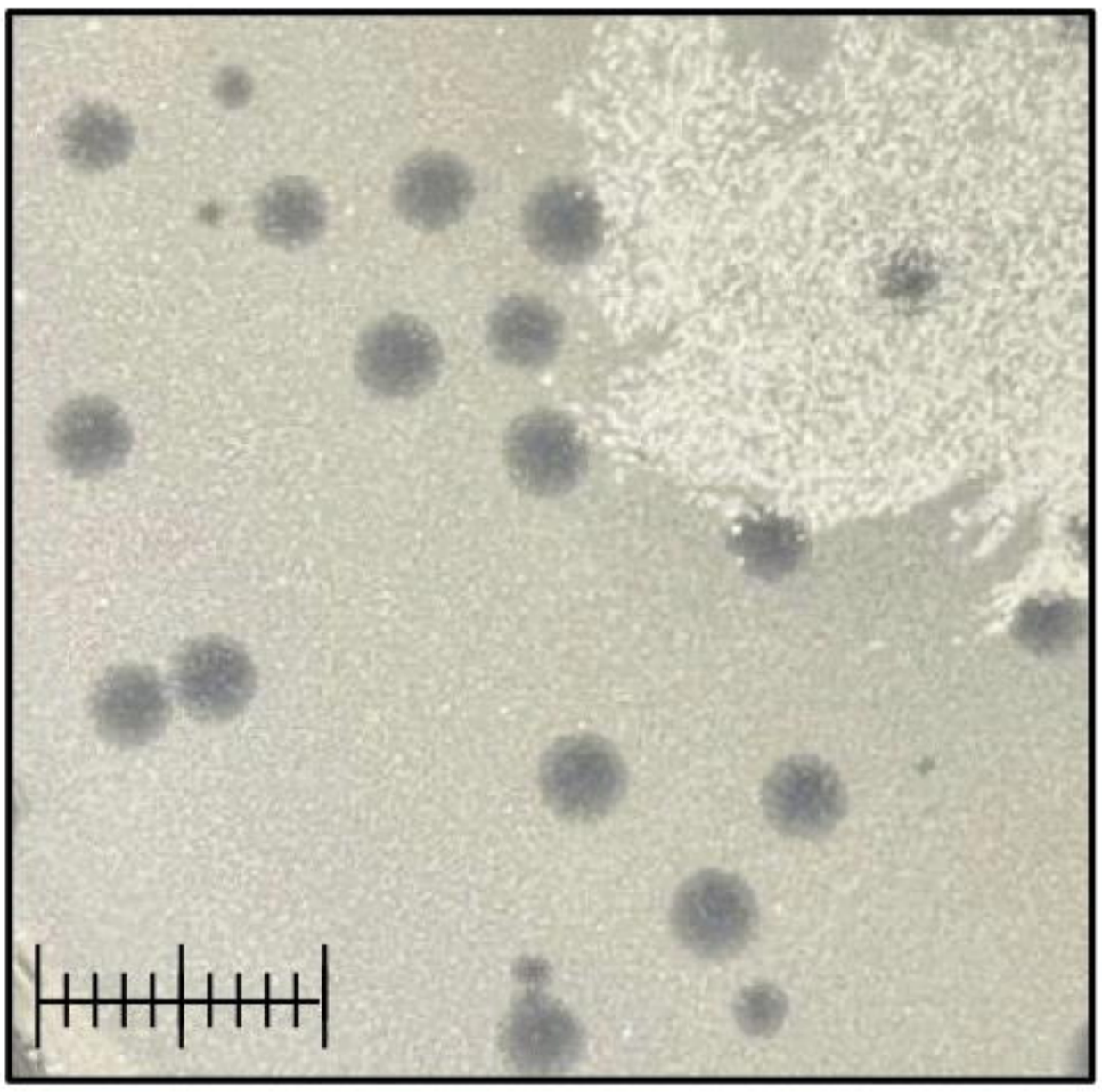

Girr_*ΔlysF1a*
M. Smegmatis
pExTra-Girr*34 no aTc*
2.83 +/- 0.353 mm

A.

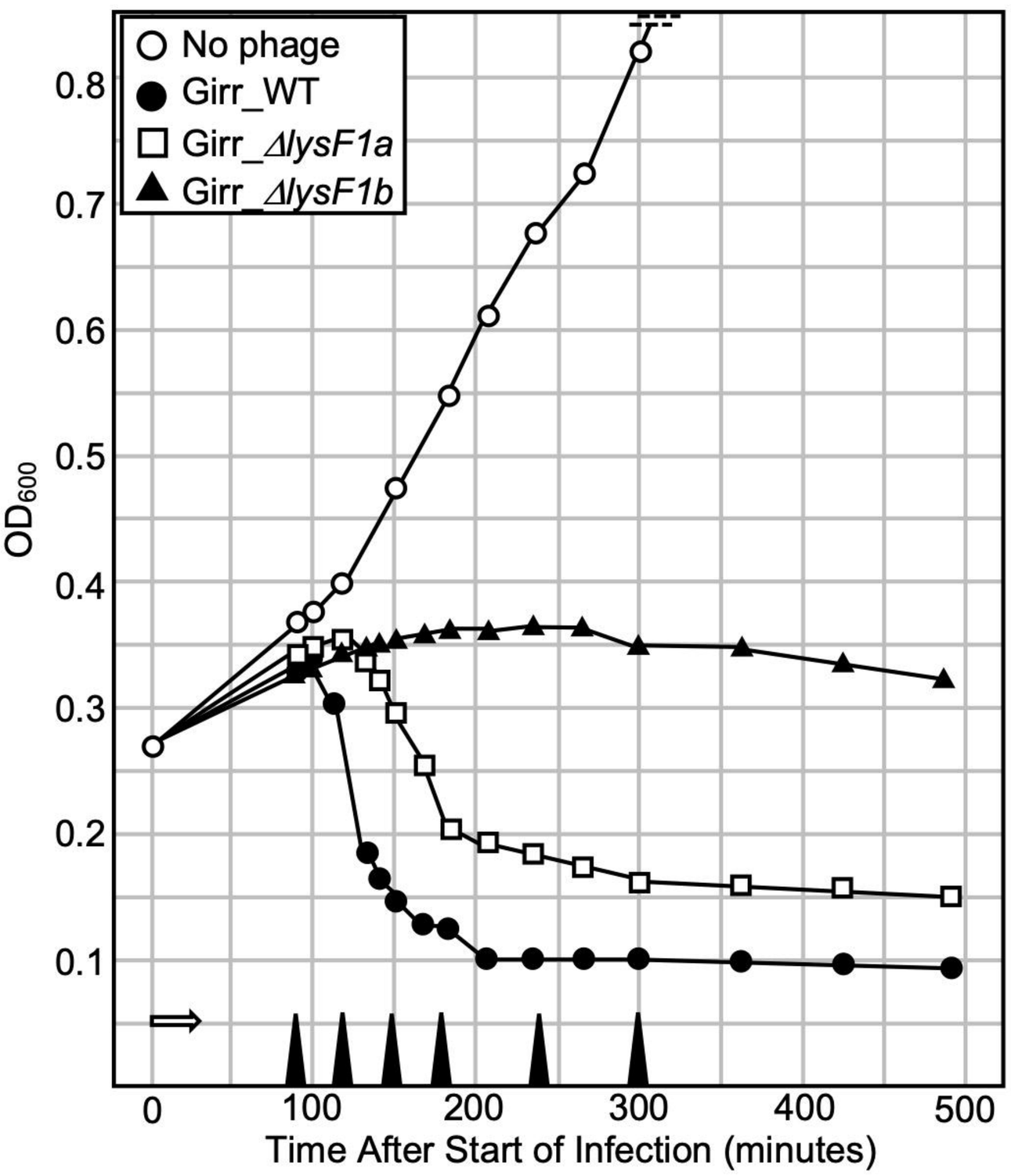
No phage
Girr_WT
Girr_ΔlysF1a
Girr_ΔlysF1b
OD600
0.8
0.7
0.6
0.5
0.4
0.3
0.2
0.1
0
100
200
300
400
500
Time After Start of Infection (minutes)

B.

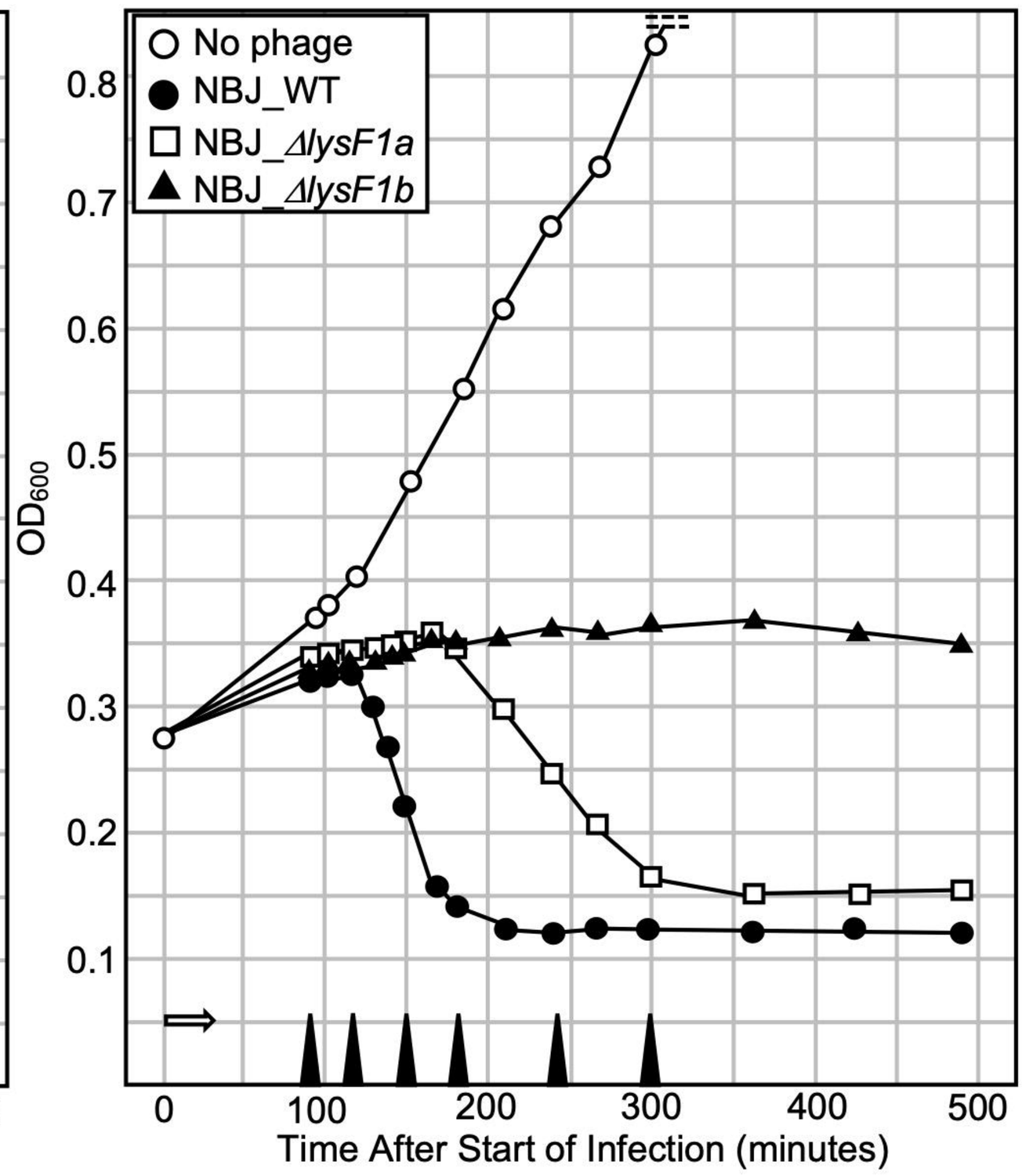
No phage
NBJ_WT
NBJ_ΔlysF1a
NBJ_ΔlysF1b
OD600
0.8
0.7
0.6
0.5
0.4
0.3
0.2
0.1
0
100
200
300
400
500
Time After Start of Infection (minutes)

C.

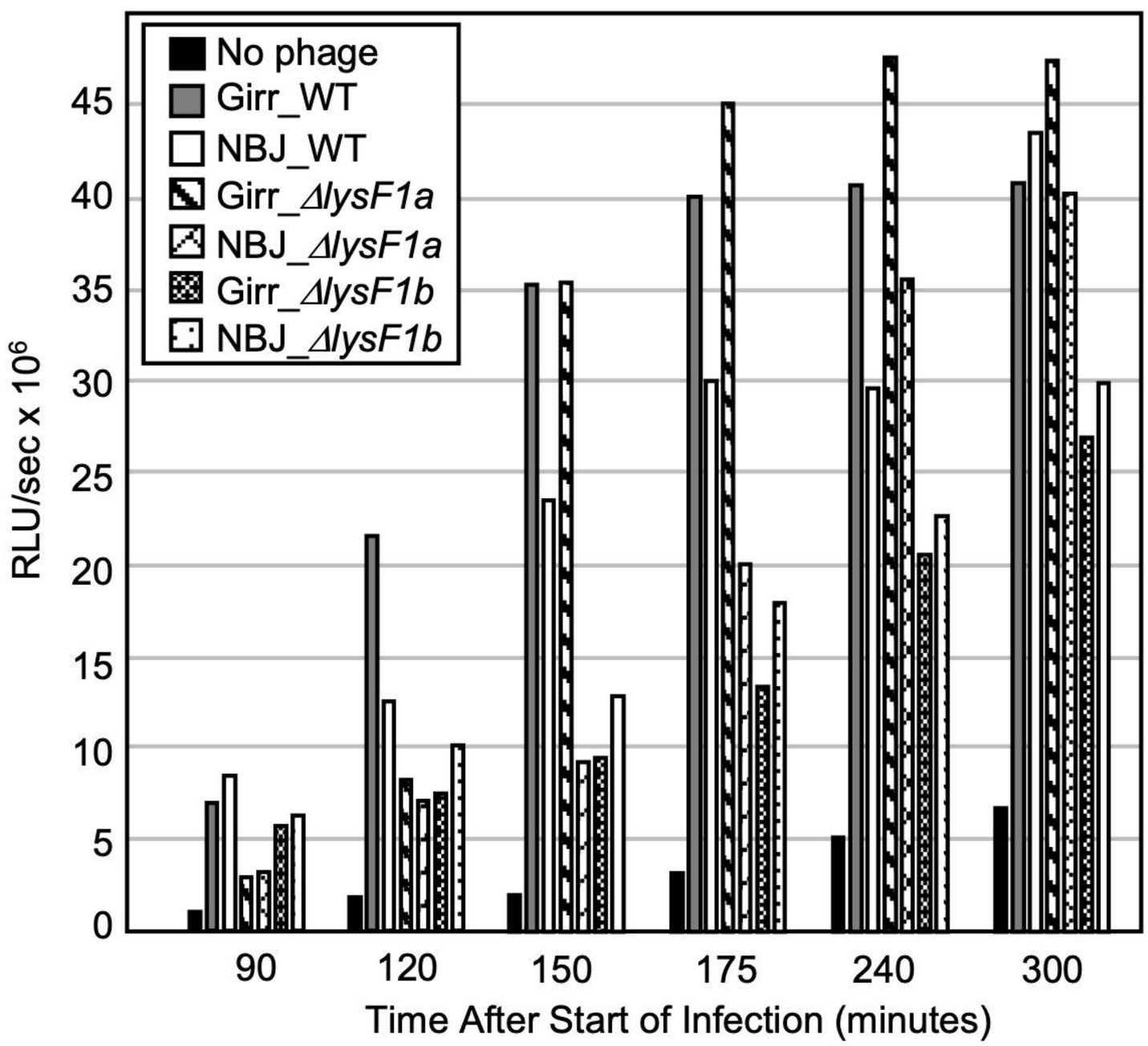
No phage
Girr_WT
NBJ_WT
Girr_ΔlysF1a
NBJ_ΔlysF1a
Girr_ΔlysF1b
NBJ_ΔlysF1b
RLU/sec x 10^6
45
40
35
30
25
20
15
10
5
0
90
120
150
175
240
300
Time After Start of Infection (minutes)

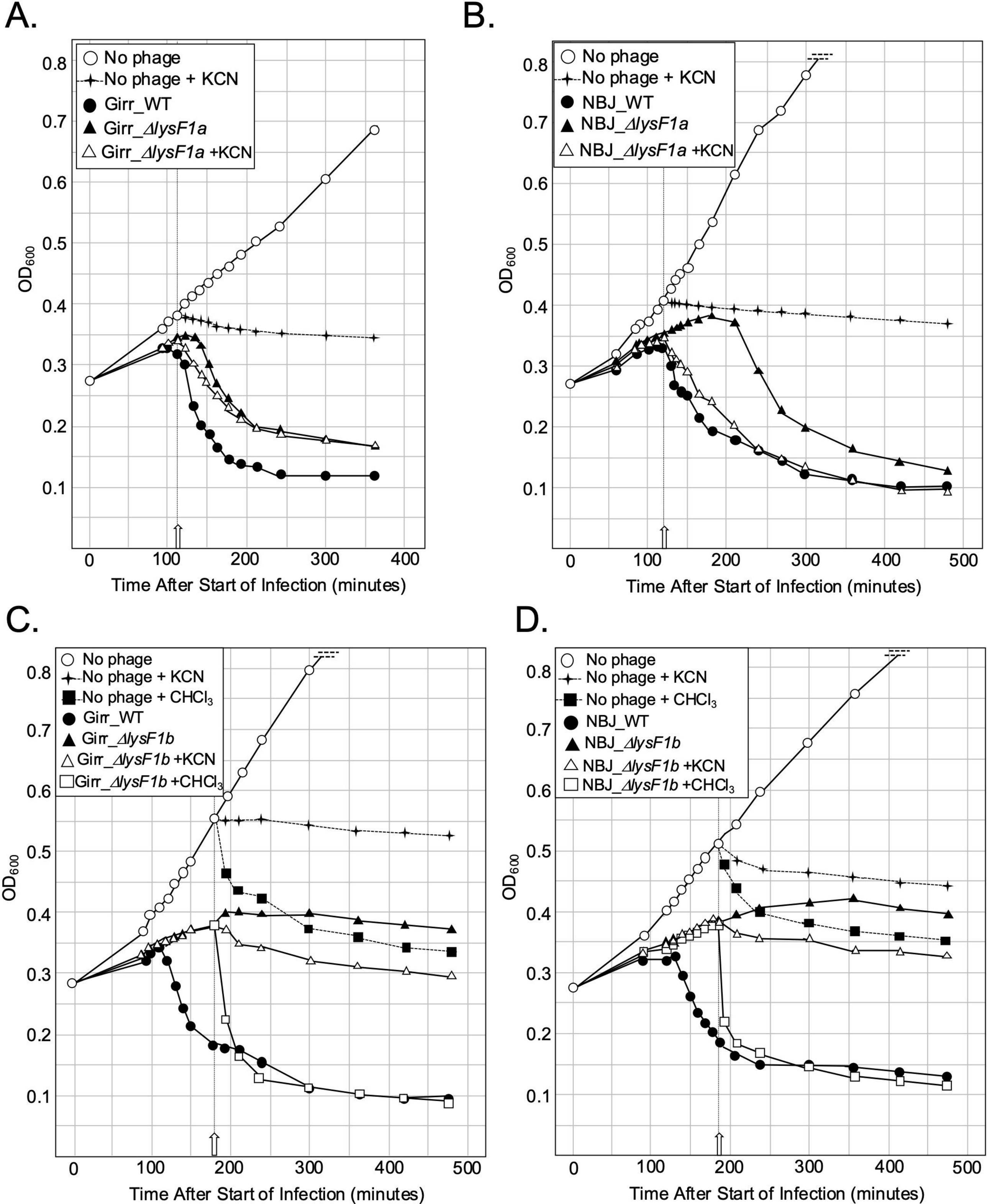
A.
No phage
No phage + KCN
Girr_WT
Girr_ΔlysF1a
Girr_ΔlysF1a +KCN
OD600
Time After Start of Infection (minutes)
B.
No phage
No phage + KCN
NBJ_WT
NBJ_ΔlysF1a
NBJ_ΔlysF1a +KCN
OD600
Time After Start of Infection (minutes)
C.
No phage
No phage + KCN
No phage + CHCl3
Girr_WT
Girr_ΔlysF1b
Girr_ΔlysF1b +KCN
Girr_ΔlysF1b +CHCl3
OD600
Time After Start of Infection (minutes)
D.
No phage
No phage + KCN
No phage + CHCl3
NBJ_WT
NBJ_ΔlysF1b
NBJ_ΔlysF1b +KCN
NBJ_ΔlysF1b +CHCl3
OD600
Time After Start of Infection (minutes)

A.

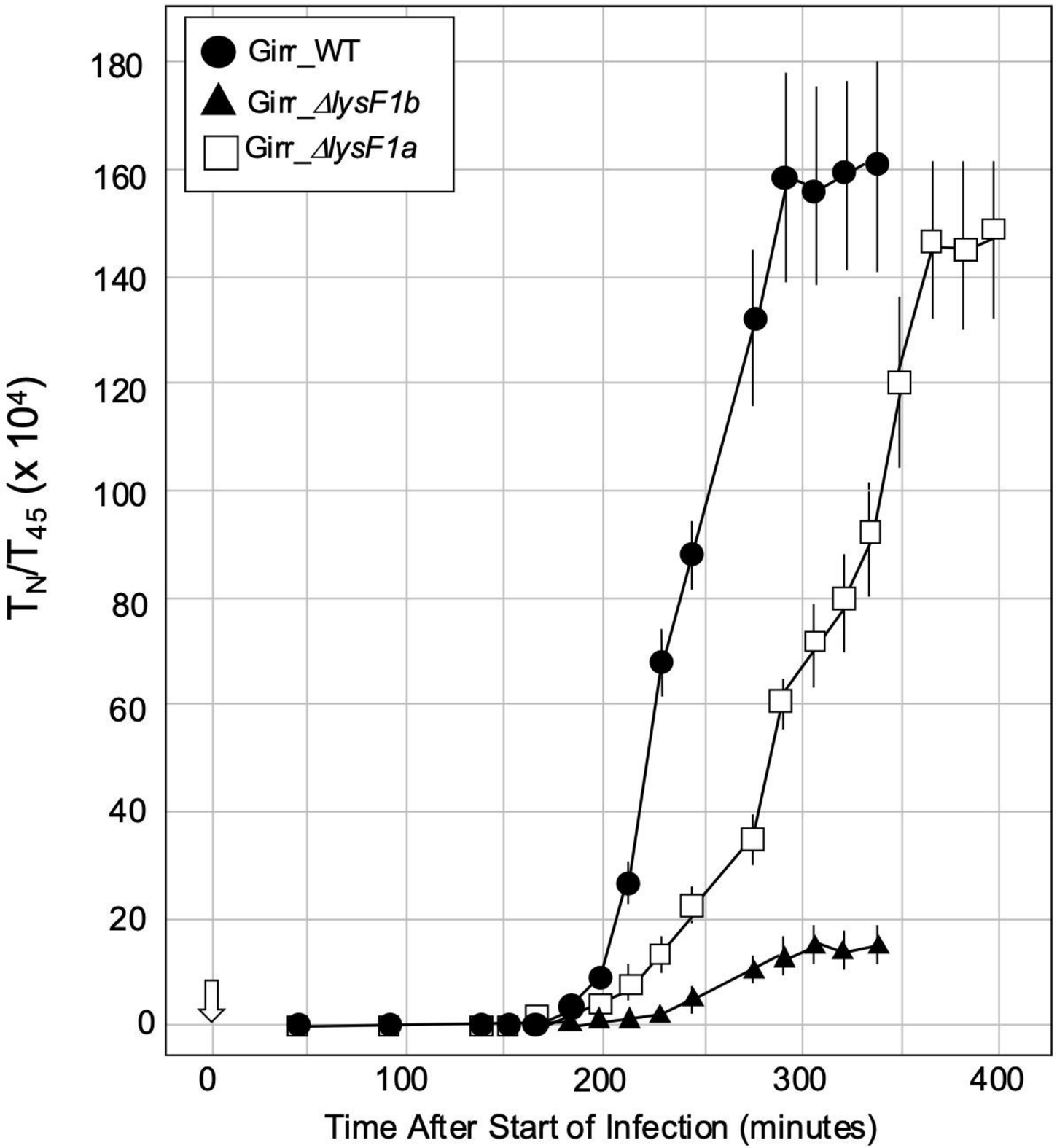

B.

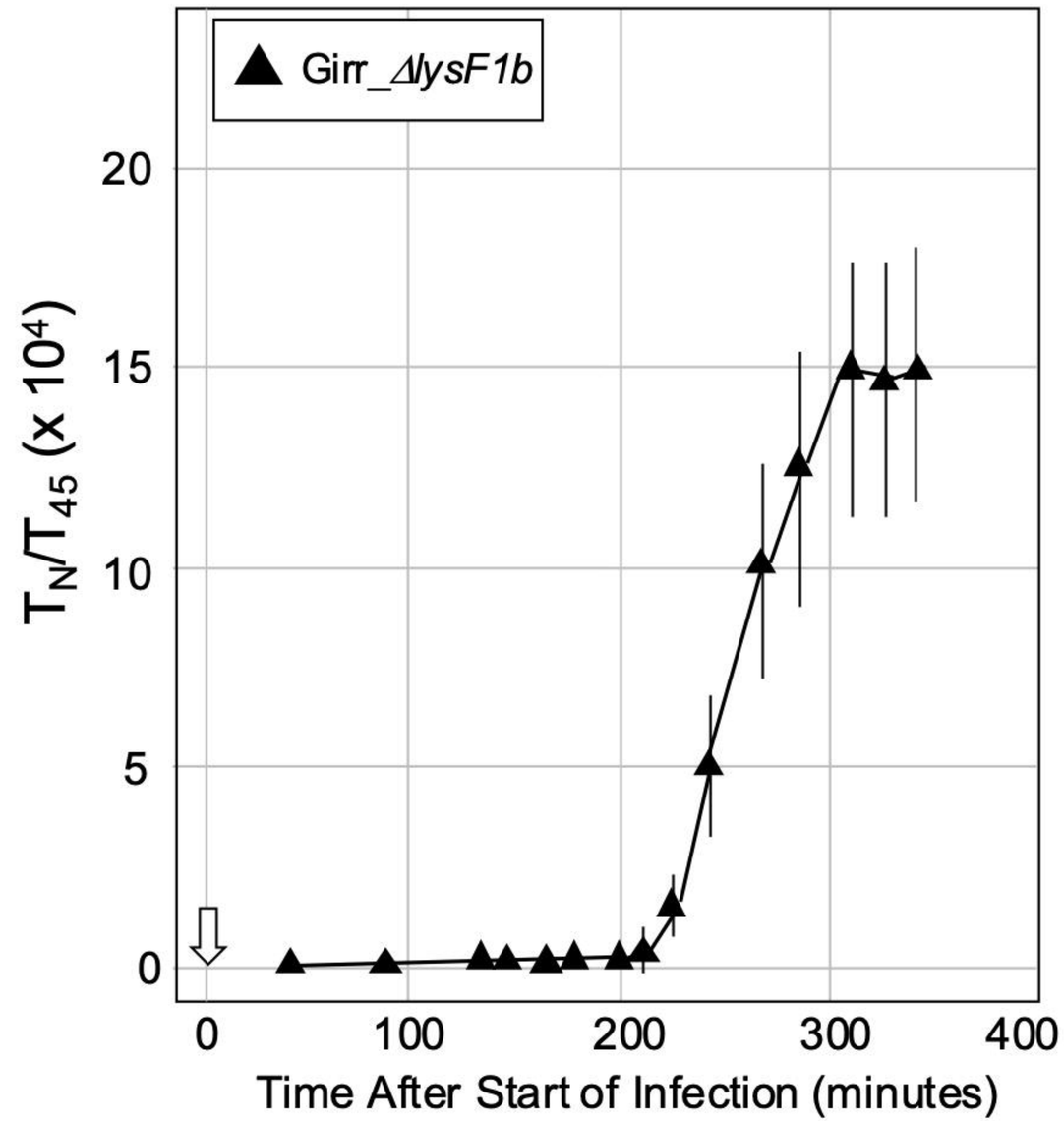

C.

phage	Burst Size PFU/cell
Girr_WT	277 +/- 81
Girr_*ΔlysF1a*	255 +/- 75
Girr_*ΔlysF1b*	*29.2 +/- 36

*statistically significant from WT phage *p<0.0001.*

A.

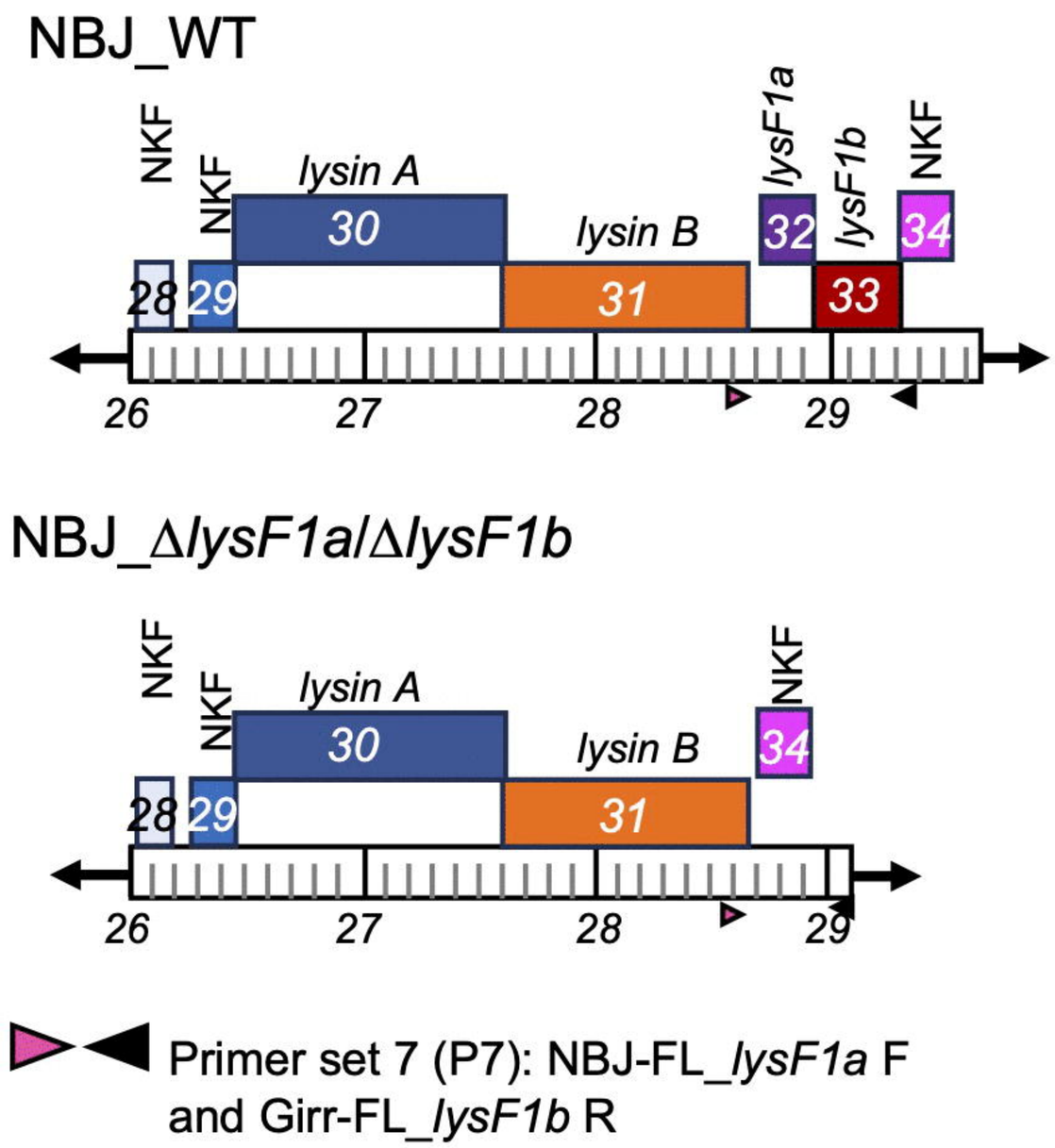
NBJ_WT
NKF
NKF
lysin A
30
lysin B
31
lysF1a
32
lysF1b
33
NKF
34
28
29
26
27
28
29
NBJ_ΔlysF1a/ΔlysF1b
NKF
NKF
lysin A
30
lysin B
31
NKF
34
28
29
26
27
28
29
Primer set 7 (P7): NBJ-FL_lysF1a F
and Girr-FL_lysF1b R

B.

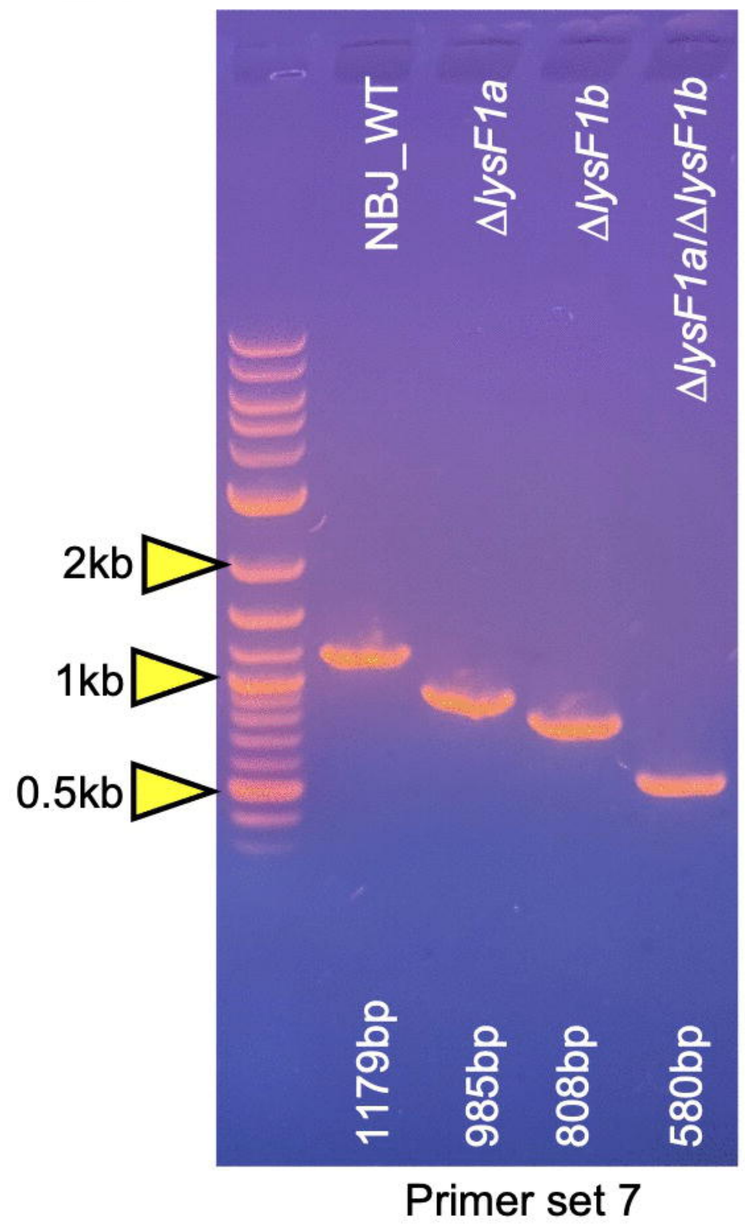
NBJ_WT
ΔlysF1a
ΔlysF1b
ΔlysF1a/ΔlysF1b
2kb
1kb
0.5kb
1179bp
985bp
808bp
580bp
Primer set 7

C.

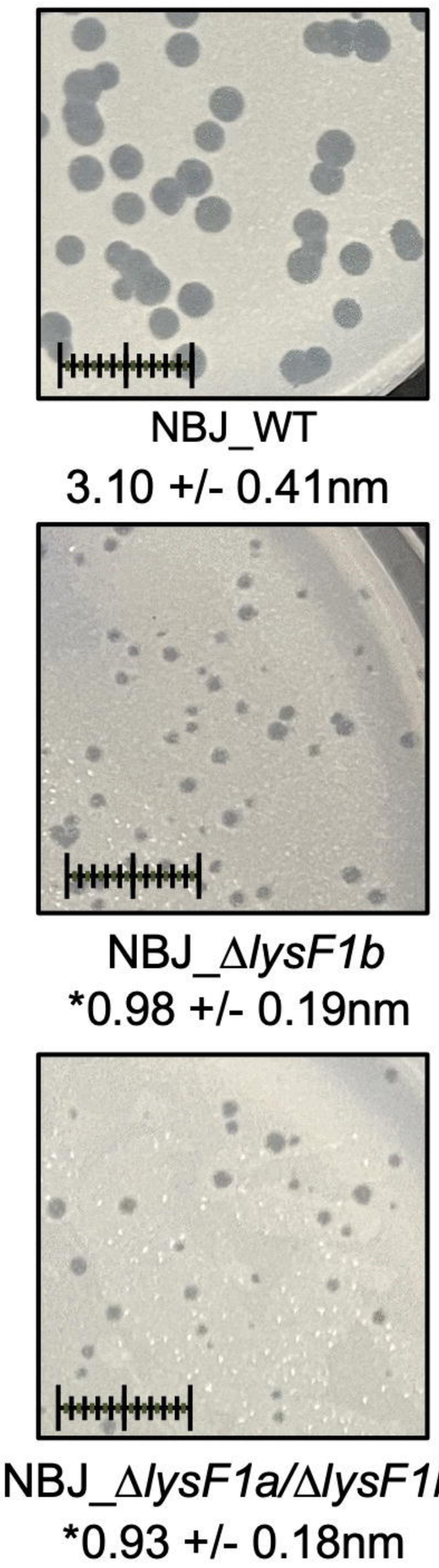
NBJ_WT
3.10 +/- 0.41nm
NBJ_ΔlysF1b
*0.98 +/- 0.19nm
NBJ_ΔlysF1a/ΔlysF1b
*0.93 +/- 0.18nm

D.

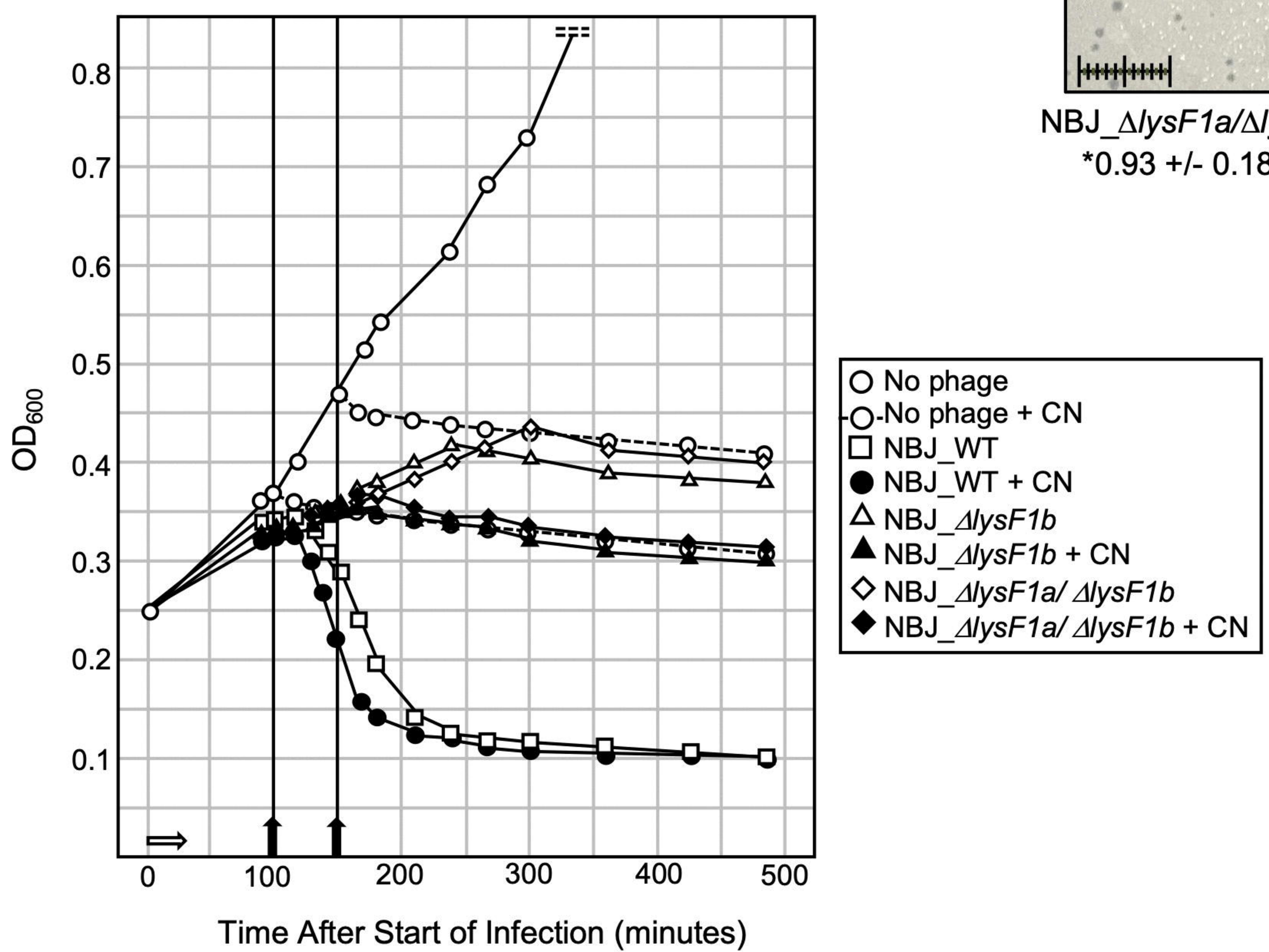
OD600
0.8
0.7
0.6
0.5
0.4
0.3
0.2
0.1
0
100
200
300
400
500
Time After Start of Infection (minutes)
No phage
No phage + CN
NBJ_WT
NBJ_WT + CN
NBJ_ΔlysF1b
NBJ_ΔlysF1b + CN
NBJ_ΔlysF1a/ ΔlysF1b
NBJ_ΔlysF1a/ ΔlysF1b + CN

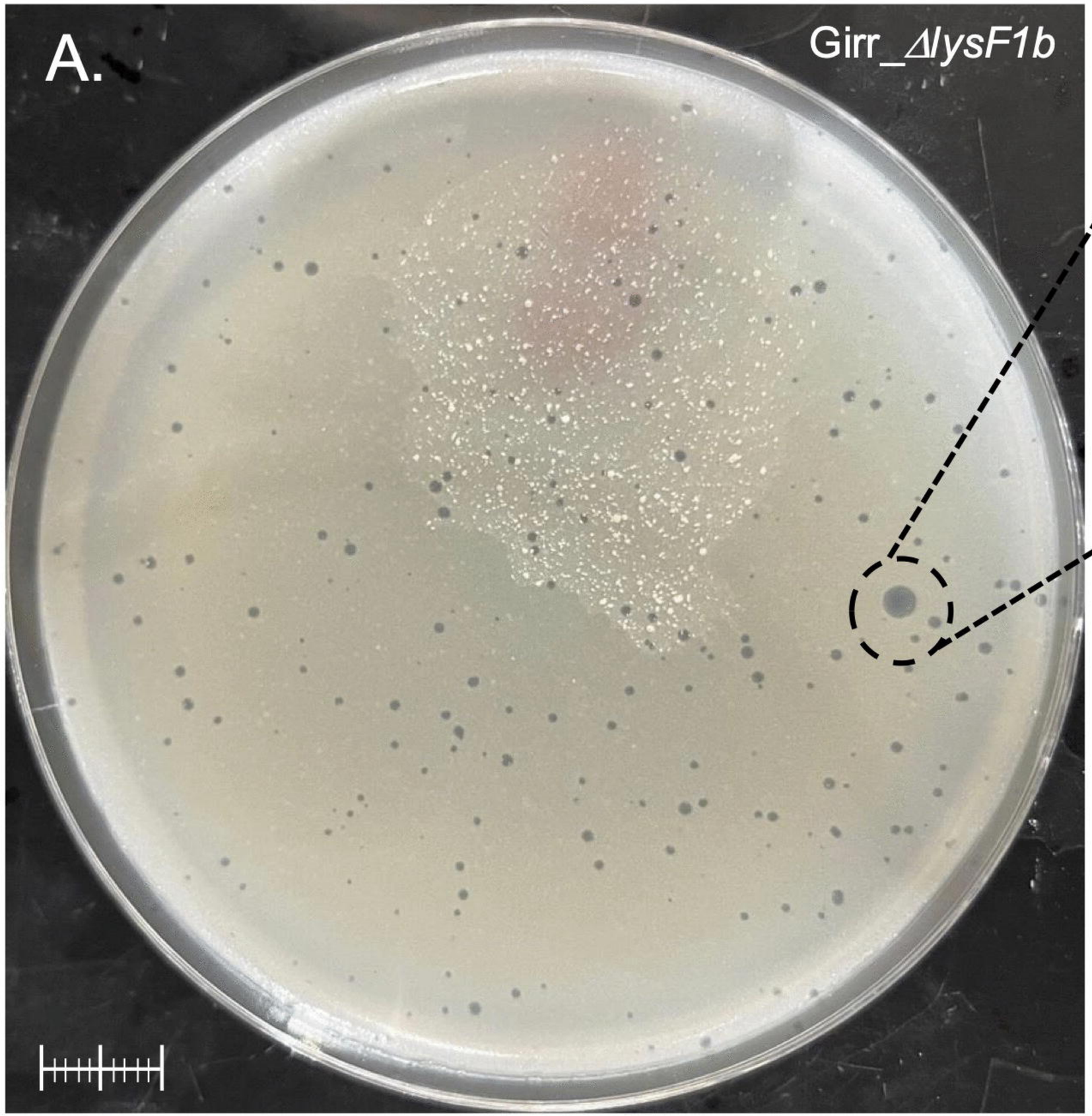

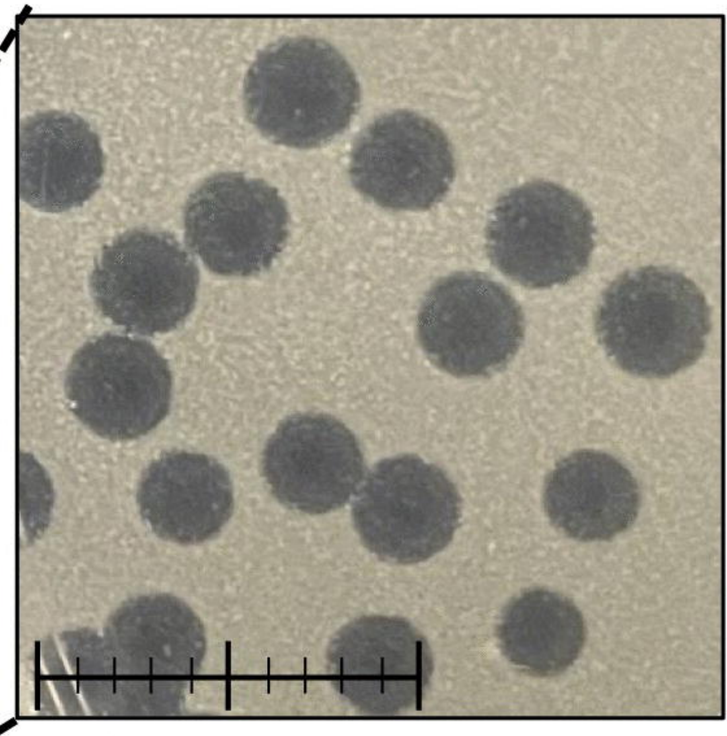

Girr_ΔlysF1b-LRM
3.01 +/- 0.26mm

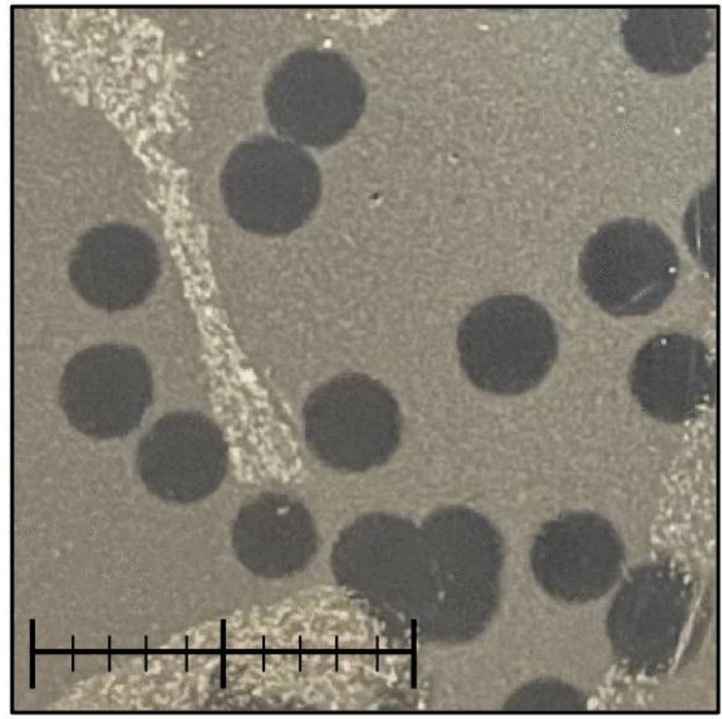

Girr_WT
2.94 +/- 0.25mm

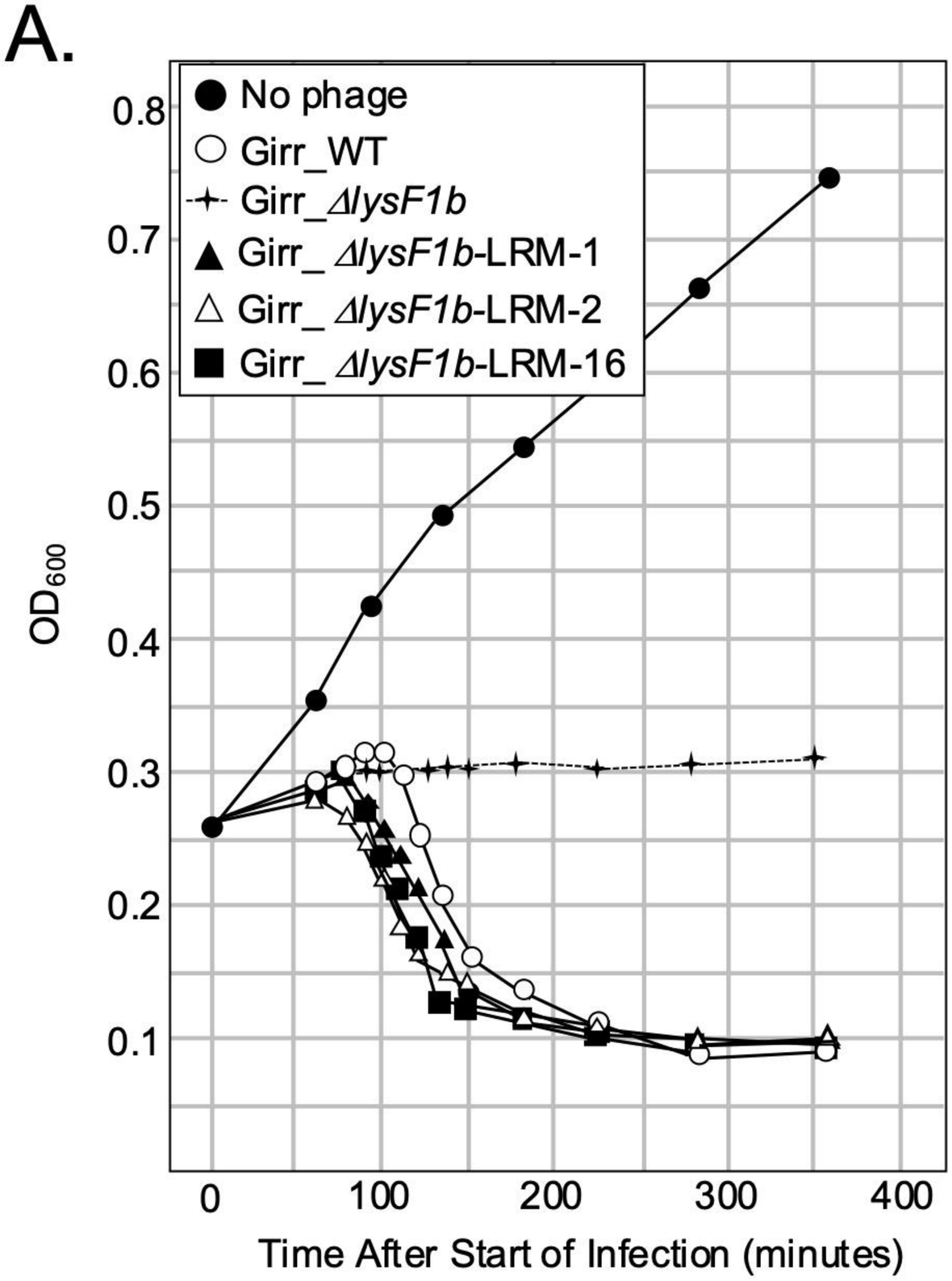
A.
No phage
Girr_WT
Girr_ΔlysF1b
Girr_ ΔlysF1b-LRM-1
Girr_ ΔlysF1b-LRM-2
Girr_ ΔlysF1b-LRM-16
OD600
0.8
0.7
0.6
0.5
0.4
0.3
0.2
0.1
0
100
200
300
400
Time After Start of Infection (minutes)

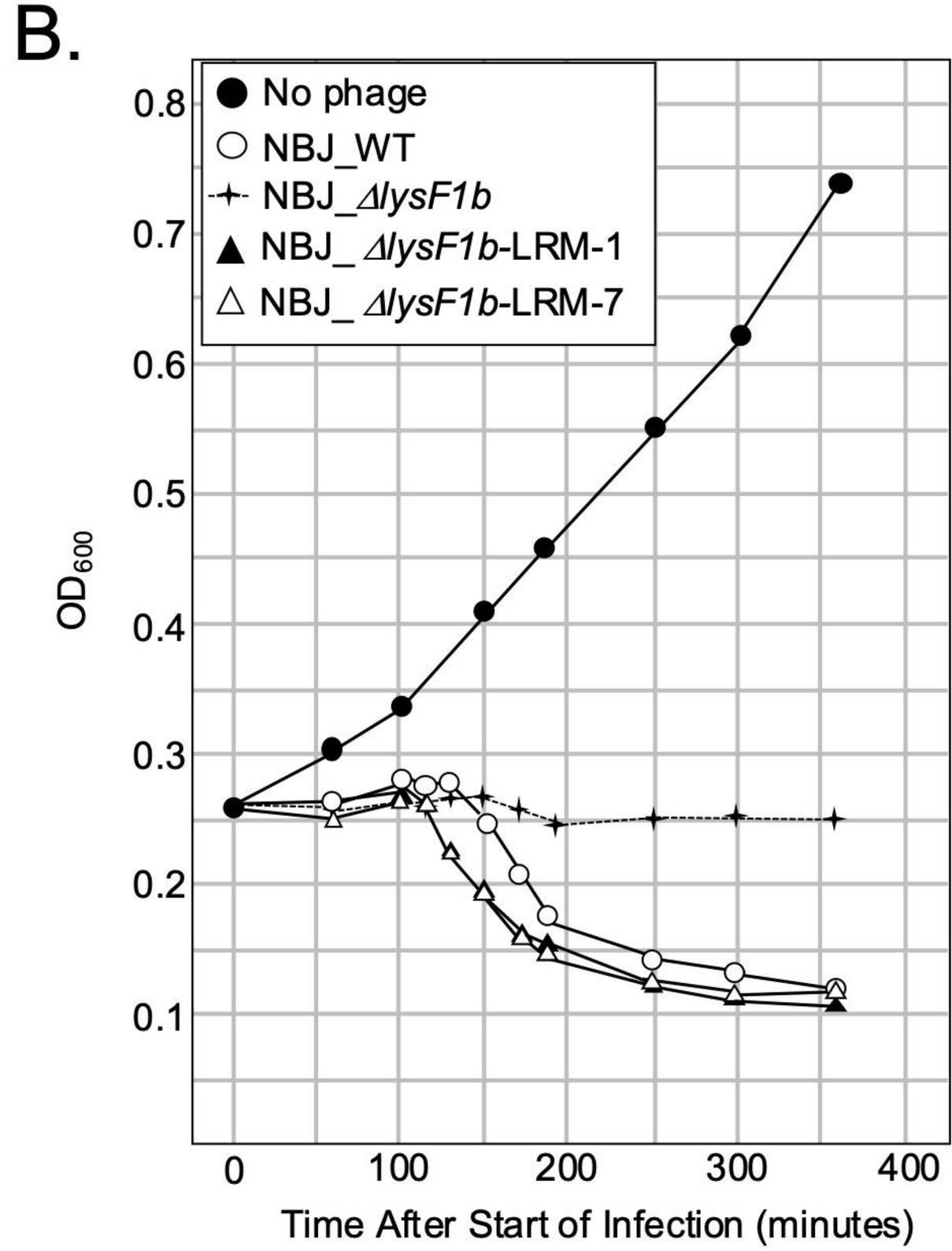
B.
No phage
NBJ_WT
NBJ_ΔlysF1b
NBJ_ ΔlysF1b-LRM-1
NBJ_ ΔlysF1b-LRM-7
OD600
0.8
0.7
0.6
0.5
0.4
0.3
0.2
0.1
0
100
200
300
400
Time After Start of Infection (minutes)

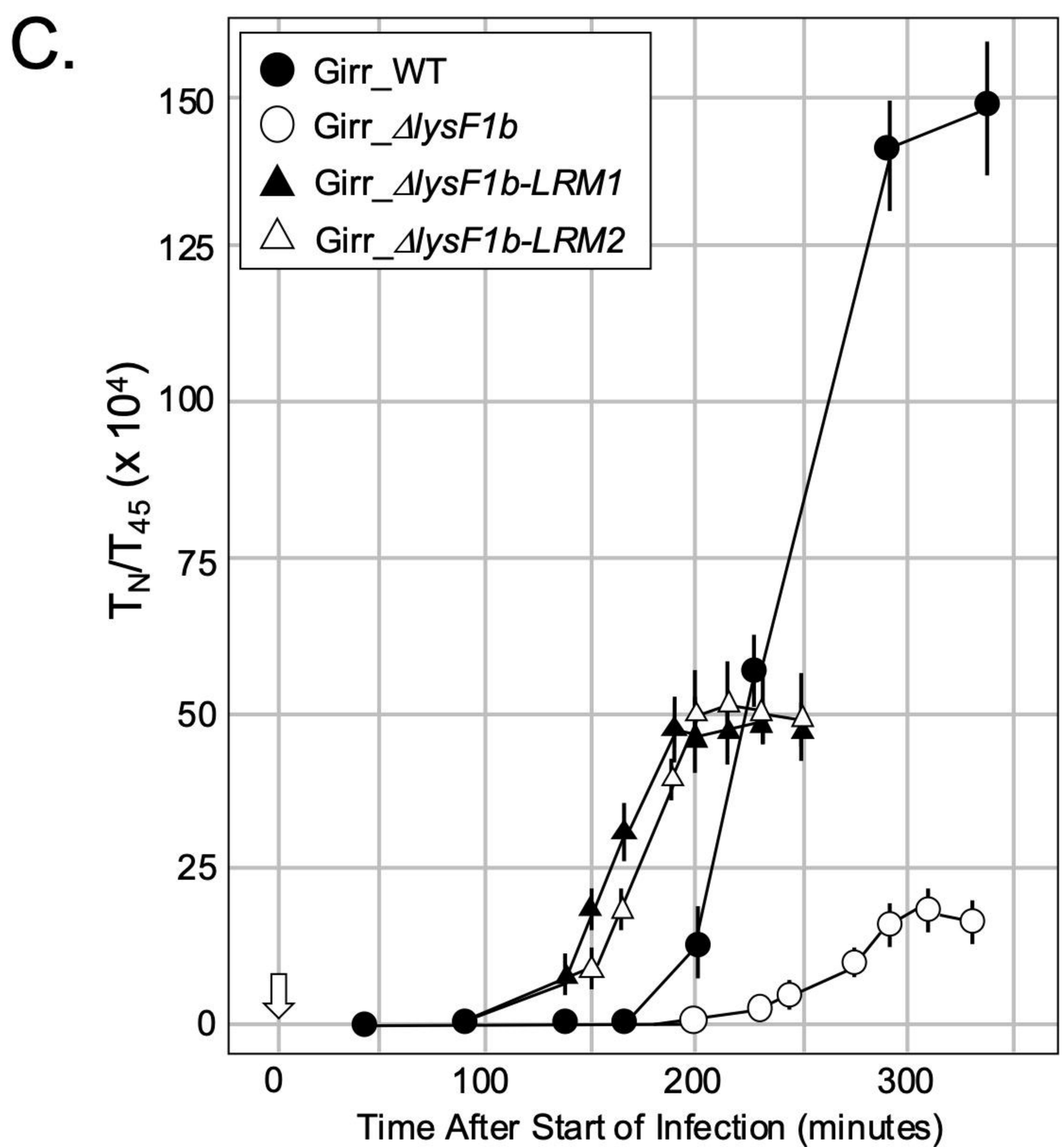
C.
Girr_WT
Girr_ΔlysF1b
Girr_ΔlysF1b-LRM1
Girr_ΔlysF1b-LRM2
TN/T45 (x 10^4)
150
125
100
75
50
25
0
0
100
200
300
Time After Start of Infection (minutes)

A.

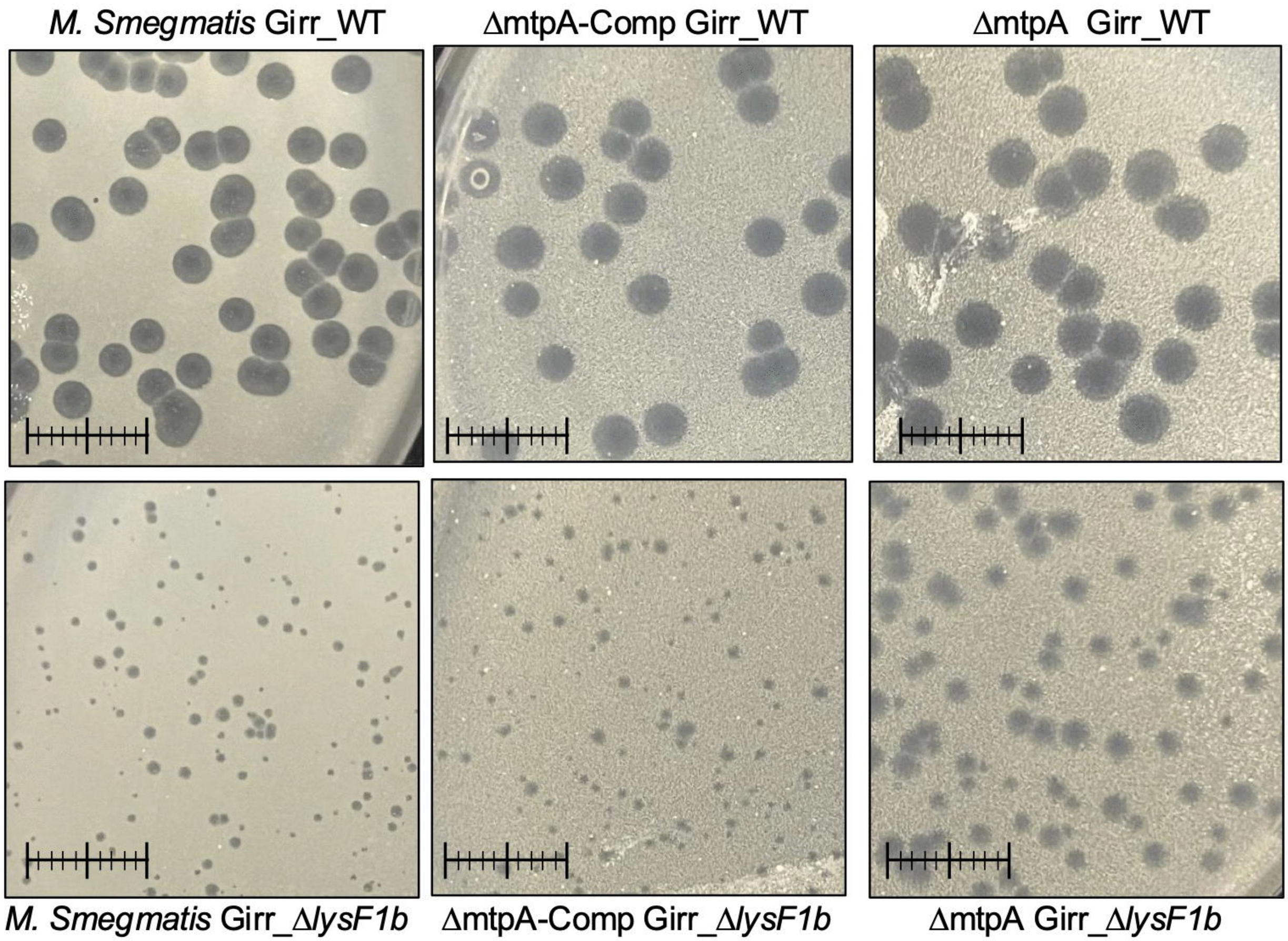
M. Smegmatis Girr_WT
ΔmtpA-Comp Girr_WT
ΔmtpA Girr_WT
M. Smegmatis Girr_ΔlysF1b
ΔmtpA-Comp Girr_ΔlysF1b
ΔmtpA Girr_ΔlysF1b

B.

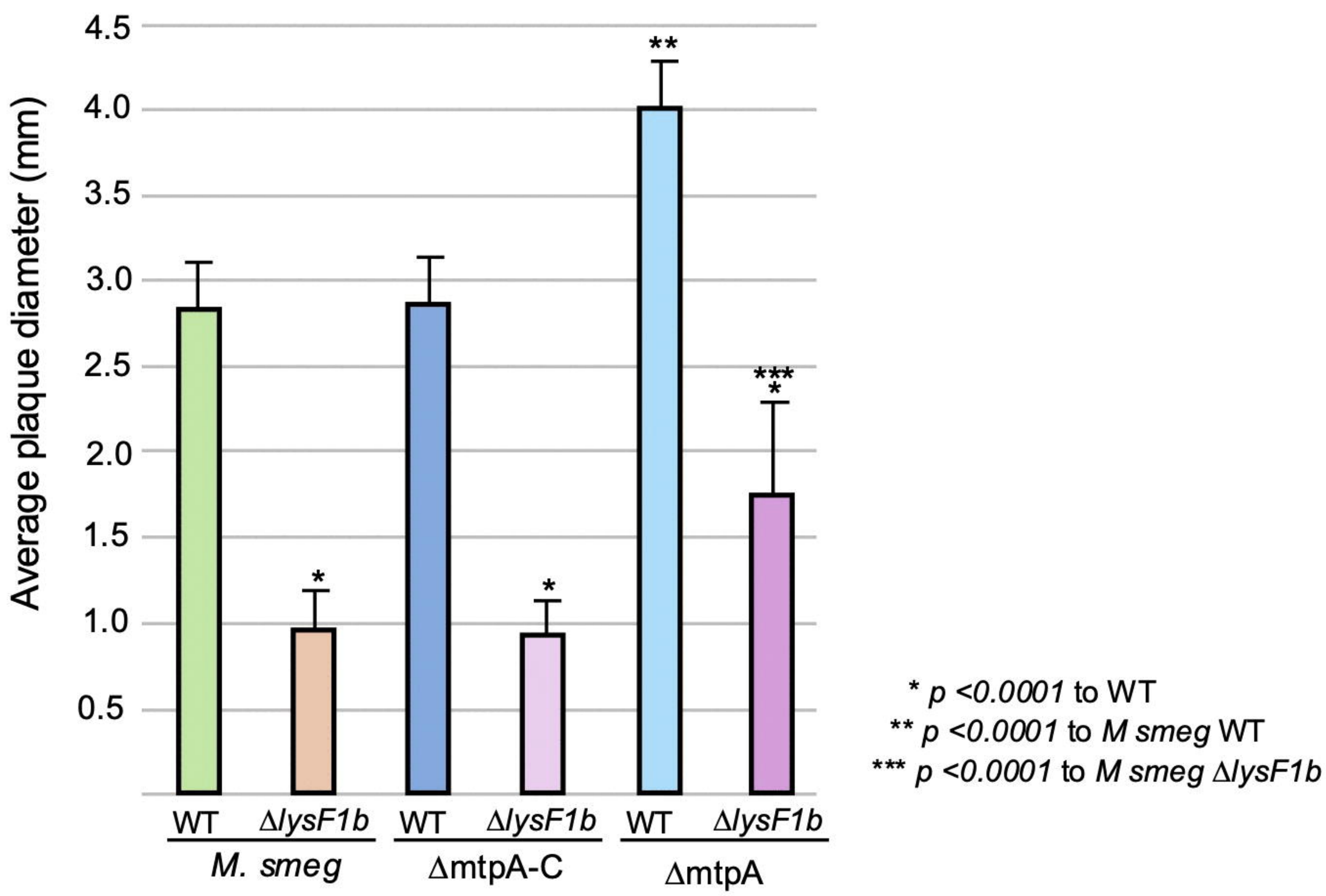
Average plaque diameter (mm)
4.5
4.0
3.5
3.0
2.5
2.0
1.5
1.0
0.5
**
***
*
*
*
WT
ΔlysF1b
WT
ΔlysF1b
WT
ΔlysF1b
M. smeg
ΔmtpA-C
ΔmtpA
* p <0.0001 to WT
** p <0.0001 to M smeg WT
*** p <0.0001 to M smeg ΔlysF1b

A.

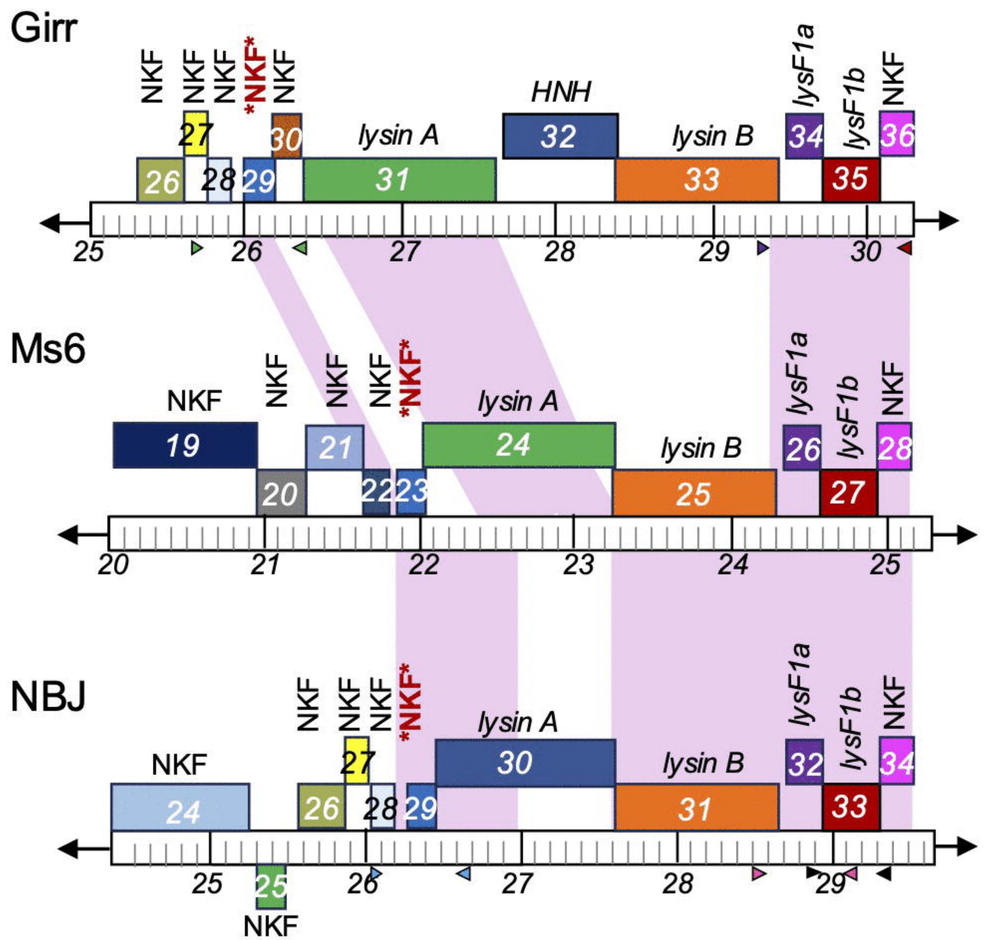

B.

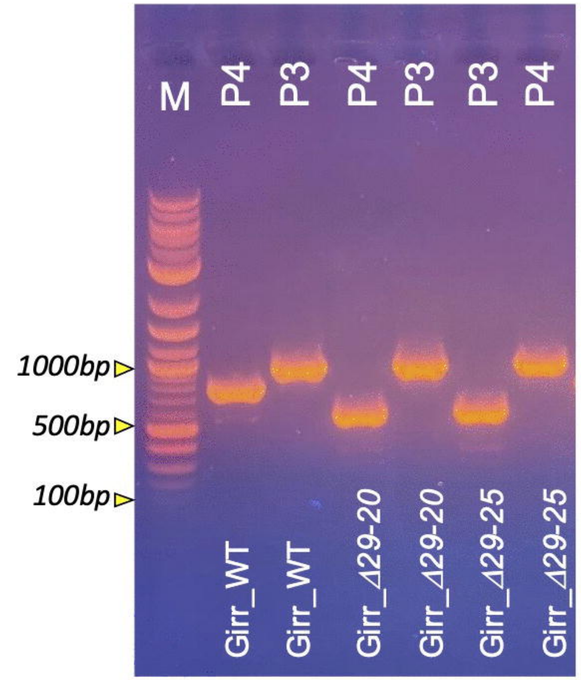

Primer set 3 (P3): Girr-FL_*lysF1a* F and Girr-FL_*lysF1b* R

Primer set 4 (P4): Girr-FL_*29* F & R

C.

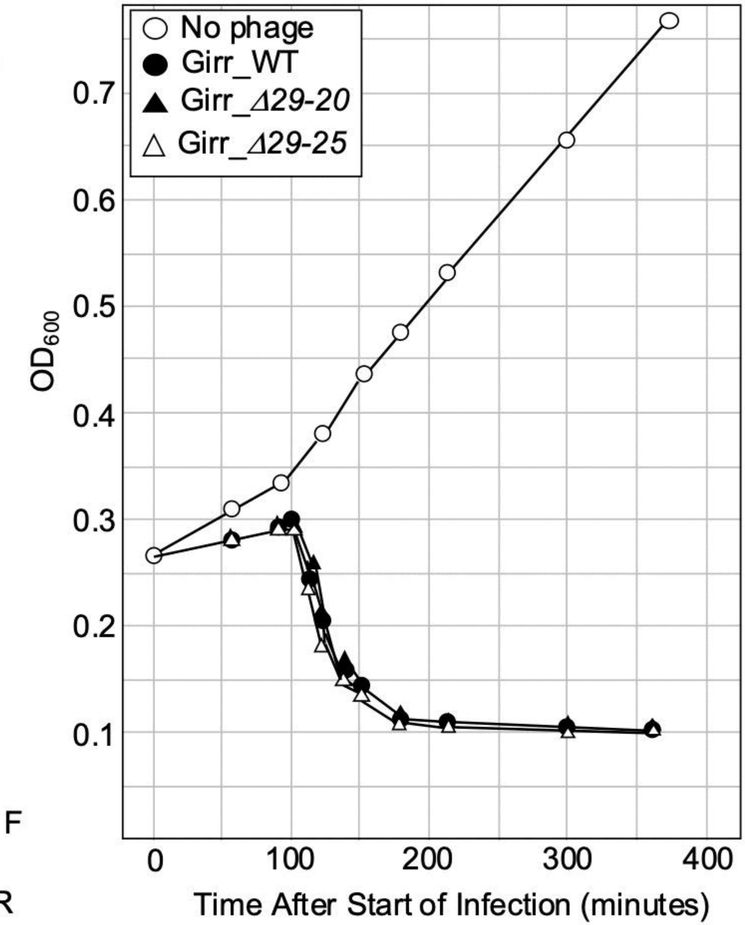

D.

```
Girr_29   MDRLGIILLKLLGPLADRIADRIADRITENLPDLSDLDDQIVAKLPDLTNLPEQVINIIGRLPRFPFLLGGKP
Ms6_23    MDRLGIVLLKLFGPLADRIADRIADRIAENLPDLSNLDDQIVAKLPDLTNLPAQVMDIIDSALRSIPVLGGILGSKR
NBJ_29    MDRLGIILLKLFGPLADRIADRIADRITENLPDLSNLDDQIVAKLPDLTNLPAQVMDIIDGALRSIPVLGGILGSKR
```

E.

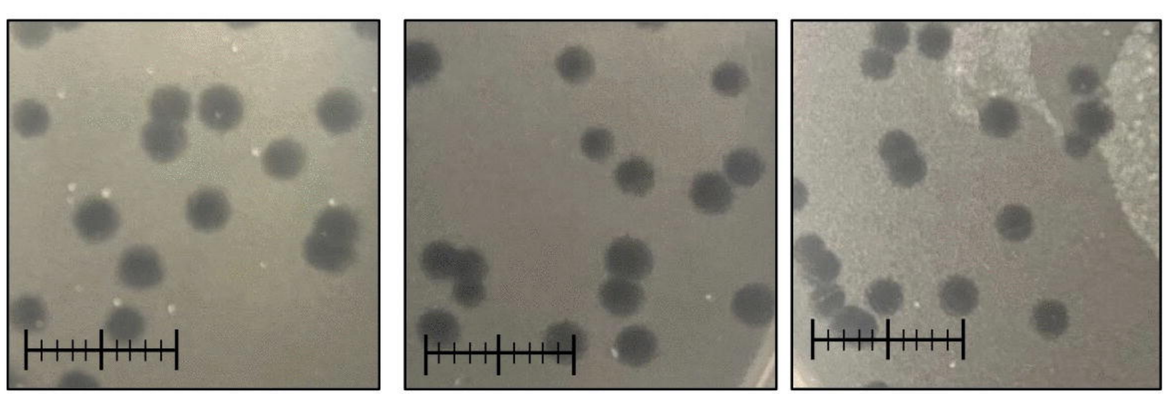

Girr_WT
3.11 +/- 0.12 nm

Girr_*Δ29-20*
2.98 +/- 0.16 nm

Girr_*Δ29-25*
3.02 +/- 0.14 nm

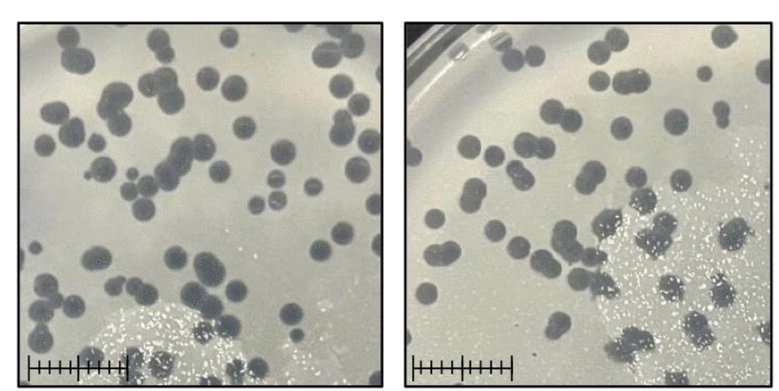

NBJ_WT
2.25 +/- 0.25 nm

NBJ_*Δ29*
2.15 +/- 0.09 nm